ELUCIDATING CAUSE-EFFECT RELATIONSHIPS BETWEEN EXTRACELLULAR MATRIX SIGNALING AND MESENCHYMAL STEM CELL DIFFERENTIATION

A Dissertation

by

SILVIA MILENA BECERRA-BAYONA

Submitted to the Office of Graduate Studies of
Texas A&M University
in partial fulfillment of the requirements for the degree of

DOCTOR OF PHILOSOPHY

Chair of Committee,	Mariah Hahn
Committee Members,	Zhilei Chen
	Arul Jayaraman
	Mike McShane
Intercollegiate Faculty Chair,	Ibrahim Karaman

August 2013

Major Subject: Materials Science and Engineering

ABSTRACT

Mesenchymal stem cell (MSC) differentiation is known to be influenced by a range of environmental stimuli. MSC-based bone regeneration strategies would benefit from the identification of scaffold material properties which intrinsically promote osteoblast lineage progression. The aim of this work was to contribute to the understanding of elucidating cause-effect relationships between extracellular matrix (ECM) signaling and osteogenic MSC differentiation using poly(ethylene glycol) diacrylate (PEGDA) hydrogels as a material platform. First, the effect of several ECM proteins associated with bone morphogenesis or bone fracture healing on MSC osteogenesis was investigated. Second, collagen-mimetic proteins (Scl2) were modified in order to incorporate them in a 3D network, and cell adhesion and activation of cell signaling were evaluated, as well. Finally, the influence of integrin α_1 and α_2 binding on human MSC (hMSC) osteogenesis was investigated toward the goal of deconvoluting the impact of integrin-based interactions on associated cell behavior.

In terms of the osteoinductivity of select ECM components, the results showed that both FG and LN enhanced the osteogenic response of encapsulated MSC cells. In addition, the integrin-based interactions supported by these ECM components indicated that integrin α_2 and α_6 appeared to play an important role in MSC osteogenesis.

Regarding Scl2 protein studies, Scl2-1, Scl2-2, and Scl2-3 were functionalized with photocrosslinking sites to enable incorporation into a 3D hydrogel matrix. characterization studies confirmed that the functionalization of the Scl2 proteins did not

disrupt triple helix conformation, integrin binding, or cell adhesion. Also, initial cell studies confirmed specific hMSC adhesion to Scl2 proteins and appropriate activation of different MAP kinase pathways.

Finally, Scl2 proteins were conjugated into PEGDA hydrogels and their effect on hMSC osteogenesis was evaluated. The results indicated that both PEG-Scl2-2 and PEG-Scl2-3 were osteoinductive, but in different ways. Therefore, to gain insight into the origins of the observed osteogenic responses, the influence of p38 pathway in osteogenesis of hMSC was investigated in order to establish its potential causative relationship with Scl2 proteins. The results of the p38 inhibition studies suggested p38 pathway may regulate osteogenesis in hMSCs. Further research is needed for investigation of detailed mechanism of osteogenesis regulation.

DEDICATION

To my parents Lucia and Carlos Julio who have supported and encouraged me during all my life.

Thanks for your unconditional love that motivates me to keep walking, dreaming and living. You are my life!

ACKNOWLEDEMENTS

I would like to thank to my advisor, Dr. Mariah Hahn, for her guidance, support, and patience throughout the course of my research. I would also like to thank my committee members, Dr. Mike McShane, Dr. Zhilei Chen and Dr. Arul Jayaraman, for their support. Also, I want to extend my gratitude to Dr. Melissa Grunlan for participating in my defense committee.

Thanks also to all my group members and friends for having made my time during all these years a great experience. Thanks to my parents for their encouragement, patience and love. I could not have succeeded in this goal without the assistance and support from each of you.

TABLE OF CONTENTS

CHAPTER Page

CHAPTER Page

LIST OF FIGURES

LIST OF TABLES

CHAPTER I

INTRODUCTION

1.1. PROBLEM STATEMENT

Tissue engineering combines cells, soluble stimuli and/or a matrix (biomaterial scaffold) to guide regeneration. This paradigm has proven to be powerful and has transformed our understanding of the cell and its interactions with its environment. The extracellular matrix (ECM), long considered a passive structural component of tissues, is now understood to be a rich source of biochemical and biophysical cues which direct cell behavior. Indeed, a seemingly bewildering array of matrix-mediated stimuli are now recognized to impact cell responses, including matrix-induced organization and rigidity of the actin cytoskeleton, the identity and concentration of extracellular biochemical cues, and the nanoscale clustering of bioactive ligands. In face of this array of complex and often interdependent signals, it is difficult to rationally design biomaterials to elicit desired cell behavior.

The proposed research activities focused on developing a platform to enable the exploration of the impact of various matrix-mediated stimuli on mesenchymal stem cell (MSC) signaling and osteogenic lineage progression. A unique biosynthetic hydrogel, based on the crosslink of diacrylate-derivatized poly(ethylene glycol) (PEGDA) with collagen-mimetic proteins (Scl2s) was employed. Collagen-mimetic protein (Scl2.28) is a recently discovered protein which contains the GXY repeats and triple helical structure

characteristic of native collagen, but lacks collagen's array of cell adhesion, cytokine binding, and enzyme cleavage sites. Thus, Scl2 provided a "blank-slate" into which desired collagen-based, cell adhesion sequences can be programmed by site-directed mutagenesis while maintaining the triple helical context natively associated with these motifs. In evaluating cell signaling, the focal adhesion kinase (FAK) and mitogen activated protein kinase (MAPK) pathways were explored due to their known roles in regulating cell responses to integrin-mediated stimuli. The research objectives of this work were to:

- Investigate the effects of several ECM proteins associated with bone morphogenesis or bone fracture healing on MSC osteogenic differentiation.
- Functionalize collagen-mimetic proteins and validate a 3D hydrogel system incorporating these proteins.
- Confirm integrin-adhesion specificity of Scl2 proteins as well as appropriate activation of cell signaling.
- Investigate the effect of collagen-mimetic proteins in human mesenchymal stem cell osteogenesis.
- Conduct preliminary studies in order to elucidate the causative mechanisms underlying MSC osteogenic response to integrin-mediated bioactivity by inhibiting the p38 MAP kinase signaling pathway.

1.2. BACKGROUND

Tissue engineering holds great promise for the treatment of millions of people worldwide suffering from organ damage or failure [1-3]. However, several obstacles currently hinder the rapid progress of this field. Two of the major limitations involve: (1) the issue of cell source [2] and (2) the difficulties associated with biomaterial design due in part to the complexity of cell-matrix interactions. Until recently, most tissue engineering research focused on building new tissues using adult somatic cells. However, adult cells tend to display low rates of matrix production and many differentiated adult cells have limited proliferative and functional regenerative capacities [2]. In addition, most organs contain a range of cell types organized into complex interconnecting structures. Thus, organ repair generally requires that multiple different adult cell types be isolated and recombined into organized, functional units, further complicating regeneration.

Recent advances in adult MSC research have shown these cells to be a promising patient-derived cell source that may address many of the limitations of differentiated adult cells [3, 4]. Not only are they capable of extensive proliferation, but they have the capacity to differentiate into a range of cell types [3, 5]. There are currently two general approaches to harnessing the multipotent character of MSCs for tissue regeneration. In one approach, MSCs are first separately differentiated into each of the desired cell types, after which the differentiated cells are organized and combined into a functional structure [3]. The second major approach generally involves placing MSCs within a 3D

biomaterial context and then providing specific spatial and temporal cues to drive the MSCs to differentiate, interconnect, and organize into a functional organ [3, 6]. In the former approach, the tissue engineer has greater control over the differentiated cell populations but generally must fabricate their structural organization, which constitutes a major challenge due to the complex arrangement of elements underlying cell extracellular matrix functionality.

However, a major limitation to the use of MSCs in tissue regeneration is the conflicting literature base regarding matrix-mediated stimuli that drive specific lineage progression. Despite a number of advances, understanding of MSC behavior is not yet sufficient to enable the rational selection of stimuli to elicit desired cell responses [7, 8]. Indeed, the literature contains a number of examples of the same apparent stimuli being applied to MSCs with markedly different outcomes [9-12]. For instance, a recent study found that MSCs cultured in alginate gels in the presence of TGF-β and dexamethasone displayed decreased chondrogenic potential with increasing levels of integrin-adhesion peptide RGD [12]. In contrast, a separate study reported that MSCs cultured in PEG-based hydrogels, also in the presence of TGF-β and dexamethasone, showed increased chondrogenic potential with increasing RGD concentration [11]. Since neither PEG [13] nor alginate[14] interact significantly with cells and since neither study characterized gel modulus, the source of the discrepancy between the two studies is, as is often the case, unclear. Such inconsistencies limit our ability to rationally guide MSC lineage progression.

A potential source of the inconsistency in literature may arise from the complexity of the native biopolymers often used in the studies [15-18]. Aside from issues associated with variations in biopolymer purity, biopolymers, such as collagen, are complex molecules containing an array of signals which guide cell behavior [19-21]. These signals include cell adhesion sites, enzyme cleavage sequences, as well as growth factor and cytokine binding regions [20, 21]. These intricate biological interactions make it difficult to deconvolute the impact of individual biopolymer motifs on associated cellular signaling.

To address this challenge, many researchers have employed integrin-blocking peptides or antibodies to reduce the ability of cell to interact with specific biopolymer sequences [11, 12]. These studies have yielded significant insight into the influence of various integrins and specific ECM sequence motifs on cell behavior. However, they are limited in that they do not account for the fact that the cells continue to receive remaining ECM signals; in other words, they do not account for the context in which the loss of signaling is occurring. This observation is significant because cells do not generally respond additively to signals they receive from the surroundings. Thus, recognition and, if possible, control over the contextual presentation of a given stimulus is critical to the development of cause-effect relationships.

To overcome the obstacles associated with biopolymer signaling context, many researchers have explored the use of bioactive peptides, such as RGD, in place of full biopolymers [22-24]. This approach has greatly advanced our understanding of cell responses to matrix-mediated biochemical cues. Unfortunately, this approach removes a

critical aspect of the 3D context provided by the parent biomolecule, namely the regional protein folding. It also has limited capacity for the re-introduction of additional biopolymer signals for studies of synergistic interactions among biopolymer signaling motifs.

An underlying premise of this research proposal is that providing MSCs with the spatial and temporal signals needed to direct functional organ regeneration requires a deeper understanding of MSC responses to external stimuli than currently exists. Therefore, we propose to investigate the effects of native ECM constituents as well as ECM mimics on MSC osteogenic differentiation in 3D contexts. In order to achieve this, poly(ethylene glycol) diacrylate (PEGDA) hydrogel networks will be used as the material platform due to the broad tunability of their mechanical properties, their previous use in bone regeneration applications as well as their biological "blank slate" nature. The latter feature of PEGDA hydrogels allows initial cell interactions with the matrix to be isolated to the proteins specifically tethered to the scaffold. To investigate potential causative signaling mechanisms regulating MSC differentiation in response to specific matrix-mediated stimuli, we conducted preliminary studies in which we inhibited p38 in the FAK/MAP kinase signaling cascade and characterized associated changes in cell response. Understanding the dominant signaling underlying particular cell behavior will allow biomaterials to be specifically designed to modulate these signaling cascades. We hypothesize that there is a subset of external stimuli which dominate cell responses and that the discovery of these stimuli, and the key signaling

mechanisms through which they actuate cell behavior, will allow us to predict, and therefore dictate, cell behavior.

The understanding gained from this research will contribute to the rational development of biomaterial matrices designed to "program" or evoke desired MSC lineage commitment via modulation of specific input stimuli and/or signaling elements. This would represent a significant advance in biomaterials design for complex organ regeneration.

CHAPTER II

INFLUENCE OF SELECT EXTRACELLULAR MATRIX PROTEINS ON MESENCHYMAL STEM CELL OSTEOGENIC COMMITMENT IN THREE-DIMENSIONAL CONTEXTS*

2.1. OVERVIEW

Mesenchymal stem cells are being increasingly recognized as a viable cell source for bone regeneration applications due to their ability to be expanded in vitro and to differentiate into a number of cell lineages. Thus, the ability to promote MSC osteogenic differentiation via the manipulation of scaffold material properties would be beneficial. The current work examines the influence of select extracellular matrix (ECM) proteins on MSC osteogenesis toward the goal of developing scaffolds with osteoinductive properties. Fibrinogen (FG), fibronectin (FN) and laminin-1 (LN) were chosen for evaluation due to their known roles in bone morphogenesis or bone fracture healing.

---

*Reprinted with permission from "Influence of select extracellular matrix proteins on mesenchymal stem cell osteogenic commitment in three-dimensional contexts" by Silvia Becerra-Bayona, Viviana Guiza-Arguello, Xin Qu, Dany J. Munoz-Pinto, Mariah S. Hahn, 2012. *Acta Biomaterialia*, 8, 4397-4404, Copyright [2012] by Acta Materialia Inc. Published by Elsevier Ltd.

These proteins were conjugated into poly(ethylene glycol) diacrylate (PEGDA) hydrogels and their effects on encapsulated 10T½ MSCs were evaluated. Specifically, following 1 week of culture, mid-term markers of various MSC lineages were examined in order to assess the strength and specificity of the observed osteogenic responses. PEG–LN gels demonstrated increased levels of the osteogenic transcription factor osterix relative to day 0 levels. In addition, PEG–FG and PEG–LN gels were associated with increased deposition of bone ECM protein osteocalcin relative to PEG–FN gels and day 0. Importantly, the osteogenic response associated with FG and LN appeared to be specific in that markers for chondrocytic, smooth muscle cell and adipocytic lineages were not similarly elevated relative to day 0 in these gels. To gain insight into the integrin dynamics underlying the observed differentiation results, initial integrin adhesion and temporal alterations in cell integrin profiles were evaluated. The associated results suggest that α_2 and α_6 integrin subunits may play key roles in integrin-mediated osteogenesis.

2.2. INTRODUCTION

Mesenchymal stem cells are being increasingly recognized as a viable cell source for bone regeneration applications due to their ability to be expanded in vitro and to differentiate into a number of cell lineages. However, MSC differentiation is known to be influenced by a range of environmental stimuli. Thus, MSC-based bone regeneration

strategies would benefit from the identification of scaffold material properties which promote osteoblast lineage progression.

A number of two-dimensional (2-D) studies have demonstrated MSC osteogenic differentiation to be tightly regulated by cellular interactions with the surrounding extracellular matrix (ECM) [16, 18, 24-34]. However, comparatively little is known regarding the effects of various ECM components in regulating MSC osteogenesis in three-dimensional (3-D) scaffold environments [17, 35, 36]. This is significant since recent studies suggest that effects observed in two dimensions may not be indicative of the effects of the same scaffold variables in more biomimetic 3-D culture systems [37-39]. Therefore, the current work focuses on elucidating the influence of select ECM constituents on MSC osteogenic differentiation in 3-D contexts.

Towards this goal, we incorporated specific ECM molecules into hydrogel scaffolds designed to have moduli within the ‘‘osteogenic’’ range identified in the 3-D human and mouse MSC studies of Huebsch et al. [40]. In selecting molecules for examination, we chose to focus on several ECM proteins associated with bone morphogenesis (fibronectin [41] and laminin-1 [42, 43]) and/or bone fracture healing (fibrinogen [44]). These proteins were then conjugated into poly(ethylene glycol) diacrylate (PEGDA) hydrogel networks. PEGDA hydrogels were selected as the base scaffold due to the broad tunability of their mechanical properties and their previous use in bone regeneration applications [45-48]. In addition, pure PEGDA hydrogels function as biological ‘‘blank slates’’ in that they do not significantly adsorb cell adhesive serum proteins and therefore do not intrinsically promote cell adhesion [13]. Thus, cell

interactions with PEGDA gels are initially isolated to the proteins specifically tethered to the scaffold as well as the interactions supported by these proteins (e.g. growth factor binding).

In the present study, 10T½ MSCs were encapsulated within PEGDA hydrogels containing defined amounts of fibronectin (FN), fibrinogen (FG) or laminin-1 (LN). The levels of various markers of osteoblast, chondrocytic, smooth muscle cell and adipocytic fates were then monitored with time in culture toward assessing the strength and specificity of observed osteogenic responses. Due to the critical role of integrins in transducing the signals provided by glycoproteins such as FN, FG and LN [49], initial integrin adhesion profiles as well as temporal alterations in cell integrin profiles were also characterized.

2.3. MATERIAL AND METHODS

2.3.1. Polymer synthesis and characterization

2.3.1.1. PEG-diacrylate synthesis

PEGDA was prepared as previously described [50] by combining 0.1 mmol ml^{-1} dry PEG (10 kDa, Fluka), 0.4 mmol ml^{-1} acryloyl chloride and 0.2 mmol ml^{-1} triethylamine in anhydrous dichloromethane and stirring under argon overnight. The resulting solution was washed with 2 M K_2CO_3 and separated into aqueous and dichloromethane phases to remove HCl. The organic phase was subsequently dried with

anhydrous $MgSO_4$, and PEGDA was precipitated in diethyl ether, filtered and dried under vacuum. Acrylation of the PEG end hydroxyl groups was characterized by proton nuclear magnetic resonance (^{1}H-NMR) to be ~95%.

2.3.1.2. Synthesis of acrylate-derivatized proteins

Proteins FN (human plasma, BD Biosciences), FG (human plasma, Sigma Aldrich) and LN (mouse, BD Biosciences) were lightly functionalized in their folded state by reaction with acryloyl-PEG-N-hydroxysuccinimide (ACRL-PEG-NHS, 3.4 kDa, Nektar) at a 1:2 M ratio at pH 8.5 [50]. The resulting acrylate-derivatized products were purified by dialysis against a 100 kDa membrane, lyophilized and stored at -20 °C until use. ACRL–PEG conjugation to the target proteins was confirmed using ^{1}H-NMR. A representative ^{1}HNMR spectrum for acrylate-derivatized FG is shown in Figure 1.

To confirm the ability of the modified proteins to be incorporated within PEGDA hydrogel networks, hydrogel precursor solutions were prepared with 0.5 mg ml^{-1} protein and 100 mg ml^{-1} PEGDA (10kDa). Following the addition of 10 µl ml^{-1} of a 300 mg ml^{-1} solution of UV photoinitiator 2,2-dimethoxy-2-phenyl-acetophenone (DMAP) in N-vinylpyrrolidone (NVP), gels were polymerized by 4 min exposure to long-wave UV light (Spectroline, ~6 mWcm^{-2}, 365 nm). The gels were then immersed in PBS overnight, after which they were transferred to a 0.12 M NaOH solution to hydrolyze the PEGDA crosslinks and release encapsulated protein. The levels of protein released were compared to the levels in the precursor solution using the CBQCA assay (Invitrogen), and the average level of protein incorporation was found to be consistent across protein

types at 86.7 ± 7.2%. In addition, to assess the ability of cells to interact with proteins incorporated into the hydrogel network, 10T½ cells were seeded onto the surface of each gel formulation. Cell adhesion and spreading were confirmed for each PEG–ECM gel type (Figure 2).

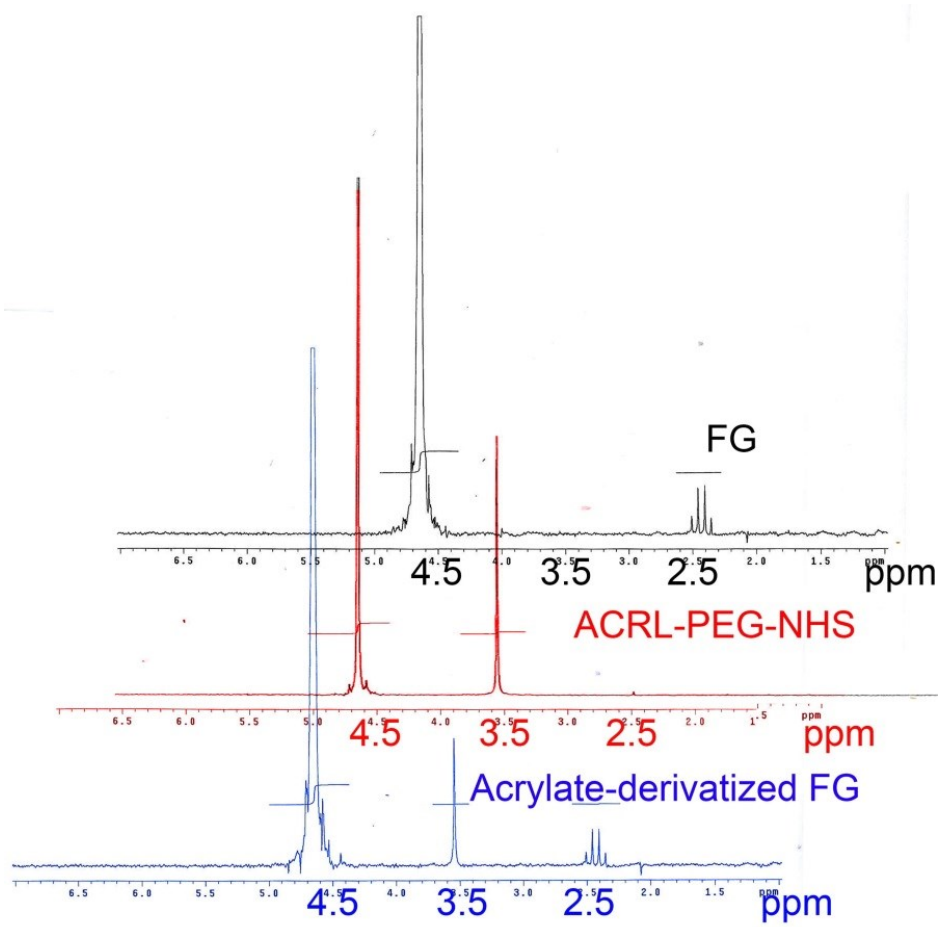

Figure 1. ^{1}H-NMR spectrum of functionalized FG confirming conjugation of FG with ACRL-PEG-NHS.

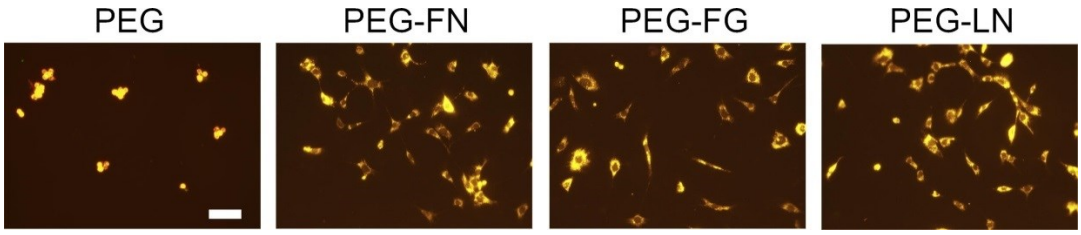

Figure 2. PEG-functionalized protein hydrogels were fabricated by combining 100 mg ml^{-1} PEGDA (10kDa) with photoinitiator (DMAP in NVP) and 0.5 mg ml^{-1} functionalized protein of FG, FN and LN. PEGDA hydrogel served as a negative control. 10T½ cells were stained with 5μM CellTracker Orange CMTMR (5-(and-6)-(((4-chloromethyl)benzoyl)amino)Tetramethylrhodamine) and seeded at a density of 6,000 cells cm^{-2} on the surface of the hydrogels. Attached cells were allowed to spread for 3 hours and imaged by fluorescence microscopy. The scale bar applies to all images and equals 100 μm.

2.3.2. Cell culture, initial characterization and encapsulation

Cryopreserved 10T½ mouse MSCs (American Type Culture Collection; ATCC) at passage 2 were thawed and expanded in monolayer culture per ATCC protocols. Prior to encapsulation, cells were maintained at 37 °C and 5% CO_2 in Dulbecco's modified Eagle's medium (DMEM, Hyclone) supplemented with 10% heat-inactivated fetal bovine serum (FBS, Hyclone). Cells at passage 4–6 were termed ''day 0'' and were harvested and allocated for either protein extraction, integrin blocking studies or hydrogel encapsulation.

2.3.2.1. Protein extraction

Proteins were extracted from day 0 10T½ cells by the addition of Trizol (Invitrogen) per manufacture's protocols. The resulting solutions were centrifuged, and each supernatant was mixed with chloroform (Sigma), vigorously shaken for 15 s and centrifuged. The lower protein-rich phenol–chloroform phase of each sample (n = 4) was

mixed with ethanol to precipitate residual DNA. The resulting phenol–ethanol phase was transferred to a 3.4 kDa SnakeSkin dialysis membrane (Pierce). The solution was dialyzed for ~60 h at 4 °C against an aqueous solution of 0.1% sodium dodecyl sulfate (SDS), with buffer exchange every 18 h. By the end of the third 18 h dialysis period, the samples had partitioned into three phases: (1) a supernatant, (2) a globular mass and (3) a colorless, viscous liquid. The globular mass, containing the bulk of sample proteins [51], was resuspended in PBS containing 0.5% SDS and 1% Triton X-100. The isolated sample proteins were subsequently used in quantitative ELISA assays.

2.3.2.2. Integrin blocking studies

Standard adhesion blocking studies were performed to determine the integrin alpha subunits through which the 10T½ cells initially interacted with the PEG–ECM gels. In brief, functionalized FG, FN and LN were resuspended in PBS at 100 μg ml^{-1}, after which they were applied to a 96-well, high protein binding plate at 100 μl per well for 12 h at 4 °C. The wells were then blocked with 3% bovine serum albumin (BSA). Harvested 10T½ cells were washed with PBS and resuspended in serum-free DMEM supplemented with 1 mM Ca^{2+} and 1 mM Mg^{2+}. Cells were then exposed to 50 μg ml^{-1} of α_1, α_2, α_5, α_v or α_6 integrin antibodies or to 50 μg ml^{-1} of appropriate negative control antibodies for 30 min at room temperature. Further details regarding antibodies are given in Table 1. The cell suspensions were subsequently applied to the coated wells at 10,000 cells cm^{-2}. Following 30 min incubation at 37 °C and 5% CO_2, wells were rinsed three times with PBS. Adherent cells were then lysed, and the number of adherent cells in

each well was measured using a lactate dehydrogenase assay kit (Roche). Percentage inhibition was evaluated relative to the corresponding negative control. At least five sample wells per antibody were analyzed for each protein type.

Table 1. Antibodies employed in adhesion blocking, immunostaining, and ELISA assays.

Antibody	Clone	Supplier	Adhesion Blocking	Immunostaining	ELISA
Integrin α_1	Ha31/8	BD	√		
Integrin α_2	HMα2	BD	√		
Integrin α5	HMα5-1	BD	√		
Integrin αv	RMV-7	BD	√		
Integrin α6	NKI-GoH3	Chemicon	√		
Osterix	M-15	SCBT			√
Osteocalcin	M-15	SCBT		√	√
Osteopontin	AKm2A1	SCBT		√	
PPARγ	H-100	SCBT		√	
A-FABP	C-15	SCBT			√
Sox 9	C-20	SCBT			√
Collagen II	N-19	SCBT			√
Myocardin	H-300	SCBT		√	
SM22α	P-15	SCBT			√
Integrin α_1	F-19	SCBT			√
Integrin α_2	N-19	SCBT			√
Integrin α5	P-19	S CBT			√
Integrin αv	N-19	SCBT			√
Integrin α_6	N-19	SCBT			√
B-actin	13E5	CS			√

[†]Abbreviations: BD – BD Pharminogen; SCBT – Santa Cruz Biotechnology; CS: Cell Signaling

2.3.2.3. Cell encapsulation and culture

Hydrogels were fabricated by preparing: (1) a 20 wt.% PEGDA solution in HEPES-buffered saline (HBS) and (2) separate solutions of 1 mg ml^{-1} acrylate-derivatized FN, FG or LN in HBS. A 300 mg ml^{-1} solution of DMAP in NVP was added at 2% (v/v) to the PEGDA mixture. The PEGDA and protein solutions were then separately sterilized by filtration, after which each protein solution was mixed with an equal volume of the 20 wt.% PEGDA solution. Harvested 10T½ cells were resuspended in the resulting precursor solutions at 1 x 10^6 cells ml^{-1}. The cell suspensions were then pipetted into molds composed of two glass plates separated by 0.5 mm polycarbonate spacers and polymerized by 4 min exposure to long-wave UV light (Spectroline, ~6mWcm^{-2}, 365 nm). A set of the resulting hydrogels were harvested for ‘‘day 0’’ analyses as described in the following section. The remaining hydrogel slabs were transferred to Omnitrays (Nunc) fitted with four sterile polycarbonate bars to simultaneously prevent gel flotation and prevent gel contact with the tray bottom. Hydrogels were immersed in DMEM supplemented with 10% FBS, 100 U ml^{-1} penicillin and 100 mg l^{-1} streptomycin. Gels were maintained at 37 °C and 5% CO_2, with media changes every 2 days.

2.3.3. Day 0 hydrogel characterization

2.3.3.1. Average mesh size

PEGDA hydrogel mesh structure cannot be visualized using standard techniques

such as scanning electron microscopy. In the present study, average hydrogel mesh size was therefore characterized via a series of dextran diffusion experiments based on an adaptation of the methodology of Watkins and Anseth [52]. In brief, samples were collected from the freshly prepared PEG– ECM hydrogels and allowed to swell overnight at 37 °C in PBS containing 0.05% azide (PBS-azide). Eight-millimeter-diameter discs were then harvested from each gel formulation, and solutions containing 0.05 mg ml^{-1} fluorescently labeled dextran (10 kDa, Invitrogen) in PBS-azide were added at 1 ml per hydrogel disc. Dextran solutions were allowed to diffuse into the hydrogels for 24 h at 37 °C. Each gel disc was then gently blotted and transferred to 1 ml fresh PBS-azide. Dextran that had penetrated into the hydrogels was then permitted to diffuse out into the surrounding solution at 37 °C. After 24 h, the fluorescence of the PBS-azide solution surrounding each disc was measured at ex/em 488/532. Dextran standard curves were used to convert each fluorescence signal to a concentration. For each hydrogel, the measured dextran concentration was divided by gel weight [53]. The resulting value served as a quantitative indicator of hydrogel permissivity.

2.3.3.2. Hydrogel mechanical properties

Samples were collected from each freshly prepared hydrogel formulation and allowed to swell overnight in PBS-azide. Eight mm discs (n = 4 per formulation) were then cored from each gel sample and mechanically tested under unconfined compression using a DMA 800 (TA Instruments). Following application of a 0.01 N preload, each disc was subjected to compression at a rate of 0.1 mm min^{-1}. The compressive modulus

of each hydrogel was extracted from the resulting stress–strain data over a 10–25% strain range.

2.3.3.3. Cell density

Samples (n = 4) were collected from each freshly prepared hydrogel formulation following 24 h immersion in culture media. Hydrogel samples were digested for 72 h at 37 °C in 1 ml of 0.12 M NaOH per 0.2 g hydrogel wet weight [54, 55]. Aliquots of the hydrolyzed samples were neutralized, and their DNA content determined using the Invitrogen PicoGreen assay [56]. DNA measures were translated to cell number using a conversion factor of 6.6 pg DNA per cell [57]. Calf thymus DNA (Sigma) subjected to the same association with PEGDA and to the same digestion conditions as the samples served as a standard.

2.3.4. Endpoint analyses

At day 7 of culture, samples were harvested from each hydrogel formulation for mechanical, mesh size, DNA, ELISA and histological analyses. Samples collected for histological analyses (n = 4–8 per formulation) were fixed in 10% formalin for 30 min and embedded in Tissue-Tek freezing medium. Samples harvested for mechanical (n = 4 per formulation), mesh size (n = 4 per formulation) and DNA (n = 4 per formulation) assessments were evaluated according to the same protocols as the day 0 specimens. Similarly, samples harvested for ELISA analyses (n = 6–9 per formulation) were

homogenized in Trizol using a Bead-Beater homogenizer (Biospec), after which sample proteins were isolated as described for day 0 specimens.

2.3.4.1. ELISA analyses

Proteins extracted from the day 0 cells and the day 7 constructs were evaluated for various lineage markers and integrin alpha subunits via competitive ELISAs. Further details regarding the antibodies employed are given in Table 1. For each antibody examined, high binding EIA 96-well plates (Costar) were coated overnight at 4 °C with appropriate competitive peptide. The concentration of applied competitive peptide was 200 ng per well, except for b-actin (50 ng per well). The coated wells were then blocked with BSA and rinsed with PBS. Aliquots of each sample were incubated with primary antibody for 1 h, after which the sample–antibody mixtures were applied to coated wells for 1 h. Standard curves were similarly prepared by incubating primary antibody with varying levels of competitive peptide for 1 h, followed by solution application to coated wells. For both samples and standards, primary antibody which had bound to the coated wells was detected using an appropriate HRP-conjugated secondary antibody (Jackson Immunoresearch), followed by the application of 2,20-azino-bis(3-ethylbenzthiazoline-6-sulphonic acid) (Sigma) and monitoring of absorbance at 410 nm. Each target protein was analyzed in duplicate for each sample (n = 6–9 per day 7 gel type; n = 4 for day 0) and normalized to the housekeeping protein b-actin.

2.3.4.2. Histological analyses

Bone ECM deposition (osteopontin and osteocalcin) was further analyzed using standard immunohistochemical techniques. In brief, 35 μm sections were cut from each embedded histological sample (n = 4–8 per formulation) using a cryomicrotome. Rehydrated sections were blocked for peroxidase for 30 min followed by 30 min exposure to Terminator (Biocare Medical). Primary antibodies for osteopontin and osteocalcin were diluted in PBS containing 3% BSA and then applied to the sections for 1 h. Bound primary antibody was detected using HRP-conjugated secondary antibody (Jackson Immunoresearch) followed by the application of chromogens AEC (LabVision) or DAB (Biocare Medical). For the detection of intracellular differentiation markers (myocardin and PPARγ), rehydrated sections were permeabilized (10 mM HEPES, pH 6.8, 100 mM NaCl, 3 mM $MgCl_2$, 300 mM sucrose, 0.5% Triton X-100) for 30 min prior to Terminator application. Further details regarding the antibodies employed are given in Table 1.

Stained sections were imaged using a Zeiss Axiovert microscope, and cell counts were carried out to semi-quantitatively evaluate immunostaining results for intracellular markers myocardin and PPARγ. These counting assessments were conducted according to established methods [45, 58, 59] on sections from each sample (n = 4–8 per gel formulation). For each cell, *i*, in a given section, a single observer blinded to outcome assigned a staining intensity, d_i, on a scale of 0–3 (0 = ‘‘no staining’’ and 3 = ‘‘highest intensity among all formulations for that antibody’’). The cumulative staining intensity, *d*, for a given antibody in a particular section was calculated using the following

equation: $d=(\sum d_i)/(\text{total cell number})$. In addition, since deposited ECM remained localized around the parent cells in each hydrogel formulation, as is characteristic for PEGDA gels [60], the relative levels of osteocalcin and osteopontin among hydrogel formulations were also evaluated by cell counts per the above procedure. Osteocalcin counts were used to internally validate the counting approach by direct comparison with corresponding quantitative ELISA data (Figure 3). The degree of correlation between the two assessment techniques was 98.9% by Pearson's correlation coefficient method.

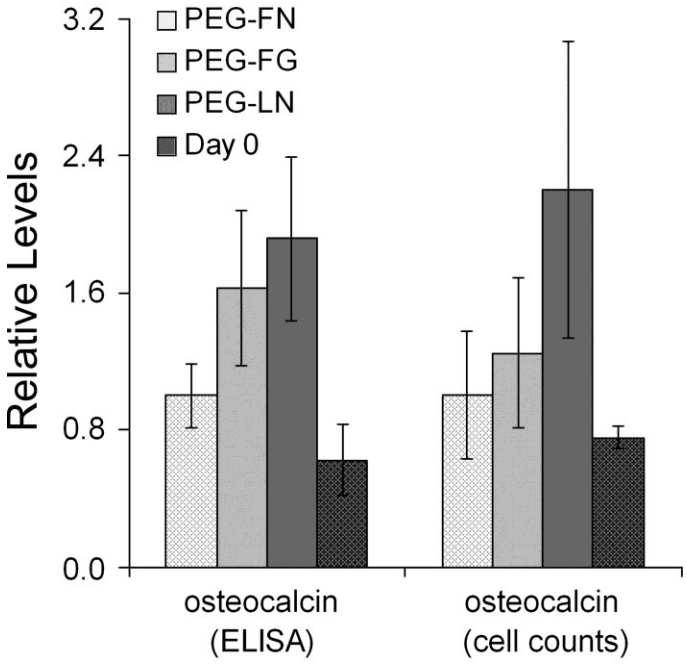

Figure 3. Comparison of osteocalcin measures by ELISA and cell counting assessments. For ELISA assays, 6-9 samples per formulation were analyzed. For cell counts, sections from 4 separate discs of each formulation were evaluated. The degree of correlation between the two assessment techniques was 98.5% by Pearson's correlation coefficient method.

2.3.5. Statistical analyses

Data are reported as mean ± standard deviation. Comparison of sample means was performed by ANOVA followed by Tukey's post hoc test (SPSS software), $p < 0.05$.

2.4. RESULTS

2.4.1. Hydrogel material properties and cell density

A range of scaffold properties, including modulus, permeability and degradation rate, have been found to impact MSC lineage progression. Therefore, in order to attribute differences in 10T½ cell behavior across hydrogel formulations specifically to initial differences in gel protein composition, it was important that the remaining hydrogel material properties could be considered consistent across gels. Hydrogels formed from pure PEGDA degrade slowly (over a period of 1–2 years) and resist cell-mediated gel contraction, ensuring consistent bulk gel properties over a broad time range [55, 56, 61-63]. In the present study, a 200:1 weight ratio of PEGDA to protein was therefore selected to ensure that the network properties of the resulting gels would be dominated by PEGDA. To confirm this, the modulus, mesh size, thickness and mass of the PEG–ECM hydrogels were characterized both at day 0 and at day 7.

As shown in Table 2, the initial elastic moduli of the PEG–FG, PEG–FN and PEG–LN gels were similar at ~33 kPa. Importantly, each of these initial moduli were within the osteogenic range identified by the 3-D studies of Huebsch et al. [40]. To assess degradation and cell-mediated contraction, hydrogel modulus and thickness were evaluated across time in culture.

Comparison of initial and endpoint mechanical data indicated that, although the modulus decreased by ~15% over the 7 day culture time for each gel formulation, hydrogel modulus remained consistent across formulations (Table 2). Similarly, average mesh size was consistent across hydrogels at both day 0 and day 7 (Table 2). The initial and endpoint thickness data for 8 mm gel discs indicated a negligible alteration in gel volume with time. In addition, net cell proliferation and loss were examined for each PEG–ECM hydrogel over the 7 day culture period. The cell density in each PEG–ECM hydrogel following 7 days of culture was between 78 and 86% of the initial seeding density (Table 3), consistent with PEG hydrogel literature [26, 31, 35, 47, 64-66]. Combined, the above data indicate that: (1) each hydrogel formulation maintained an osteogenic modulus throughout the study [40] and (2) differences in cell responses among formulations can be attributed to differences in the initial proteins tethered to the gel network, their interactions with other molecules and subsequent neo-matrix deposition.

Table 2. Comparison of the average modulus and mesh size of 8 mm discs of each PEG–ECM hydrogel formulation with time in culture.[a]

Gel type	Modulus (kPa)		Mesh size (μg dextran/g-gel)	
	Day 0	Day 7	Day 0	Day 7
PEG-FN	33.3 ± 0.7	29.2± 0.8*	11.8 ± 0.3	12.4± 0.3
PEG-FG	33.9 ± 1.9	29.9± 1.5*	11.4 ± 0.3	11.7± 0.2
PEG-LN	33.7 ± 2.0	28.7± 1.2*	11.6 ± 0.3	11.8± 0.6

[a] Property results represent an average of n = 4 samples for each PEG-ECM formulation
* Significantly different from the corresponding day 0 value, $p < 0.05$.

Table 3. Comparison of the average thickness, mass, and cell density in discs of each PEG–ECM hydrogel formulation with time in culture.[a]

Gel type	Thickness (mm)		Mass of 8mm discs (mg)		Cell density ($x10^6$)	
	Day 0	Day 7	Day 0	Day 7	Day 0	Day 7
PEG-FN	0.550 ± 0.01	0.560± 0.01	29.1 ± 0.2	29.5± 0.2	1.01± 0.06	0.88± 0.08*
PEG-FG	0.550 ± 0.01	0.560± 0.01	29.2 ± 0.2	29.4± 0.5	0.96± 0.05	0.72± 0.02*
PEG-LN	0.540 ± 0.01	0.560± 0.01	29.2 ± 0.4	29.3± 0.3	1.01± 0.06	0.82± 0.02*

[a] Results represent an average of n = 4 samples for each PEG–ECM formulation.
* Significantly different from the corresponding day 0 value, $p < 0.05$.

2.4.2. Cell differentiation

Following 7 days of culture, cell differentiation was examined by quantitative ELISA or by cell counts (as validated in figure 3). As shown in figure 4, day 7 levels of various osteogenic markers indicated significant differences relative to day 0 and/or among hydrogel formulations. Specifically, cells in PEG–LN gels expressed significantly higher levels of the osteogenic transcription factor osterix than day 0 cells ($p = 0.032$), while osterix expression in PEG–FN gels could not be distinguished from

day 0 levels. In addition, PEG–LN gels retained day 0 osteopontin expression levels, whereas osteopontin levels in day 7 PEG–FN gels had fallen to approximately half of day 0 levels ($p = 0.005$). Similarly, day 7 PEG–FN gels contained significantly lower levels of the bone ECM protein osteocalcin relative to PEG–FG ($p = 0.042$) and PEG–LN ($p = 0.002$) gels, whereas PEG–FG and PEG–LN gels contained 2.4- and 2.9-fold greater osteocalcin levels than day 0 ($p = 0.004$ and $p < 0.001$, respectively).

To assess the specificity of the osteogenic response associated with the PEG–FG and PEG–LN gels, mid-term markers of chondrogenesis, smooth muscle progression and adipogenesis were evaluated (Figure 5). Day 7 expression of smooth muscle transcription factor myocardin was similar to day 0 levels and across hydrogel formulations. In addition, day 7 levels of SM22α, a cytoskeletal protein associated with smooth muscle differentiation, could also not be distinguished among gel formulations or from day 0 levels. PPARγ expression was similar to day 0 levels across the day 7 gels, and the day 7 levels of the adipocyte intracellular protein A-FABP were statistically indistinguishable from day 0 levels and among formulations. Furthermore, day 7 expression of chondrogenic transcription factor sox9 did not vary significantly with gel formulation or relative to day 0, and day 7 levels of the cartilage-associated ECM protein collagen II could also not be distinguished among the PEG–ECM gels or relative to day 0. Representative immunostaining images for proteins evaluated by cell counts (myocardin, PPARγ, and osteopontin) are given in Figure 6.

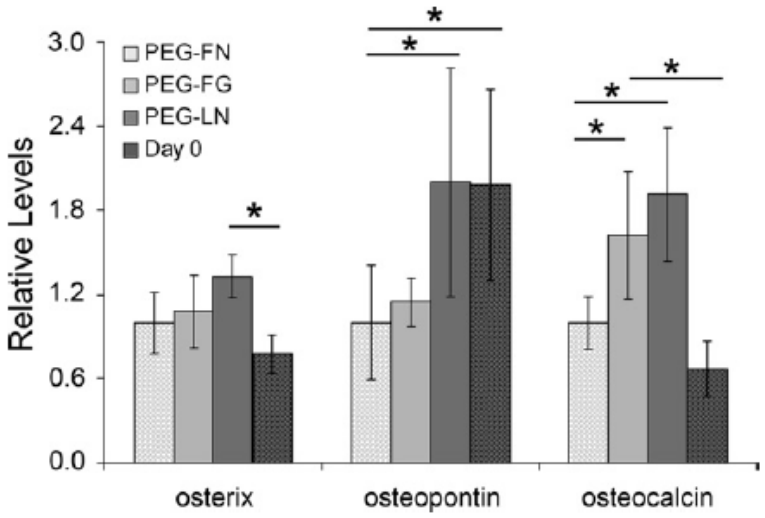

Figure 4. Expression of osteogenic markers osterix, osteopontin and osteocalcin by ELISA (osterix and osteocalcin) and cell counts (osteopontin). For ELISA assays, six samples per day 7 formulation were analyzed. The day 0 ELISA sample number was n = 4. For cell counts, sections from 4-8 separate samples of each formulation were evaluated. Validation of the cell counting assessment method is given in Figure. 3. For the purpose of comparison, ELISA and cell count measures for each protein have been normalized to the corresponding measure for PEG-FN gels.
*indicates a significant difference, $p < 0.05$.

2.4.3. Integrin expression

Integrin-associated signaling has been demonstrated to play a key role in MSC osteogenic lineage progression [18, 25, 26, 30, 31, 33]. Therefore, initial integrin adhesion and temporal alterations in cell integrin profiles were evaluated in order to gain insight into the integrin dynamics underlying the observed differentiation results.

2.4.3.1. Initial integrin adhesion

Inhibition studies were conducted to characterize the integrins through which cells initially interacted with the various PEG–ECM hydrogels. As illustrated in Table 4,

the day 0 population of 10T½ cells interacted with each PEG–ECM gel via a distinct panel of integrins. Specifically, cell adhesion to functionalized FG was inhibited by antibodies to α_v and α_5 integrin subunits, although integrin α_v appeared to be dominant. In contrast, cell binding to FN was significantly inhibited by antibodies to α_2, α_v and α_5 integrin subunits, whereas LN interacted with α_1, α_v, α_5 and α_6 integrin subunits.

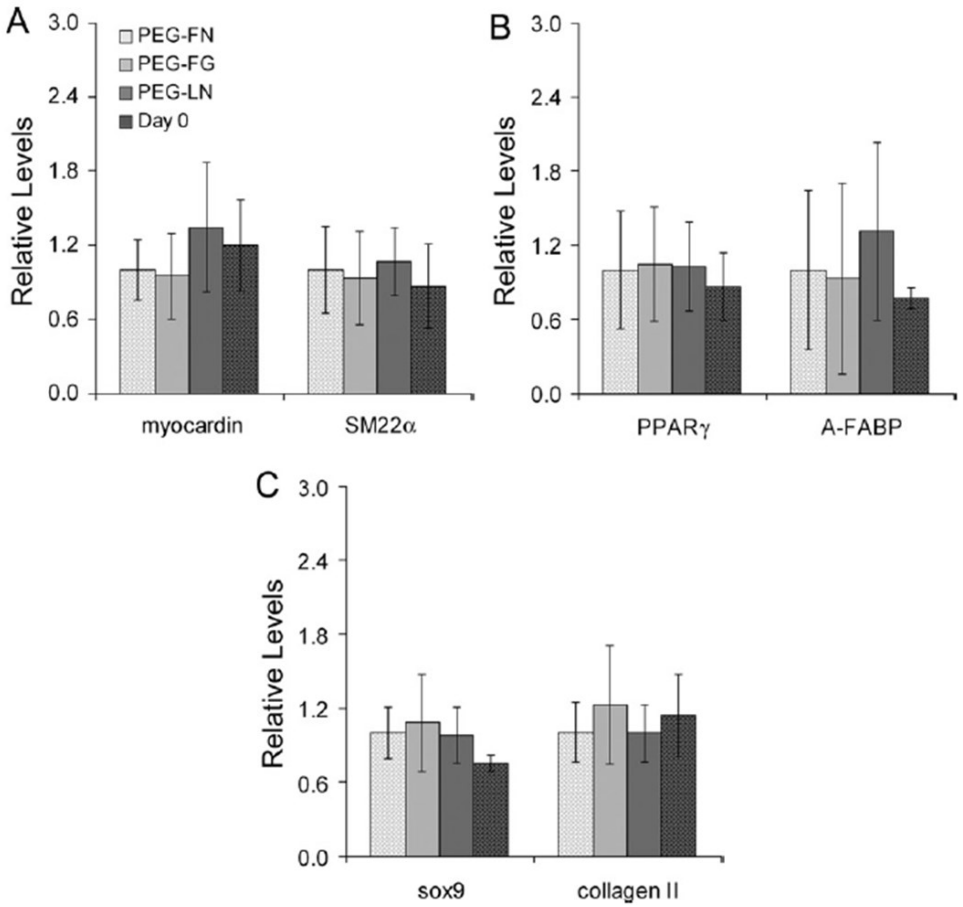

Figure 5. (A) Expression of myocardin and SM22α, as assessed by cell counting and ELISA methods, respectively. (B) Expression of PPARγ and A-FABP, as assessed by cell counting and ELISA methods, respectively. (C) Expression of sox9 and collagen II by ELISA. For ELISA assays, 6–9 samples per day 7 formulation were analyzed. The day 0 ELISA sample number was n = 4. For cell counts, sections from four separate samples of each formulation were evaluated. For the purpose of comparison, ELISA and cell count measures for each protein have been normalized to the corresponding measure for PEG–FN gels.

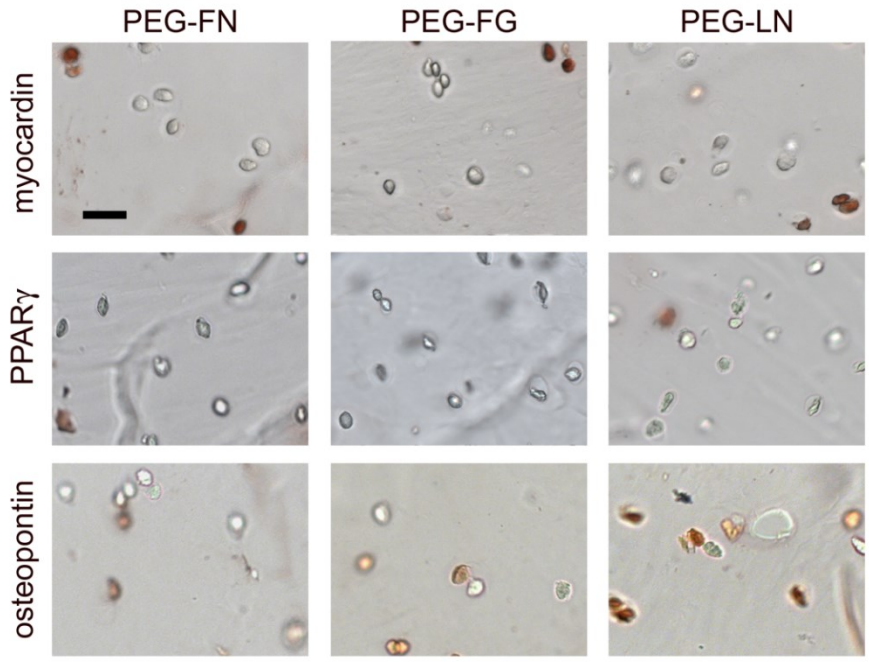

Figure 6. Representative images of day 7 immunostaining for myocardin, PPARγ and osteopontin. Positive staining is indicated by brown (PPARγ and osteopontin) or red (myocardin) coloration. Scale bar = 40 μm and applies to all images.

2.4.3.2. Endpoint integrin profiles

To investigate potential temporal alterations in cell–substrate integrin interactions, the endpoint expression of various integrins was investigated relative to day 0. Day 7 expression of integrin subunits α_1, α_v and α_5 did not significantly vary among PEG– ECM gels or relative to day 0 levels (Figure 7). However, integrin α_2 expression was ~1.6-fold higher in day 7 PEG–LN gels than at day 0 ($p = 0.034$). Similarly, integrin α_6 expression in day 7 PEG–FG hydrogels was ~2-fold higher than at day 0 ($p = 0.030$) and was significantly greater than in PEG–FN gels ($p = 0.014$). Cumulatively, the endpoint integrin profiles associated with the PEG–FG and PEG–LN gels differed from their initial integrin profiles.

Table 4. Percentage inhibition of 10T½ cell adhesion at day 0 by blocking antibodies to various integrin alpha subunits.[a]

Gel type	α_1	α_2	α_v	α_5	α_6
PEG-FN	-	31.9 ± 26.5	52.9 ± 22.8	15.2 ± 5.0	-
PEG-FG	-	-[*]	97.5 ± 8.7[*]	2.4 ± 7.7[*]	-
PEG-LN	31.7 ± 10.7[*,#]	-[*]	24.9± 9.6[#]	26.4 ± 5.9[*,#]	17.0 ± 7.8[*,#]

[a] Integrin inhibition results represent an average of n = 5–10 sample wells per antibody per ECM molecule. ''–'' indicates no inhibition detected.
[*] Significantly different from the corresponding PEG–FN gels, $p < 0.05$.
[#] Significantly different from the corresponding PEG–FG gels, $p < 0.05$.

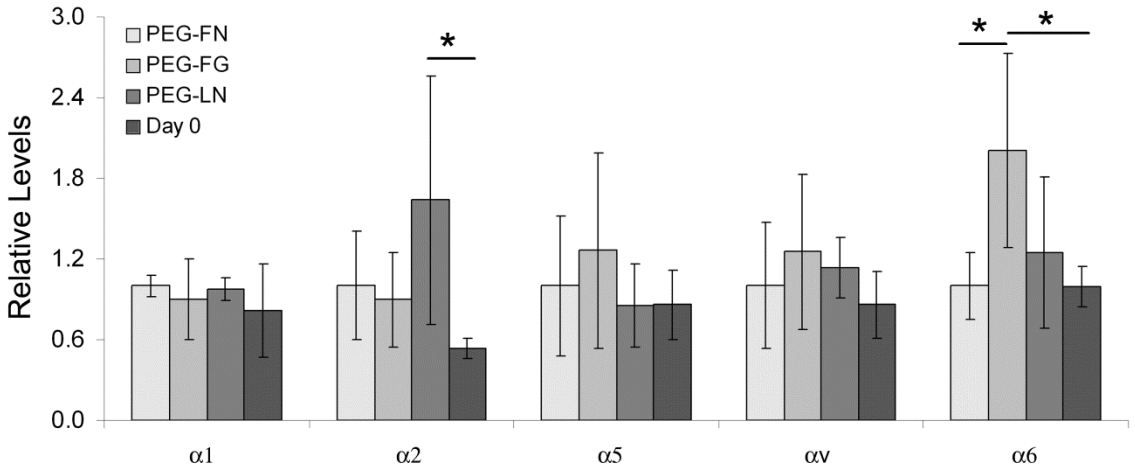

Figure 7. Day 7 and day 0 expression of various integrin alpha subunits as assessed by ELISA (n = 6–9 per day 7 formulation; n = 4 for day 0). For the purpose of comparison, ELISA measures for each protein have been normalized to the corresponding measure for PEG–FN gels.
[*]indicates a significant difference, $p < 0.05$.

2.5. DISCUSSION

The aim of the present work was to compare the osteoinductivity of select ECM components in defined 3-D environments toward the improved design of osteogenic

scaffolds. These ECM components were examined within the context of scaffolds with osteogenic moduli (~30 kPa) [40]. The associated temporal evolution in MSC lineage progression and integrin profiles were then characterized. Present data indicated that both FG and LN enhanced the osteogenic response of encapsulated 10T½ cells. Specifically, osteocalcin levels in day 7 PEG–FG and PEG–LN gels were ~2.4- and 2.9-fold greater, respectively, than day 0 levels. In addition, expression of osterix, an osteoblast-specific transcription factor required for osteogenesis, was significantly elevated in day 7 PEG–LN gels relative to day 0 levels. In contrast, the day 7 levels of markers for adipogenesis, chondrogenesis and smooth muscle lineage progression were not significantly different among formulations or relative to day 0, indicating that the osteogenic response associated with the PEG–FG and PEG–LN gels was specific.

The present results are consistent with previous 2-D studies demonstrating LN to support higher active levels of the osteogenic transcription factor Cbfα1 than FN over a 5 day culture time frame [32]. In addition, a study by Salaszynk et al. indicated that, in the absence of osteogenic media supplements, FN did not support human MSC matrix mineralization, in contrast to collagen I and vitronectin [26]. Indeed, they found little role for FN in stimulating osteogenic differentiation [27], beyond activation of alkaline phosphatase [26]. Similarly, Benoit et al. found that FN increased alkaline phosphatase production, but not osteopontin gene expression [35]. Although fibrin glue has been used extensively in bone tissue engineering [44, 67-76], literature presents conflicting reports regarding the osteoinductivity of fibrinogen. Specifically, while several studies have suggested that fibrin sealants promote osteogenesis [70, 72-74], other studies have

reported negative effects when fibrin sealants were combined with coral granules [75, 76] and poly(lactide-co-glycolic acid) scaffolds [67]. These conflicting results may arise, in part, from differences in the material properties of the various fibrin-containing scaffolds assayed. In the present study, we tightly controlled initial scaffold material properties as well as the temporal evolution of those properties in order to isolate the osteoinductive effect of FG from other matrix properties.

To gain insight into the origins of the osteogenic response associated with FG and LN, we examined the initial integrin-based interactions supported by these ECM components. Specifically, integrin blocking studies indicated that day 0 10T½ cells interacted with FG primarily through α_v integrin subunits. MSC–matrix interactions through α_v subunits have previously been correlated with osteoinductivity [12, 26]. In particular, Salaszynk et al. found that human MSCs bound to vitronectin primarily (>90% of adhesive interactions) through α_v subunits, and that vitronectin was capable of promoting osteogenic differentiation, even in the absence of added growth factors [26]. Similarly, Connelly et al. [12] and Yang et al. [48] demonstrated that the peptide RGD, which primarily supports α_v interactions, promoted expression of osteocalcin.

In contrast to FG, day 0 10T½ cells bound to FN through integrins α_2, α_v and α_v. As with integrin α_v, the α_2 subunit has been associated with osteogenic differentiation in the case of both MSCs [18, 77] and pre-osteoblasts [30]. Specifically, Shih et al. found that increased MSC osteogenesis was linked to an increase in integrin α_2 expression, and that knockdown of integrin α_2 downregulated osteogenic differentiation markers [77]. In addition, anti-α_2 integrin antibody was found to block ascorbic-acid-dependent induction

of alkaline phosphatase [34] and of the osteocalcin promoter [30] in MC3T3-E1 pre-osteoblasts. In contrast to integrin α_2, studies involving human MSCs suggest that integrin α_5 interactions do not support osteogenesis in the absence of osteoinductive media supplements [26]. Thus, the reduced osteogenic response associated with PEG–FN gels may be due, in part, to integrin α_5 signaling dominating over or interfering with pro-osteogenic integrin α_2 and α_v signals. That said, it is interesting to note that, in the presence of osteogenic media supplements, integrin α_5 interactions have been found to support osteogenesis [40].

As for FN, day 0 10T½ interactions with LN were mediated by both integrins α_v and α_5. However, LN also supported significant levels of integrin α_1 and α_6 interactions at day 0. Nevertheless, α_1 subunit did not significantly vary among PEG– ECM gels or relative to day 0 levels at 1 week of culture. As with integrins α_2 and α_v, integrin α_6 have previously been associated with osteogenesis. In particular, integrin α_6 upregulation has been associated with the MSC osteogenic responses observed on rough titanium surfaces [78, 79] and poly(lactide-co-glycolide) constructs [80]. Thus, the osteoinductive effect associated with PEG–LN gels may arise, in part, from integrin α_v and α_6 interactions predominating over integrin α_5 and α_1 interactions.

The osteoinductive role for integrins α_2 and α_6 noted in the literature was further supported by the temporal variations in integrin profiles observed in the present study. Specifically, PEG–FG gels were associated with an increase in integrin α_6 expression over the time course of the study, and PEG–LN gels were associated with an increase in integrin α_2 expression. The increased expression of these integrin subunits may therefore

have contributed to the osteogenic effects of both the PEG–LN and PEG–FG gels, although definitive statements cannot be made since the presence of a specific integrin does not necessarily imply its activity.

Several limitations of the present study merit comment. FG, FN and LN each support an array of interactions, such as cytokine and ECM protein binding, which likely influenced both integrin-mediated and non-integrin-mediated cell–hydrogel interactions. In addition, non-integrin cell–ECM interactions associated with deposited neo-matrix were not assessed. Thus, the present interpretations linking osteogenic responses to particular integrins must be treated with caution. In particular, further studies would be required to establish potential causative relationships between observed cell responses and associated integrin profiles. Finally, osteogenesis represents a complex set of processes that are mediated by a number of factors. The interplay between these factors and the precise sequences leading to osteogenic commitment are not fully understood, and the present study examined only a limited subset of the interactions and a limited panel of the markers that characterize osteogenesis. Furthermore, the present results do not enable the impact of the 3-D culture environment itself to be assessed.

Despite the limitations discussed previously, the cumulative ECM and phenotypic data indicate that LN may be the most appropriate of the biomolecules examined for promoting specific osteogenic differentiation within the context of scaffolds with osteoinductive moduli. Future studies will focus on exploring a broader range of time points and ECM protein concentrations as well as on examining potential synergy between various ECM components.

CHAPTER III

NOVEL COLLAGEN-MIMETIC PROTEINS FOR THE FABRICATION OF HYBRID POLYMERIC SCAFFOLDS*

3.1. OVERVIEW

The results from the studies described in chapter II indicated that FG and LN enhanced the osteogenic response of encapsulated 10T½ cells. Moreover, integrin α_2 and α_6 appeared to have played an important role in MSC osteogenic differentiation. Nonetheless, native biomolecules such as FG, FN and LN also support an array of additional signals which guide cell behavior. These signals include alternate cell adhesion sites, enzyme cleavage sequences, as well as growth factor and cytokine binding regions. These intricate biological interactions make it difficult to deconvolute the impact of integrin-based interactions on associated cellular signaling. Consequently, the results from the previous study cannot be definitively linked to integrin α_2 and α_6 signaling.

---

* Part of this chapter is reprinted with permission from ""Bioactive hydrogels based on Designer Collagens" by Cosgriff-Hernandez E, Hahn MS, Russell B, Wilems T, Munoz-Pinto D, Browning MB, Rivera J, Höök M, 2010. *Acta Biomaterialia*, 6, 3969-3977, Copyright [2010] by Acta Materialia Inc. Published by Elsevier Ltd.

We therefore propose to investigate the impact of integrin α_2 binding sequence and compare it to integrin $\alpha_{1,}$ which appeared to be not correlated with osteogenesis, in a more controlled format. Toward this goal, a class of collagen-mimetic proteins was used. These collagen-mimetic proteins are based on streptococcal collagen-like (Scl2) proteins that form a triple helix similar to mammalian collagens. In contrast to the numerous cell-binding sites on collagen, Scl2 from Streptococcus pyogenes serotype M28 does not contain any known cell-binding sites and thus provides a blank slate in terms of cellular interactions. In the current study, Scl2 protein was modified to include receptor binding motifs that interact with α_1 and/or α_2 integrin subunits.

Despite the potential of these Scl2 proteins in several applications, the utility of this recombinant protein family is currently limited to coatings due to the inability of Scl2 proteins to assemble into stable three-dimensional networks. To address this limitation, the Scl2 proteins were functionalized with photocrosslinking sites to enable incorporation into a hydrogel matrix. Characterization studies confirmed that the functionalization of the Scl2 proteins did not disrupt triple helix conformation, integrin binding or cell adhesion. Bioactive hydrogels were fabricated by combining the functionalized Scl2 proteins with poly(ethylene glycol) diacrylate (PEGDA) and photocrosslinking. Finally, human mesenchymal stem cell adhesion studies confirmed both cell-specific adhesion and appropriate activation of different MAP kinase signaling pathways due to selective integrin binding to the two receptor binding motifs investigated. These results serve to highlight the potential of this novel biomaterial platform in the development of improved scaffolds.

3.2. INTRODUCTION

The extracellular matrix (ECM), a complex network which is mainly composed of insoluble biomolecules, soluble biomolecules, and proteins and other factors from cell-cell interactions, is fundamental for essential biological processes such as cell migration, morphogenesis, cell proliferation, apoptosis, organogenesis and cell differentiation [81-83]. One of the biomolecules that compose the ECM is collagen. Collagens are a family of proteins that serve as structural building blocks of mammalian tissues [81, 84, 85]. Additionally, collagens have the ability to interact with specific cellular receptors, such as integrins [86, 87]. Integrins, which are considered transmembrane receptors, are large glycoproteins composed of α and β subunits [81, 87-90]. Up to now, 18 and 8 different α and β subunits, respectively, have been identified which can noncovalently combine to form 24 different heterodimers with distinct specificities [81, 90, 91]. For instance, $\alpha_2\beta_1$, $\alpha_{10}\beta_1$, and $\alpha_{11}\beta_1$ integrins are known to mediate interactions between several collagen types and the ECM [92, 93]. Integrin-ECM interactions impact cell behavior by the activation of the focal adhesion kinase (FAK) [94, 95]. Activated FAK triggers activation of mitogen-activated protein kinases (MAPKs) as is shown in Figure 8. To date, different groups of MAP kinases have been discovered to be involved in signaling cascades. These groups include signal-regulated kinases (ERKs) 1 and 2 (ERK1/2); 1, 2, and 3, p38 isoforms α, β, γ, and δ; c-Jun amino-terminal (JNK) [96-98]. Nevertheless, the most studied MAP kinases are the ERK1/2 and p38α kinases.

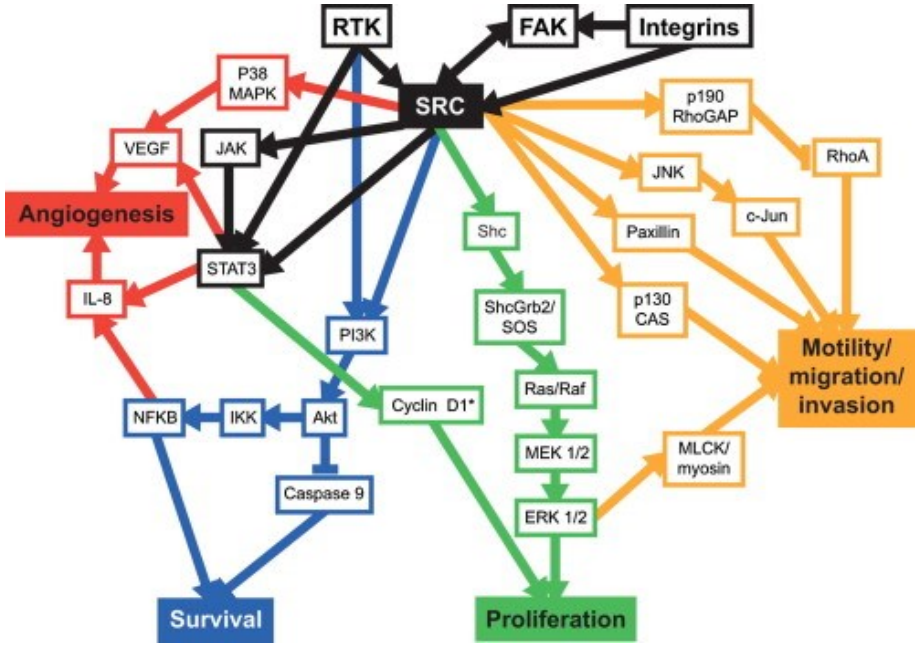

Figure 8. Schematic outline showing the activation of different MAP kinase pathways by the phosphorylation of FAK.
Adapted from [99]

In attributing mesenchymal stem cell osteogenesis to binding of a particular integrin requires that control over these and surrounding (non-integrin) interactions. This is a level of control that native biomolecules, such as collagen, cannot provide. In addition, the signaling associated with these specific integrin interactions must be characterized. Collagen-mimetic proteins are a novel protein family recently generated from streptococcal collagen-like (Scl2) proteins, isolated from group A Streptococcus. Expression of these proteins in bacterial culture enables a level of batch consistency and economies of scale not possible with solid-phase synthesis or native collagen extraction [85, 87, 100]. The unhydroxylated Scl2 proteins contain the GXY repeats associated with mammalian collagen but are able to form a stable triple helix at physiological

temperature in the absence of further modification [87, 101]. This is in contrast to recombinantly expressed human collagens, which require expensive post-translational modification to achieve the native triple helical conformation. Furthermore, whereas native collagen contains numerous binding sites that interact with integrins expressed by a wide range of cells, the Scl2 protein (scl2.28 from the serotype M28 strain MGAS6274A) functions as a biological blank slate [102-105]. Site-directed mutagenesis has been successfully utilized to insert specific receptor binding motifs into the Scl2 protein to promote cell adhesion, spreading, and migration [106]. Thus, specific mutations can be used to control the cell–material interactions of these recombinant proteins, and the Scl2 protein may be designed to induce selective cell adhesion and function.

In the present study, Scl2 proteins modified to contain the peptide sequences GFPGER or GFPGEN were selected for examination. These receptor binding motifs were based on the previously characterized GF/LOGER sequence (O; hydroxyproline), which interacts with collagen-binding α_1 and α_2 integrin I-domains [20, 107-109], and on molecular modeling of different collagen sequences in complex with α_1 and α_2 integrin I-domains. The Scl2 proteins modified to contain these integrin binding sequences have previously been shown to support cell-specific binding and spreading and migration [106]. However, unlike native fibrillar collagens, Scl2 proteins do not form stable networks and are limited to coating applications.

To use these proteins to examine the impact of specific integrin signaling on osteogenesis, the Scl2 proteins needed to be assembled into stable 3D structures. In

addition, the capacity of mesenchymal stem cells to bind to these proteins with stimulation of appropriate cellular signaling had to be demonstrated. In the current study, the Scl2 proteins were functionalized with photocrosslinking sites to enable incorporation into a three-dimensional (3-D) hydrogel matrix. Characterization studies were performed to investigate the effect of functionalization on the triple helix conformation, integrin binding and cell adhesion of the modified Scl2 proteins. Also, human mesenchymal stem adhesion studies were conducted to confirm both cell-specific adhesion and appropriate activation of different MAP kinase signaling pathways due to selective integrin binding to the two receptor binding motifs. Subsequent conjugation of Scl2 protein within a synthetic PEGDA network was then utilized to examine the impact of different Scl2s on cell adhesion and ascertain the potential of these materials in the future development of bioactive scaffolds.

3.3. MATERIALS AND METHODS

3.3.1. Materials

All chemicals were used as received. Poly(ethylene glycol)-acrylate-N-hydroxysuccinimide (3400 g mol^{-1}) (Ac-PEG-NHS) was purchased from JenKem Technology (Allen, Texas). All other chemicals were purchased from Sigma Aldrich (Milwaukee, WI). Recombinant α_1 I-domains were expressed in *E. coli* BL21 and purified as described previously [20]. Recombinant proteins were dialyzed against

phosphate-buffered saline (PBS), pH 7.4 and protein concentrations were determined using a calculated extinction coefficient for each protein.

3.3.2. Collagen-mimetic proteins based on streptococcal collagen-like protein (Scl2)

The scl2.28 sequence was amplified from the serotype M28 strain MGAS6274A (Scl2-1) and purified as previously described [87]. Scl2-1 served as the negative control as it does not contain binding sites for $\alpha_1\beta_1$ or $\alpha_2\beta_2$ and has previously been shown to be non-adhesive [85, 102-106]. Variants of this protein containing the sequence GFPGER (Scl2-2) or GFPGEN (Scl2-3) were generated by single amino acid mutations introduced in Scl2-1 using synthesized PCR primers (Integrated DNA Technologies) and the QuikChange site-directed mutagenesis kit per the manufacturer's instructions (Stratagene) (Figure 9). The mutations were verified by sequencing (SeqWright, Houston, TX). Recombinant proteins were expressed using standard recombinant protein procedures in E. coli BL21 (Novagen) and purified by affinity chromatography on a StrepTrap HP column (GE Healthcare). Protein purity was determined by SDS-PAGE followed by coomassie blue staining. Proteins were stored at 4°C in PBS (pH 7.4) until use.

3.3.3. Scl2 conjugation to PEG linker with photoreactive crosslinks

Scl2 proteins and a rat tail collagen I control (Sigma Aldrich) were

functionalized with photoreactive crosslink sites to enable hydrogel formation according to a protocol adapted from Sebra et al. (Figure 10) [110]. Scl2 proteins contain ~9% lysine groups that readily facilitate bioconjugation chemistry via the established NHS - lysine ε−amino group reaction. Briefly, Scl2s were reacted with acrylate-PEG-N-Hydroxysuccinimide (Ac-PEG-NHS, MW 2000) in 50 mM sodium bicarbonate buffer (pH 8.5) at room temperature. A molar ratio of 2:1 Ac-PEG-NHS:NH_2 was used and the reaction was allowed to proceed for 18 h at room temperature with shaking. Excess Ac-PEG-NHS and other reaction byproducts were removed via dialysis (MWCO = 20,000). Functionalization of the modified proteins (Collagen-F, Scl2-F) was confirmed with infrared (IR) spectroscopy and gel electrophoresis (data not shown).

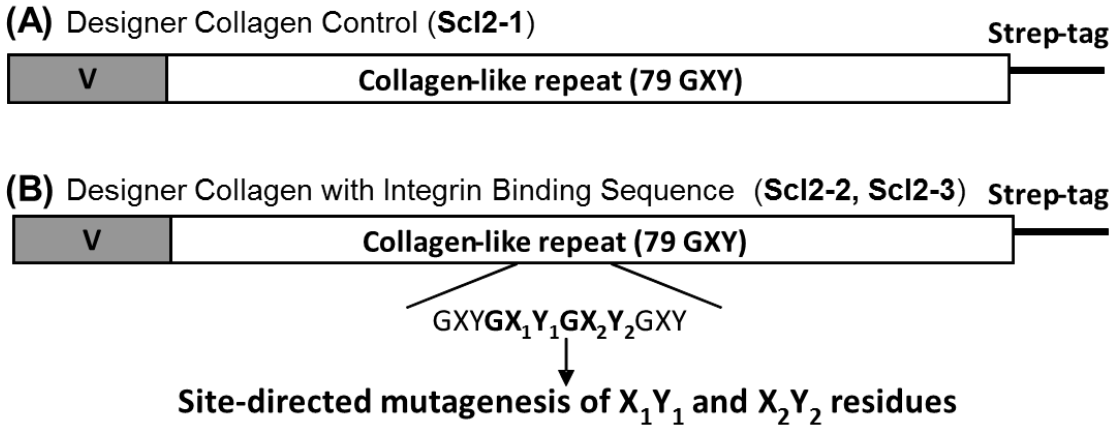

Figure 9. Schematic representation of the site-directed mutagenesis of Scl2 to create Scl2-2 and Scl2-3 with integrin binding motifs. PCR primers were used to generate the integrin binding sequences $GX_1Y_1GX_2Y_2$.

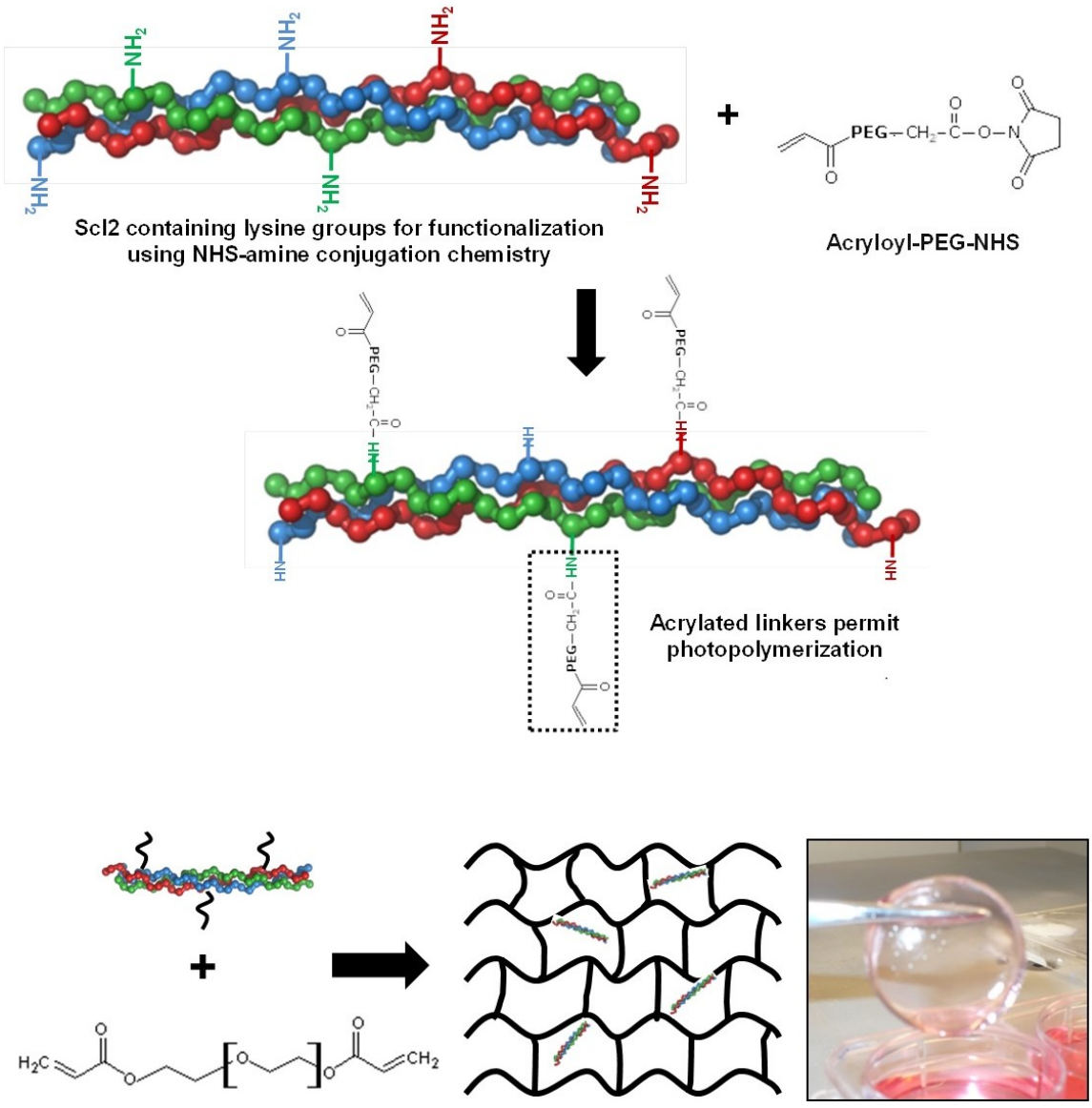

Figure 10: Schematic representation of the functionalization of Scl2 proteins with photoreactive crosslink sites to enable hydrogel formation. An image of a PEGDA-Scl2 hydrogel and schematic of the associated hydrogel network structure are provided.

3.3.4. Characterization of integrin specificity of functionalized Scl2 proteins

An enzyme-linked immunosorbant assay ELISA) was utilized to assess the

specificity of recombinant α_1 I-domain binding to control and functionalized Scl2 proteins. Microtiter wells were coated with 1 μg per well of Scl2-1, Scl2-2, Scl2-3, or rat tail derived collagen type I (Cultrex R&D) in PBS containing 1 mM $MgCl_2$ or 1 mM EDTA overnight at 4°C. The samples were blocked with PBS containing 1% BSA (w/v) for 1 h at room temperature. Five μM α_1 I-domains (0.12 mg ml^{-1}) were added to the wells and incubated for 2 h at room temperature. A mouse monoclonal anti-His-HRP conjugate (Alpha Diagnostics) followed by SigmaFast OPD (Sigma) incubation at 1 h was used to detect bound I-domains. The absorbance at 450 nm was measured using a Thermomax plate reader (Molecular Devices Corp, Menlo Park, CA). Experiments were performed in triplicate.

To confirm that each Scl2 protein retained appropriate cell interactions following conjugation to PEG, the ability of three distinct cell populations to interact with the functionalized proteins was examined in two dimension (2D): (1) C2C12 cells, which do not natively express α_1 and α_2 integrin subunits; (2) C2C12 cells modified to stably express human α1 integrin subunits (C2C12-α_1); and (3) C2C12 cells modified to stably express human α_2 integrin subunits (C2C12-α_2). Mouse myoblast C2C12, C2C12-α_1, and C2C12-α_2 cells were kindly provided by Dr. Donald Gullberg (University of Bergen, Bergen, Norway) and maintained in DMEM with 10% FBS (Hyclone) supplemented with no antibiotic, 1 mg ml^{-1} geneticin (Invitrogen), or 10 μg ml^{-1} of puromycin (InvivoGen), respectively. The expression of α_1 or α_2, and β1 integrin subunits on the surface of the modified C2C12 cells was confirmed by immunocytochemistry prior to cell culture studies (data not shown).

3.3.5. Cell adhesion to functionalized Scl2 proteins

For cell adhesion studies, microtiter plates were coated with functionalized and unmodified Scl2-1, Scl2-2, and Scl2-3. Rat tail collagen I coated wells served as positive controls. Microtiter wells were coated with 1 μg per well of Scl2 1, Scl2-2, Scl2-3, or rat tail derived collagen type I (Cultrex R&D) in PBS overnight at 4°C. The Scl2 protein solutions were filter-sterilized using a 0.22 μm PDVF membrane (Millipore) prior to application to the microtiter plate. For each Scl2 protein, 15 wells (3 wells per cell type examined) were coated. After blocking with PBS containing 1% BSA for 1 h, the wells were rinsed extensively with PBS and cells were seeded onto the coated surfaces at 6,000 cells cm^{-2}.

Prior to seeding, cells were adapted to serum free media (DMEM containing 1mM $CaCl_2$ and 1mM $MgCl_2$) for 3 h, after which cells were harvested by brief exposure to 0.125% trypsin (Mediatech) and resuspended in serum free media supplemented with 0.2% BSA. Following 3 h exposure to the coated surfaces at 37 °C / 5% CO_2, cells were fixed with 4 % paraformaldehyde and stained with rhodamine phalloidin (Invitrogen) and SybrGreen (Invitrogen). Rhodamine- labeled phalloidin in combination with SybrGreen were chosen as cell markers because phalloidin binds to F-actin, which is present in abundance in cell cytoplasm, and SybrGreen binds DNA, which indicates the location of the nucleus of each cell. Representative fluorescence images were obtained using a Zeiss Axiovert microscope.

3.3.6 Cell chip studies

Agilent 2100 analyzer and the Cell Fluorescence LabChip®Kit (Agilent) were used to characterize integrin specificity of human mesenchymal stem cells (hMSCs). hMSCs (approximately 0.4 million per staining) were collected and washed with cold D-PBS (Gibco) once and resuspended in staining buffer (PBS supplemented with 1% BSA) to reach 2 million cells ml^{-1}. 2 μM Calcein solution (Molecular Probes) was used to stain the live cells for 30 minutes at room temperature and protected from light. Before applying the primary antibody, cells were washed twice with staining buffer. Integrin α_1, integrin α_2, and appropriate positive and negative controls were used to perform the staining. Specifically, 1μg of each primary antibody and appropriate isotype controls IgG diluted in staining buffer was used. Further details on antibodies are given in Table 5. All samples were incubated on ice for 30 minutes protecting from light. Subsequently, cells were washed twice with staining buffer, and fluorescence-labeled secondary antibodies (Jackson Immunoresearch) were added to the cell suspension in order to label the cells using a 1:50 dilution in staining buffer. Cell suspensions were incubated on ice for 30 minutes protecting from light. Labeled cells were spun down and resuspended in 80ul of cell buffer (Cell Fluorescence LabChip®Kit, Agilent) and 10ul of sample were loaded onto the cell chip per manufacturer's protocol.

Table 5. Antibodies employed in cell chip and western blot assays.

Antibody	Clone	Supplier	*Cell chip*	*Western blot*
Integrin α_1	FB12	MP	√	
Integrin α_2	P1E6	MP	√	
CD105	MJ7/18	SCBT	√	
FAK	C-20	SCBT		√
p-FAK	Tyr 397	MP		√
ERK1	K-23	SCBT		√
p-ERK1/2	12E4	SCBT		√
p38α	F-9	SCBT		√
p-p38	Thr 180/ Tyr 182	SCBT		√

[†]Abbreviations: MP – Millipore; SCBT – Santa Cruz Biotechnology

3.3.7. Human mesenchymal stem cell adhesion to functionalized Scl2 proteins

To assess the ability of hMSCs to interact with the functionalized proteins, cell adhesion was examined in two dimensions (2D). The expression of α_1 and α_2 integrin subunits on the surface of the hMSCs was confirmed by flow cytometry, as described previously, prior to cell culture studies. Cryopreserved hMSCs (Lonza) at passage 2 were thawed and expanded in monolayer culture per Lonza protocols. Prior to seeding, cells were maintained at 37 ºC and 5% CO_2 in MesenPRO RS^{TM} Media (Gibco) supplemented with 2% MesenPRO RS^{TM} growth supplement (Gibco). Cell adhesion studies were performed following the procedure previously described in 3.3.5.

3.3.8. Cell signaling studies

To further study the interaction between hMSCs and Scl2 proteins, the activation of important cell signaling pathways was investigated. Cryopreserved hMSCs (Lonza) at passage 2 were thawed and expanded in monolayer culture per Lonza protocols. Prior to seeding, cells were maintained at 37 ºC and 5% CO_2 in MesenPRO RS^{TM} Media (Gibco) supplemented with 2% MesenPRO RS^{TM} growth supplement (Gibco). In brief, 12-well plates were coated with Scl2-1, Scl2-2, and Scl2-3 proteins. Proteins were resuspended in PBS at 100 μg mL^{-1}, and 1 ml well^{-1} of protein solution was applied and incubated overnight at 4 °C. The Scl2 protein solutions were filter-sterilized using a 0.22 μm PDVF membrane (Millipore) prior to application to the 12-well plate. Harvested hMSCs were washed with PBS and resuspended in serum-free DMEM (Gibco). The cell suspensions were subsequently applied to the coated wells at 10,000 cells cm^{-2}.

Prior to seeding, cells were adapted to serum free media (DMEM) overnight, after which cells were harvested by exposure to 3mM EDTA solution in PBS, pH. 7.4. Cells were resuspended in serum free media and maintained in suspension for 1 h at room temperature. Following 30 min exposure to the coated surfaces at 37 °C / 5% CO_2, cells were lysed with cell extraction buffer supplemented with protease and phosphate inhibitors (1% Triton, 0.1% SDS, 10 mM sodium fluoride, 1 mM sodium pyrophosphate, 2 mM sodium orthovanadate, 1x protease cocktail (Thermo Scientific) in PBS) for 30 minutes at 4 °C. Protein levels of the resulting lysates were measured by the Bio-Rad

DC protein assay. The activation of FAK, ERK1/2 and p38α MAP kinases was evaluated using western blots.

3.3.9. Western blot assays

For Western blot assays, equal amounts of protein (10 µg per lane) were loaded into different wells of a 10% polyacrylamide gel and proteins were separated by electrophoresis. Before loading the samples onto the gel, protein solutions were concentrated using 3,000 MWCO Amicon filter units (Millipore), following denaturing by addition of β-mercaptoethanol solution and heating at 100 °C for 10 minutes. After electrophoresis, proteins were transferred to a nitrocellulose membrane (Thermo Scientific). The blot was cut into two parts and washed twice with double deionized water for 5 minutes each time at room temperature. The blots were then blocked with a 5% BSA solution (Fraction V, Fisher Scientific) in Tris-buffered saline containing 0.1% Tween-20 (TBST; 25 mM Tris-HCl, pH. 7.5, 137 mM NaCl, 0.1% Tween 20) for 1 hour at room temperature. Following blocking incubation, blots were briefly rinsed with TBST. Each blot was incubated with the appropriate primary antibody diluted in TBST solution containing 5% BSA overnight at 4 °C. Further details on antibodies employed for this study can be found in Table 5. After washing three times with TBST solution, primary antibody bound to each blot was detected using an appropriate HRP or AP conjugated secondary antibody (Jackson Immunoresearch) diluted in TBST solution containing 5% BSA for 1 h at room temperature. Blots were further washed three times

with TBST solution, 5 minutes each time, at room temperature. Signal was detected using a luminol reagent (SCBT) or AP chemiluminescent solution (Novex). Imaging was performed using the molecular imager chemidoc XRS system (Biorad) and band intensity was quantified using Adobe Phothoshop.

3.3.10. Preparation of biologically active PEG-Scl2 hydrogels

PEGDA was synthesized by adding acryloyl chloride dropwise to a solution of PEG (3.4 kDa, Fluka) and triethylamine in anhydrous dichloromethane (DCM) under an argon blanket. The molar ratio of diester, acryloyl chloride, and triethylamine was 1:2.5:2.1, respectively. The reaction was maintained at low temperature to reduce undesired side reactions utilizing a salt/ice bath. After the addition of acryloyl chloride, the reaction was stirred overnight. The resulting solution was washed with 2 M K_2CO_3 to remove acidic byproducts. The DCM phase was subsequently dried with anhydrous $MgSO_4$, and the PEGDA product was then precipitated in diethyl ether, filtered, and dried under vacuum. Acrylation of the PEG end hydroxyl groups was characterized by proton nuclear magnetic resonance (^{1}H-NMR) to be ~85%.

The ability of Scl2-2F and Scl2-3F proteins to mediate cell adhesion following incorporation within PEGDA hydrogels 3D networks was also examined. Scl2-F and Collagen-F proteins were dissolved at 6 mg protein ml^{-1} in 20 mM acetic acid. PEGDA powder was then added to each solution to 5 wt%, followed by the addition of 10 μL mL^{-1} of a 300 mg ml^{-1} solution of UV photoinitiator 2,2-dimethoxy-2-phenyl-

acetophenone in N-vinylpyrrolidone. The resulting solutions were sterile-filtered, pipetted between glass plates separated by 200 μm spacers (cell studies) or 1 mm spacers (mechanical testing), and polymerized by 10 min exposure to longwave UV light (~ 6 mW cm^{-2}, Spectroline).

The resulting hydrogels were immersed in PBS for 24 h, after which a set of 8 mm punches were collected from the swollen gels. Punches from hydrogels reserved for mechanical testing were measured using a digital caliper. Following application of a 0.05 N preload, each hydrogel was subjected to compression at a rate of 6 mm min^{-1} using an Instron 3342. The compressive modulus of each hydrogel formulation was extracted from the resulting stress-strain data. For cell adhesion studies, C2C12, C2C12-α_1, and C2C12-α_2 were harvested, resuspended in media containing 10% FBS, and seeded onto the swollen Scl2-containing gels at 10,000-20,000 cell cm^{-2}. After 3 h at 37 °C / 5% CO_2, cells were fixed with paraformaldehyde and stained with rhodamine phalloidin and SybrGreen. Representative fluorescence images were obtained using a Zeiss Axiovert microscope. Rat tail collagen I-containing hydrogels served as positive controls.

3.3.11. Statistical analyses

Data are reported as mean ± standard deviation. Comparison of sample means was performed by ANOVA followed by Tukey's post hoc test (SPSS software), $p < 0.05$.

3.4. RESULTS AND DISCUSSION

The present study was designed to extend the potential utility of Scl2 proteins in tissue engineering applications by functionalizing specific Scl2 proteins to permit their conjugation into PEGDA hydrogel networks. Toward this goal, the ability to functionalize Scl2 without disrupting the native conformation, integrin binding affinity, appropriate cell signaling and cell interactions of Scl2 proteins was examined.

3.4.1. Confirmation of Scl2 functionalization

The functionalized Scl2 proteins, denoted Scl2-F, were first analyzed using IR spectroscopy. IR absorbance peaks assigned to the peptide (amide, C=O) at 1630 cm^{-1} and PEG (ether, C-O-C) at 1110 cm^{-1} were both present in the purified product (data not shown). Control experiments confirmed that non-bonded PEG was removed by dialysis over the selected time period (data not shown); thus, the presence of PEG in the product was concluded to be coupled to the Scl2 and collagen control. As an additional confirmation of functionalization, collagen and Scl2 peptides exposed to Ac-PEG-NHS were heat denatured and run on a native SDS-PAGE gel. SDS-PAGE is a straightforward method of monitoring the PEGylation of proteins because the grafting of PEG has a detectable effect on the mobility of the protein in acrylamide gels [111-113]. The smeared bands associated with the products as compared to the unmodified controls confirmed conjugation and reflect the polydispersity of the products (Figure 11).

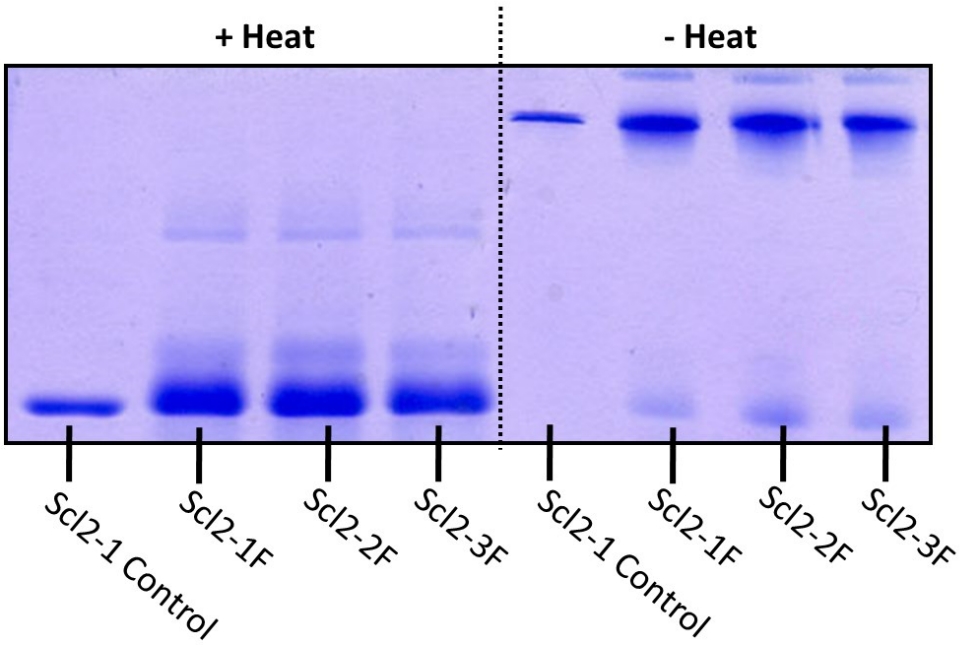

Figure 11. Coomassie-stained 12% SDS–PAGE analysis of functionalized Scl2 proteins (Scl2-1 Control, Scl2-1F, Scl2-2F, Scl2-3F) with and without heat denaturation.

3.4.2. Maintenance of triple helical structure and bioactivity following PEGylation

Extensive protein functionalization has been shown in some cases to disrupt protein conformation and adhesion site availability [114]. It was therefore important to confirm that Scl2-F proteins retained their triple helical conformation and biological activity. Scl2-F proteins ran as homogeneous trimers, with an estimated molecular weight of ~120 kDa, under non-denaturing electrophoretic conditions, in comparison to their heat-denatured counterparts, which exhibited molecular masses of ~35 kDa (Figure 11).

Retention of expected bioactivity was qualitatively evaluated by solid phase binding assays. Microtiter wells were coated with Scl2-1, Scl2-2, Scl2-3, Scl2-1F, Scl2-2F, Scl2-3F, or collagen type I and exposed to recombinant human α_1 integrin I-domains. As expected, Scl2-1 bound minimal and collagen type I exhibited maximal α_1 integrin I-domain binding levels (Figure 12). Furthermore, Scl2-2, containing the GFPGER integrin adhesion sequence, and Scl2-3, containing the GFPGEN integrin adhesion sequence, bound α_1 integrin I-domain at levels intermediate between collagen I and Scl2-1. Similar trends were observed with the Scl2-F proteins, which indicated that appropriate integrin binding was retained on functionalization. A modest decrease was observed between the functionalized and non-functionalized proteins; however, this difference was not statistically significant.

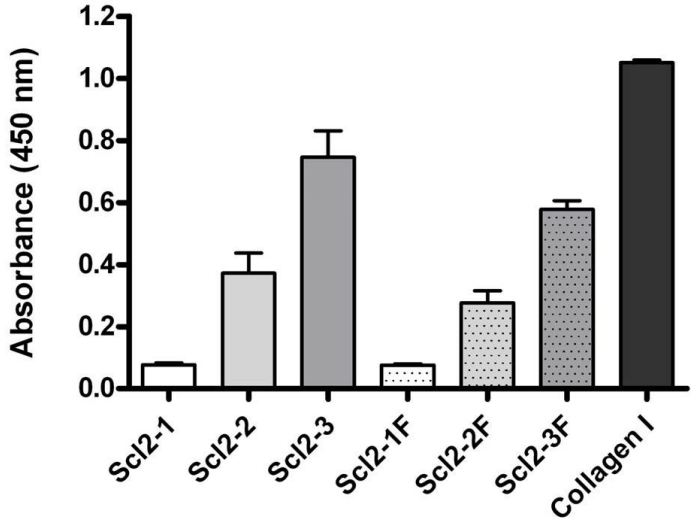

Figure 12. Microtiter plates were coated with Scl2s and functionalized Scl2s at a concentration of 1 mg per well. Recombinant α_1 integrin I-binding domains (5 mM) were allowed to adhere for 2 hours and ELISA performed to quantify integrin binding.

3.4.3. Cell adhesion to functionalized Scl2 proteins

As previously discussed, the receptor binding motifs GFRGER and GFPGEN were selected for examination based on the previously characterized GF/LOGER sequence [20, 107-109] and on molecular modeling of different collagen sequences in complex with α_1 and α_2 integrin I-domains. To confirm that cells could recognize and bind these integrin binding motifs in Scl2-F proteins, cell adhesion and spreading studies were performed using mouse C2C12 cells or stably transfected cell lines expressing the human integrin α_1 subunit, C2C12-α_1, or the human integrin α_2 subunit, C2C12-α_2. Since C2C12 cells do not normally express collagen-binding α_1 or α_2 integrins, comparison of the binding of unmodified C2C12 cells with that of C2C12-α_1 and C2C12-α_2 could be utilized to evaluate the extent to which observed cell adhesion to Scl2-2F and Scl2-3F was due exclusively to α1 or α2 integrin mediated interactions.

C2C12, C2C12-α_1, or C2C12-α_2 cells were allowed to adhere and spread for 3 h on microtiter plates coated with 1 μg protein per well. As anticipated, Scl2-1F coated surfaces displayed similar cell adhesion and spreading as BSA-coated negative controls. Scl2-2F and Scl2-3F induced spreading of C2C12-α_1 (Figure 13, second column), as did the collagen-F positive control. In contrast, C2C12-α_2 cells (Figure 13, third column) adhered and spread on Scl2-2F and collagen-F but not on Scl2-3F while unmodified C2C12 cells were unable to significantly adhere to either Scl2-2F or Scl2-3F. Cumulatively, these cell adhesion results indicate that 1) Scl2-2F and Scl2-3F mediate cell adhesion via binding to α_1 and/or α_2 integrins (C2C12 results), 2) Scl2-2F interacts

with both α1 and α2 integrins (C2C12-α_1 and C2C12-α_2 results), and 3) Scl2-3F binds only α_1 integrins (C2C12-α_1 and C2C12-α_2 results), consistent with the expected integrin binding of each protein.

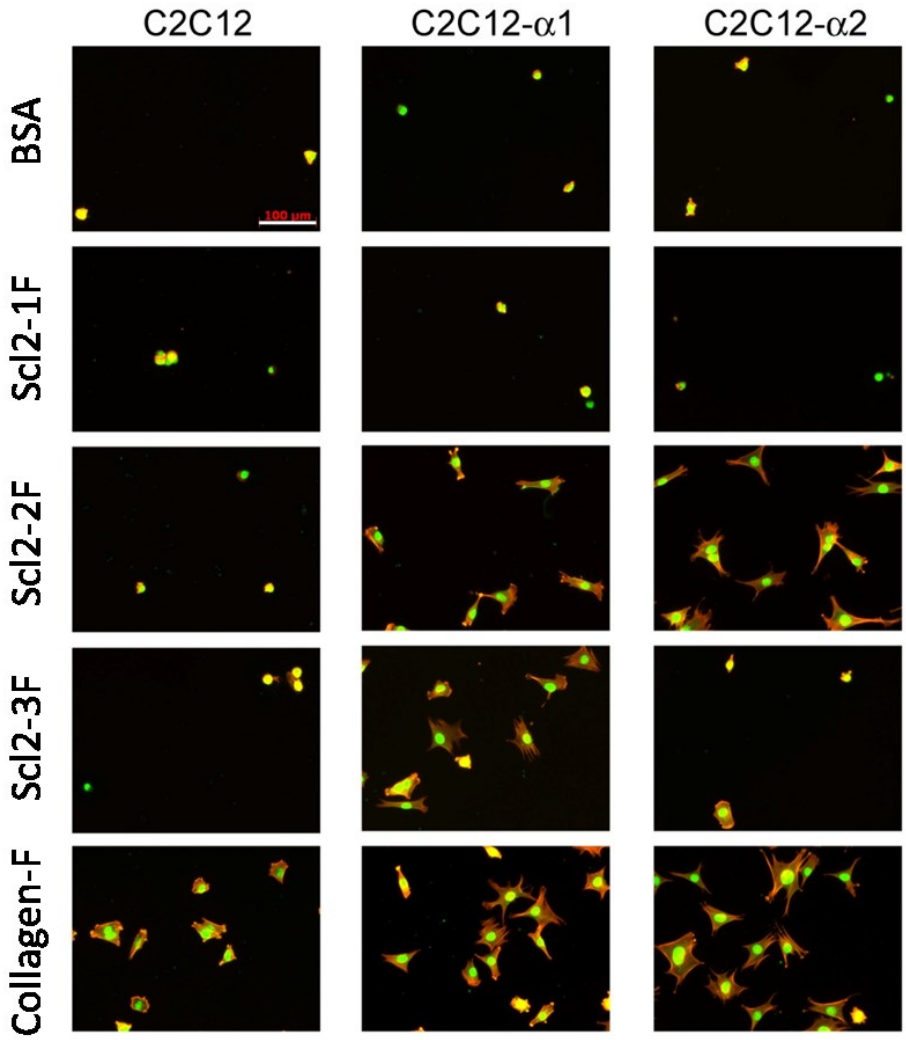

Figure 13. High binding polystyrene 96 well plates were coated with Scl2-1F, Scl2-2F, Scl2-3F, and functionalized type I collagen (collagen-F) at 1 µg protein per well. Unmodified C2C12 cells, C2C12-α1 cells, C2C12-α2 were seeded at a density of 6,000 cells cm^{-2} and allowed to spread for 3 hours. Attached cells were fixed with 4% paraformaldehyde, stained with rhodamine phalloidin (F-actin) and SybrGreen (nucleus), and imaged by fluorescence microscopy. Large circles in the Scl2-1 images are a result of floating, non-adherent cells outside of the focal plane Scale bar applies to all images and equals 100 µm.

3.4.4. Scl2 proteins promote hMSC adhesion and appropriate intracellular signaling

To assess the ability of hMSCs to interact with the Scl2 functionalized proteins, cell adhesion was examined in two dimensions (2D). First, integrin expression levels in hMSCs were analyzed using a cell fluid-based microchip, whose working principle is similar to that of flow cytometry [115]. hMSCs were stained using specific antibodies for integrin α_1 and integrin α_2 since adhesion to the Scl2 proteins is mediated by these two integrin subunits. Appropriate negative and positive controls were used, and fluorescently-labeled secondary antibodies were employed for the detection of primary antibody binding. As shown in Figure 14, hMSCs stained positive for both integrin α_1 and integrin α_2 subunits. However, integrin α_2 expression was higher (~90%) compared to integrin α_1 expression (~55%).

On the other hand, hMSC attachment and spreading was also investigated (Figure 15). hMSCs strongly spread on collagen-F coated surfaces (data not shown). Furthermore, Scl2-2F and Scl2-3F coated surfaces mediated hMSC attachment and spreading whereas hMSC adhesion on Scl2-1F coated wells was minimal. Compared to Scl2-3F samples, hMSC spreading was higher in Scl2-2F coated surfaces. Therefore, Scl2-2F and Scl2-3F appeared to selectively mediate the attachment and spreading of hMSC. Cumulatively, these cell adhesion and cell fluid-based microchip studies suggest that: 1) the selectivity of hMSC adhesion to the Scl2 proteins may be due to the differences in α_1 and α_2 integrin expression, 2) hMSC adhesion to Scl2-2F coated

surfaces occurs through α_1 and α_2 integrin subunits, and 3) hMSC α_1 integrin expression mediates binding to Scl2-3F coated surfaces.

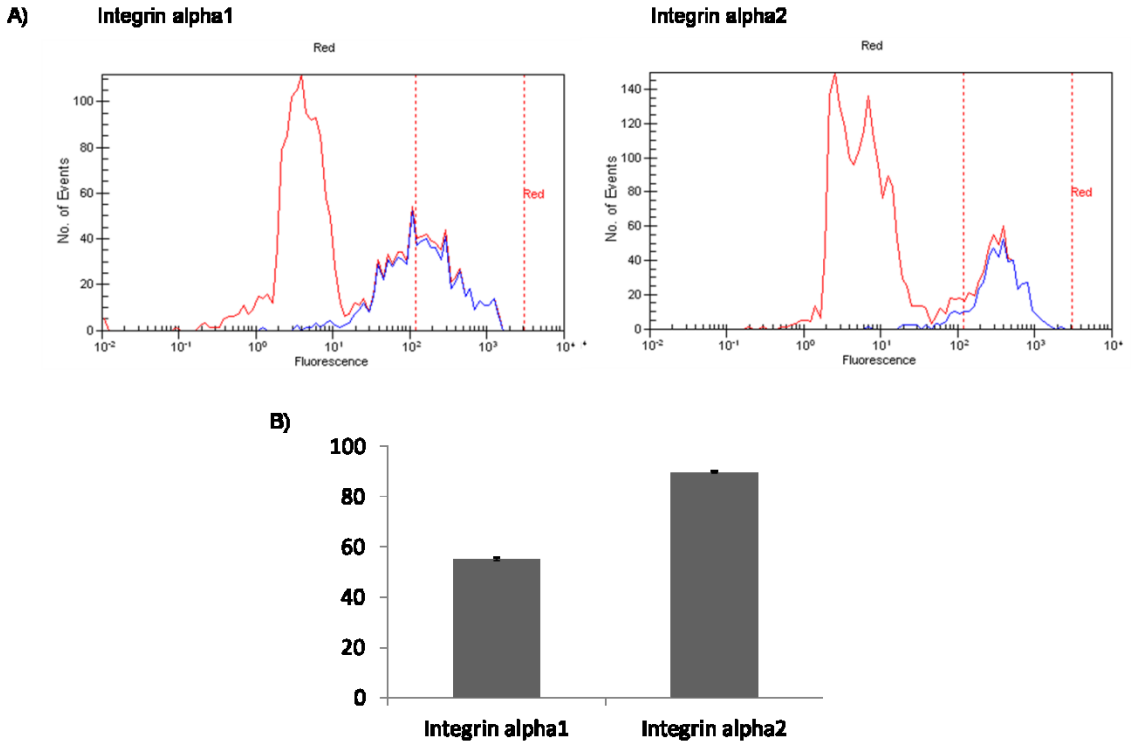

Figure 14. Integrin α_1 and α_2 characterization of hMSCs by cell chip based flow cytometry. A) Single parameter histograms showed the relative fluorescence intensity of staining and the cell counts. B) Isotype control was used to set up the gate in order to calculate the positive cells that were stained for each integrin (data not shown).

To further investigate the interactions between hMSCs and Scl2 proteins, the activation of important cell signaling pathways involved in cell adhesion was studied. Mitogen-activated protein kinases (MAPKs) play a fundamental role in the regulation of gene expression, cell adhesion, cell motility and cell differentiation [116]. In addition, it has been shown that cell adhesion is mediated by integrin signaling events that involve

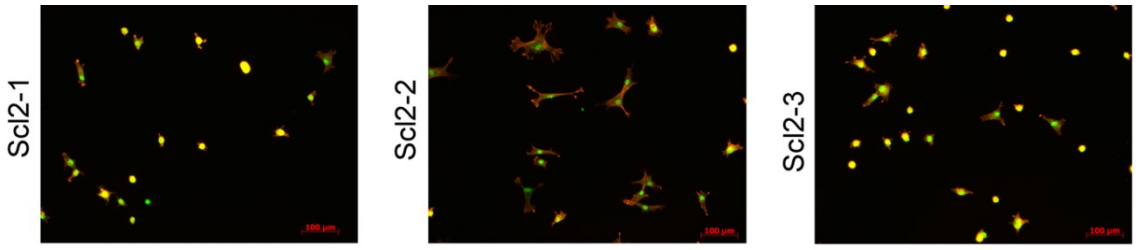

Figure 15. High binding polystyrene 96 well plates were coated with Scl2-1F, Scl2-2F and Scl2-3F at 1 μg protein per well. hMSCs were seeded at a density of 6,000 cells cm^{-2} and allowed to spread for 3 hours. Attached cells were fixed with 4% paraformaldehyde, stained with rhodamine phalloidin (F-actin) and SybrGreen (nucleus), and imaged by fluorescence microscopy. Scale bar applies to all images and equals 100 μm.

the phosphorylation of focal adhesion kinase (FAK), which initiates signaling through multiple intracellular MAP kinase pathways such as ERK1/2 and p38 [117-119]. Therefore, phosphorylation and activation of these two pathways was investigated. As a result, hMSCs were allowed to adhere for 30 minutes (time required for FAK activation [120-122]) on 12-well plates coated with 10 μg protein per well. Afterwards, cells were lysed and lysates were prepared and analyzed through immunoblotting with phosphorylated site-specific primary antibodies directed against TYR 397 FAK, T202/Y204 ERK and T180/Y182 p38. The respective total proteins (FAK, ERK and p38) were also analyzed using immunoblots. Band intensities were computed, and the activated fraction of each MAP kinase protein under study was calculated by dividing the band intensity of the phosphorylated protein by the respective band intensity of total protein. As illustrated in Table 6, a significant increase in the activated fraction of FAK, ERK1/2 and p38 was observed for Scl2-2 and Scl2-3 samples relative to Scl2-1. Comparison of activation levels between Scl2-2 and Scl2-3 indicates that phosphorylation of FAK and p38 was significantly lower in response to adhesion onto

Scl2-3 relative to Scl2-2 coated surfaces. Specifically, the active fractions of FAK and p38 for Scl2-2 were ~1.17 and 1.25 greater than those for Scl2-3, respectively. Likewise, ERK1/2 activation was apparently lower in Scl2-3 relative to Scl2-2; however, a significant difference was not observed. Cumulatively, the present data associated with MAP kinase signaling suggests that 1) integrin α_1 and integrin α_2 dependent adhesion to Scl2-2 and Scl2-3 enhanced the activation of FAK, ERK1/2 and p38 proteins, 2) Scl2-2 had a higher effect in MAP kinase-associated protein phosphorylation compared to Scl2-3, and 3) protein activation in Scl2-2 samples was the most enhanced for FAK and p38, relative to ERK1/2. Thus, activation of FAK and p38 pathways might be related to cell adhesion interactions through integrin α_2 subunit.

Table 6. Activated fraction of each of the MAP kinase proteins that was investigated. Data of Scl2-1 was used for normalization.

Protein type	pFAK/FAK	pERK/ERK	pp38/p38
Scl2-1	1.00 ± 0.11	1.00 ± 0.04	1.00 ± 0.05
Scl2-2	1.64± 0.05*	1.18 ± 0.03*	1.17 ± 0.04*
Scl2-3	1.40 ± 0.05$^{*,\#}$	1.16 ± 0.03*	0.93± 0.04$^{*,\#}$

* Significantly different from the corresponding Scl2-1, $p < 0.05$.
$^{\#}$ Significantly different from the corresponding Scl2-2 gels, $p < 0.05$.

3.4.5. Bioactive hydrogels with cell-specific adhesion

Scl2-F proteins were conjugated within 5 wt% PEGDA hydrogels resulting in stable three dimensional gel networks (Figure 10). PEGDA was selected as the base-material for the hydrogel network due to the broad tunability of PEG gel mechanical

properties, making these gels particularly desirable for tissue engineering applications. However, in the present study, the biological blank slate character of PEGDA also allowed observed cell binding to Scl2-F containing gels to be attributed to the presence of the Scl2-F protein alone. At the Scl2-F levels employed in the present study, the modulus and mesh structure of the PEG-Scl2 gel network can be expected to be dominated by PEGDA. To confirm this, the modulus of the prepared PEG-Scl2 hydrogels was compared to that of pure 5 wt% PEG (3.4 kPa) hydrogels. Mechanical testing showed the compressive modulus of the PEG-Scl2 gels to be 139 ± 13 kPa, statistically indistinguishable from the 128 ± 11 kPa modulus of the pure PEG gel counterparts. The close agreement between these initial moduli indicates that the material properties of the PEG-Scl2 hydrogels are dominated by the PEGDA at the Scl2 concentrations employed. Thus, these hybrid hydrogels appear to retain many of the beneficial properties of pure PEG gels, such as the ability to broadly tune modulus by varying the PEGDA M_w and/or concentration [123].

To confirm the continued ability of gel-associated Scl2-F proteins to mediate specific cell adhesion, C2C12, C2C12-α_1 and C2C12-α_2 were seeded onto various hydrogel surfaces (Figure 16). As anticipated, each cell type spread on collagen-F containing gels, although the extent of this spreading was in general significantly lower than on collagen-F. This observation is consistent with previous studies demonstrating a reduction in cell spreading with decreasing substrate stiffness, although increased steric hindrance resulting from collagen conjugation to the PEGDA network may also contribute [63]. Similarly, Scl2-2F promoted adhesion of C2C12-α_1 and C2C12-α_2. Scl2-

3F gels, however, were unable to support C2C12-α_2 adhesion, as can be seen by comparison with Scl2-1F gels and PEG negative controls (Figure 16). These observations confirm that functionalized Scl2 proteins can be incorporated into 3D matrices to generate cell selective, bioactive hydrogels. This result has significant implications for the tissue engineering field, where controlled attachment is needed to provide a bioactive graft interface in order to have a better control of scaffolds and investigate cell fate decisions.

3.5. CONCLUSION

In the current study, the collagen-mimetic proteins Scl2-1, Scl2-2, and Scl2-3 were functionalized with photocrosslinking sites to enable incorporation into a three dimensional hydrogel matrix. Bioactive hydrogels were then fabricated by combining the functionalized Scl2s with PEGDA and photocrosslinking via exposure to UV light. Characterization studies confirmed that the functionalization of the Scl2 proteins did not disrupt triple helix conformation, integrin binding, or cell adhesion. Initial cell studies also confirmed specific hMSC adhesion to Scl2-2 and Scl2-3 proteins and appropriate activation of different MAP kinase pathways due to selective integrin binding.

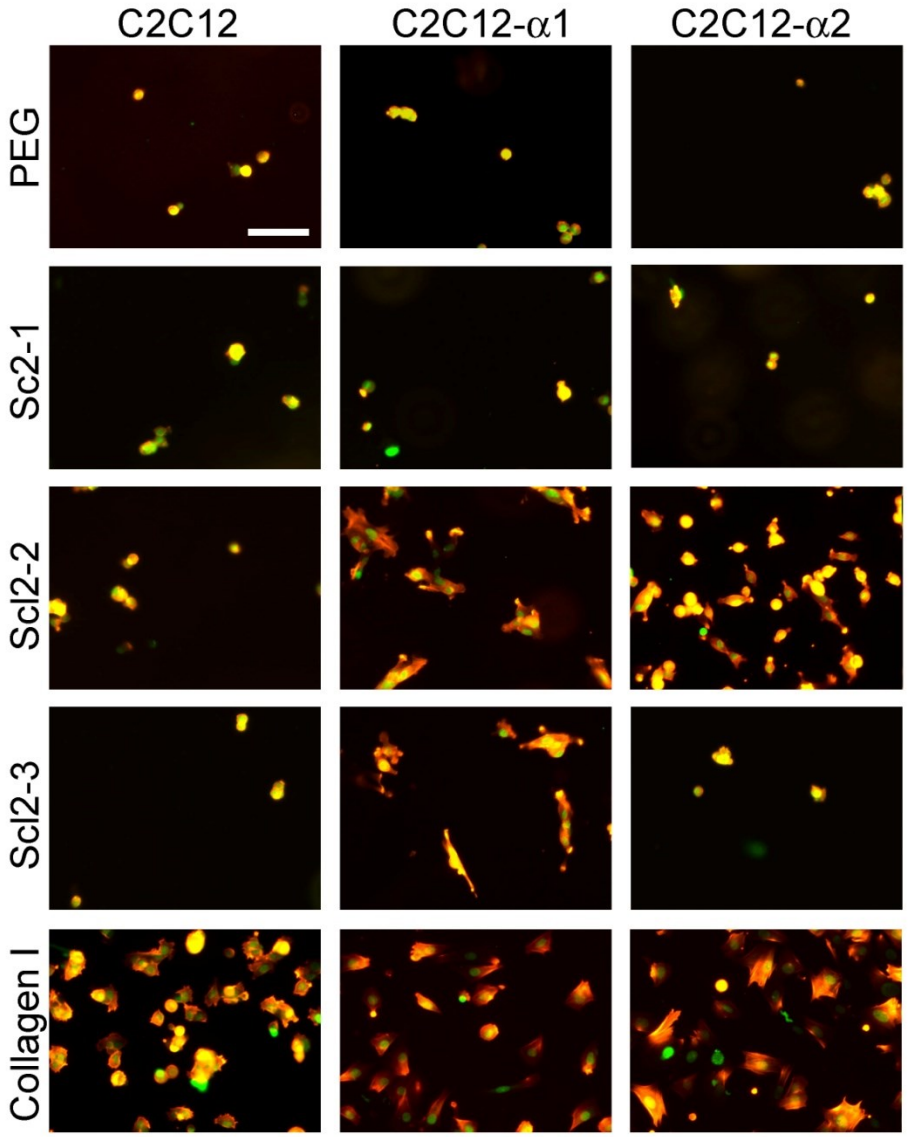

Figure 16. PEG-Scl2 hydrogels were fabricated by combining 5 wt.% PEGDA (3.4 kDa) with photoinitiator (Irgacure 2959), 6 mg protein ml^{-1} of Scl2-1F, Scl2-2F, Scl2-3F or functionalized type I collagen. PEG hydrogels served as a negative control. Cells were seeded at a density of 10,000 cell cm^{-2} and allowed to spread for 3 h. Attached cells were fixed with 4% paraformaldehyde, stained with rhodamine phalloidin and SybrGreen, and imaged by fluorescence microscopy. Large circles in the Scl2-1 images are a result of floating, non-adherent cells outside of the focal plane. The scale bar applies to all images and equals 100 μm.

CHAPTER IV

EVALUATION OF THE EFFECT OF COLLAGEN-MIMETIC PROTEINS IN HUMAN MESENCHYMAL STEM CELL OSTEOGENESIS

4.1. OVERVIEW

The results from the study of the novel collagen-mimetic proteins for the fabrication of hybrid polymeric scaffolds indicated that collagen-mimetic proteins Scl2-1, Scl2-2, and Scl2-3 can be functionalized with photocrosslinking sites and therefore, incorporated into hydrogel matrices. In addition, human mesenchymal stem cell (hMSC) adhesion studies confirmed that these cells are able to bind specifically to Scl2-2 and Scl2-3 proteins and that appropriate MAP kinase signaling is activated due to the selective integrin binding motifs. The current work examines the influence of integrin α_1 and α_2 binding on hMSC osteogenesis toward the goal of deconvoluting the impact of integrin-based interactions on associated cell behavior.

Scl2-1, Scl2-2 and Scl2-3 proteins were conjugated into poly(ethylene glycol) diacrylate (PEGDA) hydrogels and their effects on encapsulated human MSCs were evaluated. Specifically, following 2 weeks of culture, various osteogenic markers were examined in order to assess the impact of integrin α_1 and α_2 on the observed responses. hMSCs encapsulated in PEG-Scl2-3 gels showed increased expression of osterix and osteopontin relative to PEG-Scl2-2 gels. However, calcium deposition, considered by many to be the ultimate indicator of osteogenesis, was increased in PEG-Scl2-2 gels

relative to PEG-Scl2-3. Although these results appear to be contradictory, they may also reflect distinct transitional phenotypes en route to hMSCs becoming osteoblasts.

4.2. INTRODUCTION

Recent advances in adult mesenchymal stem cell (MSC) research have shown these cells to be a promising patient-derived cell source that may address many of the limitations of differentiated adult cells [3, 4]. Not only are they capable of extensive proliferation, but they also have the capacity to differentiate into a range of cell types [3, 5]. A number of 2D studies have demonstrated MSC osteogenic differentiation to be tightly regulated by cellular interactions with the surrounding extracellular matrix (ECM) [21, 18, 26-34]. However, comparatively, little is known regarding the effects of various ECM components in regulating MSC osteogenesis in 3D scaffold environments [17, 35-36]. This is significant since recent studies suggest that effects observed in 2D may not be indicative of the effects of the same scaffold variables in more biomimetic 3D culture systems.

Over the past ~20 years, the multiple facets of matrix-mediated signaling, beyond the identity and concentration of biochemical cues, have become increasingly appreciated [124]. For example, integrins, cell surface receptors which interact with a range of ECM proteins, were first recognized for their function in translating biopolymer identity into a cell response [49]. However, they also act as mechanical transducers by serving as organizing centers for focal adhesion complexes and associated cytoskeletal

networks [124, 125]. The profound effects of integrin-mediated translation of matrix elastic modulus on MSC lineage commitment has been elegantly demonstrated in 2D using collagen I-coated polyacrylamide gels [126].

Despite these advances, our understanding of cell behavior is not yet sufficient to enable the rational selection of stimuli to elicit desired cell responses [7, 8]. Towards this goal, we propose to investigate the impact of specific integrin binding sequences (integrin α_1 and α_2) on MSC osteogenesis in 3D contexts using a collagen-mimetic protein, Scl2, which was initially discovered by Dr. Lukomski of West Virginia University and Dr. Höök of Texas A&M Health Science Center [87, 127]. The "parent" Scl2 protein maintains the native triple helical structure of native collagen but contains no known cell signaling sequences [85,105]. Thus, Scl2 provides a "blank-slate" into which desired collagen-based, cell adhesion sequences can be programmed by site-directed mutagenesis while maintaining the triple helical context natively associated with these motifs.

Scl2 proteins were conjugated into poly(ethylene glycol) diacrylate (PEGDA) hydrogel networks. PEGDA hydrogels were selected as the base scaffold due to the broad tunability of their mechanical properties and their previous use in bone regeneration applications [45-48]. In addition, PEGDA hydrogels were selected to be used as the material platform since they function as biological "blank slates" in that they intrinsically resist protein adsorption and cell adhesion [13, 128, 129]. This characteristic will permit us to focus on the bioactive signals introduced into the hydrogels by the Scl2 proteins. Furthermore, pure PEGDA gels are highly biocompatible and degrade over a

period of 1-2 years by the hydrolysis of the ester bonds [130, 131], which will allow to keep the material degradation rate approximately constant within the time frame of our experiments.

In the present study, human MSCs were encapsulated within PEGDA hydrogels containing defined amounts of Scl2-1, Scl2-2 or Scl2-3 proteins. Following 14 days of culture, the levels of various markers of osteogenic differentiation markers (Runx2, osteopontin and osterix) were monitored and the deposition of ECM components associated with mature bone (calcium phosphate) was also assessed.

4.3. MATERIALS AND METHODS

4.3.1. Polymer and protein synthesis and characterization

4.3.1.1. PEG-diacrylate synthesis

PEGDA was prepared as previously described [50] by combining 0.1 mmol ml^{-1} dry PEG (3.4 kDa, Fluka), 0.4 mmol ml^{-1} acryloyl chloride and 0.2 mmol ml^{-1} triethylamine in anhydrous dichloromethane and stirring under argon overnight. The resulting solution was washed with 2 M K_2CO_3 and separated into aqueous and dichloromethane phases to remove HCl. The organic phase was subsequently dried with anhydrous $MgSO_4$, and PEGDA was precipitated in diethyl ether, filtered and dried under vacuum. Acrylation of the PEG end hydroxyl groups was characterized by proton nuclear magnetic resonance (^{1}H-NMR) to be ~96%.

4.3.1.2. Purification, expression and mutagenesis of Scl2 proteins

Desired bioactivity can be programmed into specific regions of the triple helix via site-directed mutagenesis of the gene encoding for Scl2. In conjunction with Dr. Russell of the Höök lab (Institute of Biosciences and Technology, Texas A&M University, System Health Science Center), two "daughter" Scl2s, Scl2-2 and Scl2-3, were engineered, which incorporate $\alpha_1\beta_1$ and/or $\alpha_2\beta_1$ integrin-binding motifs based on the collagen sequences GF/LOGER [20, 107] (O; hydroxyproline). Specifically, Scl2-2 and Scl2-3 were generated by encoding for sequences GFPGER and GFPGEN, respectively, using site-directed mutagenesis of the plasmid encoding for Scl2-1. Recombinant proteins were expressed using standard recombinant protein procedures in E. coli BL21 (Novagen) and purified by affinity chromatography on a HisTrap HP column (GE Healthcare). Protein purity was determined by sodium dodecyl sulfate–polyacrylamide gel electrophoresis (SDS–PAGE) followed by Coomassie blue staining. Furthermore, Scl2 proteins were dialyzed against water and stored at -20°C followed by lyophilization.

4.3.1.3. Synthesis of acrylate-derivatized Scl2 protein

In order to conjugate the different Scl2 proteins within the PEGDA-based hydrogel networks, Scl2-1, Scl2-2 and Scl2-3 were reacted with acryloyl-PEG-N-hydroxysuccinimide (ACRL-PEG-NHS, 3.4 kDa, Nektar, San Carlos, CA) at a 1:2 molar ratio for 2 h in 50mM sodium bicarbonate buffer, pH 8.5 [50]. The resulting

acrylate-derivatized products were purified by dialysis against double deionized water using a 10 kDa membrane, lyophilized and stored at -20 °C until use.

4.3.2. Cell culture and encapsulation

4.3.2.1. Cell culture

Cryopreserved hMSCs (Lonza) at passage 3 were thawed and expanded in monolayer culture per Lonza protocols. Prior to encapsulation, cells were maintained at 37 ºC and 5% CO2 in MesenPRO RSTM Media (Gibco) supplemented with 2% MesenPRO RSTM growth supplement (Gibco). Cells at passage 5–6 were harvested and allocated for hydrogel encapsulation.

4.3.2.2. Hydrogel encapsulation

Hydrogels were fabricated by preparing: 1.) a 20 wt% 3.4kDa PEGDA solution in HEPES-buffered saline (HBS) and 2.) individual solutions of 10 mg mL^{-1} acrylate-derivatized Scl2-1, Scl2-2 or Scl2-3 in double deionized water. A 300 mg ml^{-1} solution of UV photoinitiator 2,2-dimethoxy-2-phenyl-acetophenone in N-vinylpyrrolidone was added at 2 (v/v)% to the PEGDA mixture. The PEGDA and protein solutions were then separately sterilized by filtration, after which each protein solution was mixed with an equal volume of the 20 wt% PEGDA solution. Harvested hMSCs were resuspended in the resulting precursor solutions at $1.5x10^6$ cells mL^{-1}. The cell suspensions were then pipetted into molds composed of two glass plates separated by 0.75 mm polycarbonate

spacers and polymerized by 2 min exposure to longwave UV light (Spectroline, ~6 mW cm^{-2}, 365 nm). The resulting hydrogel was removed from each mold, rinsed with phosphate buffered saline (PBS, pH 7.4; Sigma) and immersed in DMEM supplemented with 10% MSC-qualified FBS and 1% PSA (PSA. 10,000 U mL^{-1} penicillin, 10,000 mg L^{-1} streptomycin, and 25 mg L^{-1} amphotericin; Gibco) at 37 ºC and 5% CO_2. After 3 h to allow for equilibrium swelling, the hydrogel slabs were separated into uniform gels discs using an 8 mm biopsy punch (Miltex). Each disc was transferred to a distinct 12-well culture insert fitted with a porous membrane (BD Biosciences). Following transfer of the gel discs, 1.5 mL of DMEM supplemented with 10% MSC-qualified FBS and 1% PSA and osteogenic supplements (0.1 μM dexamethasone, 50 μM ascorbate-2-phosphate and 10 mM β-glycerophosphate [132]) was added to each well. After 24 h of culture at 37 ºC and 5% CO_2, the media surrounding each sample was fully exchanged, after which full media changes were performed every two days during two weeks.

4.3.3. Day 0 hydrogel characterization

4.3.3.1. Average mesh size

PEGDA hydrogel mesh structure cannot be visualized using standard techniques such as scanning electron microscopy. In the present study, average hydrogel mesh size was therefore characterized via a series of dextran diffusion experiments based on an adaptation of the methodology of Watkins and Anseth [52]. In brief, samples were collected from the freshly prepared PEG-Scl2 hydrogels and allowed to swell overnight

at 37 °C in PBS containing 0.05% azide (PBS-azide). Eight-millimeter-diameter discs were then harvested from each gel formulation, and solutions containing 0.05 mg ml^{-1} fluorescently labeled dextran (10 kDa, Invitrogen) in PBS-azide were added at 1 ml per hydrogel disc. Dextran solutions were allowed to diffuse into the hydrogels for 24 h at 37 °C. Each gel disc was then gently blotted and transferred to 1 ml fresh PBS-azide. Dextran that had penetrated into the hydrogels was then permitted to diffuse out into the surrounding solution at 37 °C. After 24 h, the fluorescence of the PBS-azide solution surrounding each disc was measured at ex/em 488/532. Dextran standard curves were used to convert each fluorescence signal to a concentration. For each hydrogel, the measured dextran concentration was divided by gel weight [53]. The resulting value served as a quantitative indicator of hydrogel permissivity.

4.3.3.2. Hydrogel mechanical assessment

Mechanical analyses were conducted using a modification of the circumferential property testing technique validated in Johnson et al. [133] and Hiles et al. [134]. In brief, the dimensions of ring segments 2–4 cm in width were measured using digital calipers. These measures served as dimension inputs for subsequent stress and strain calculations and as swelling indicators. Each ring was mounted onto an Instron 3342 by threading opposing stainless steel hooks through the segment lumen. The hooks were then uniaxially separated at a rate of 6 mm min^{-1} until construct failure. As hook separation increased, the mounted ring was drawn into an increasingly oblong oval conformation. Johnson et al. confirmed that the force applied by the hooks to this oblong

oval could be approximated as being equally distributed between two parallel rectangles, each with sides equal to the width and wall thickness, h_v, of the ring. The gauge length, l_g, was taken to be the inner diameter, D_v, of the unstretched ring plus h_v, and the elastic modulus, E, of each sample was defined as the slope of the resulting stress–strain curve at a reference stress of 20 kPa [135]. Samples remained immersed in PBS until immediately prior to mechanical analyses, and testing was completed rapidly to avoid sample dehydration.

4.3.3.3. Cell density

Samples (n = 4) were collected from each freshly prepared hydrogel formulation following 24 h immersion in culture media. Hydrogel samples were digested for 72 h at 37 °C in 1 ml of 0.12 M NaOH per 0.2 g hydrogel wet weight [54, 55]. Aliquots of the hydrolyzed samples were neutralized, and their DNA content determined using the Invitrogen PicoGreen assay [56]. DNA measures were translated to cell number using a conversion factor of 6.6 pg DNA per cell [57]. Calf thymus DNA (Sigma) subjected to the same association with PEGDA and to the same digestion conditions as the samples served as a standard.

4.3.4. Endpoint analyses

At day 14 of culture, samples were harvested from each hydrogel formulation for mechanical, mesh size, DNA, calcium deposition and protein analyses (western blots).

Samples harvested for mechanical (n = 4 per formulation), mesh size (n = 4 per formulation) and DNA (n = 4 per formulation) assessments were evaluated according to the same protocols as the day 0 specimens. Samples collected for calcium deposition and protein analyses (n = 6 per formulation) were homogenized in lysis buffer (100 mM Tris-HCl, pH 7.5, 500 mM LiCl, 10 mM EDTA pH 8.0, 1% LiDS, 5 mM dithiothreitol (DTT)) and supernatant was isolated by centrifugation. A second extraction from the pellet was performed by freezing and thawing it three times, and the final solution was centrifuged one more time to isolate the supernatant, which was combined with the supernatant obtained from the homogenization. Protein levels were assessed via CBQCA protein quantitation kit (Molecular Probes). Isolated protein solutions were used for both calcium deposition measurements and western blot analyses.

4.3.4.1. Total calcium deposition.

To assess construct calcium levels, hydrogel discs (n = 6 per formulation) were homogenized in lysis buffer (100 mM Tris-HCl, pH 7.5, 500 mM LiCl, 10 mM EDTA pH 8.0, 1% LiDS, 5 mM dithiothreitol (DTT)) as described previously. Total calcium was quantified using 10 μl aliquots of each sample homogenate via the Calcium Cresolphthalein Complexone (CPC) liquid color kit (Stanbio).

4.3.4.2. Western blot analyses

Equal amounts of protein (20 μg per lane) were loaded into different wells of a 10% polyacrylamide gel and proteins were separated by electrophoresis. Before loading

the samples onto the gel, protein solutions were concentrated using 3,000 MWCO Amicon filter units (Millipore), and proteins were denatured by addition of β-mercaptoethanol solution and heating at 100 °C for 10 minutes. After electrophoresis, proteins were transferred to a nitrocellulose membrane (Thermo Scientific). The blot was cut into two parts, and washed twice with double distilled water for 5 minutes each time at room temperature. Blots were then blocked with a 5% BSA solution (Fraction V, Fisher Scientific) in Tris-buffered saline containing 0.1% Tween-20 (TBST; 25 mM Tris-HCl, pH. 7.5, 137 mM NaCl, 0.1% Tween 20) for 1 hour at room temperature. Following blocking incubation, blots were briefly rinsed with TBST. Each blot was incubated with the appropriate primary antibody diluted in TBST solution containing 5% BSA overnight at 4 °C. After washing three times with TBST solution, primary antibody bound to each blot was detected using an appropriate HRP or AP conjugated secondary antibody (Jackson Immunoresearch) diluted in TBST solution containing 5% BSA for 1 hour at room temperature. Blots were again washed three times with TBST solution, and signal was detected using a luminol reagent (SCBT) or an AP chemiluminescent solution (Novex). Imaging was performed using the molecular imager chemidoc XRS system (Biorad) and band intensity was quantified using Adobe Phothoshop.

Detection of Runx2, osteopontin (OPN) and osterix (OSX) proteins were performed using Runx2 (M-70) (1:500, Santa Cruz Biotechnology, California, USA, sc-10758), OPN (AKm2A1) (1:500, Santa Cruz Biotechnology, sc-21742) and OSX (M-15)-R (1:500, Santa Cruz Biotechnology, sc-22538-R) antibodies, respectively. Runx2, OPN and OSX levels were normalized with respect to beta actin levels (Abcam).

4.3.5. Statistical analyses

Data are reported as mean ± standard deviation. Comparison of sample means was performed by ANOVA followed by Tukey's post hoc test (SPSS software), $p < 0.05$.

4.4. RESULTS AND DISCUSSION

4.4.1. Hydrogel material properties and cell density

A range of scaffold properties, including modulus, permeability and degradation rate, have been found to impact MSC lineage progression. Therefore, in order to attribute differences in hMSC behavior across hydrogel formulations, specifically to initial differences in gel protein composition, it was important that the remaining hydrogel material properties could be considered consistent across gels. Hydrogels formed from pure PEGDA degrade slowly (over a period of 1–2 years) and resist cell-mediated gel contraction, ensuring consistent bulk gel properties over a broad time range [55, 56, 61-63]. In the present study, a 20:1 weight ratio of PEGDA to protein was therefore selected to ensure that the network properties of the resulting gels would be dominated by PEGDA. To confirm this, the modulus, mesh size, thickness and mass of the PEG–ECM hydrogels were characterized both at day 0 and at day 7.

As shown in Table 7, the initial elastic moduli of the PEG–Scl2-1, PEG–Scl2-2 and PEG–Scl2-3 gels were similar at ~158 kPa. To assess degradation and cell-mediated contraction, hydrogel modulus and thickness were evaluated across time in culture. Comparison of initial and endpoint mechanical data indicated that, hydrogel modulus remained consistent across formulations (Table 7). Similarly, average mesh size was consistent across hydrogels at both day 0 and day 7 (Table 7). The initial and endpoint thickness data for 8 mm gel discs indicated a negligible alteration in gel volume with time. In addition, net cell proliferation and loss were examined for each PEG–Scl2 hydrogel over the 14 day culture period. The cell density in each PEG–Scl2 hydrogel following 14 days of culture did not significantly changed from the initial seeding density (Table 8). Combined, the above data indicate that: (1) each hydrogel formulation maintained a consistent modulus throughout the study and (2) differences in cell responses among formulations can be attributed to differences in the initial proteins tethered to the gel network, their interactions with other molecules and subsequent neo-matrix deposition.

Table 7. Comparison of the average modulus and mesh size of 8 mm discs of each PEG–Scl2 hydrogel formulation with time in culture.[a]

Gel type	Modulus (kPa)		Mesh size (μg dextran/g-gel)[b]	
	Day 0	Day 14	Day 0	Day 14
PEG-Scl2-1	157.50 ± 2.12	155.50± 9.19	1.00 ± 0.01	1.00± 0.03
PEG-Scl2-2	158.50 ± 7.78	167.70± 2.31	0.98 ± 0.01	1.02± 0.03
PEG-Scl2-3	160.50 ± 0.00	163.50± 4.95	0.98 ± 0.01	1.01± 0.02

[a] Property results represent an average of n = 4 samples for each PEG-Scl2 formulation
[b] Mesh size data was normalized using Scl2-1 data

Table 8. Comparison of the average thickness, mass, and cell density in discs of each PEG–Scl2 hydrogel formulation with time in culture.[a]

Gel type	Thickness (mm)		Mass of 8mm discs (mg)		Cell density ($x10^6$)	
	Day 0	Day 14	Day 0	Day 14	Day 0	Day 14
PEG-Scl2-1	0.76 ± 0.01	0.78± 0.01	23.20 ± 0.14	22.90± 0.15	1.43± 0.04	1.47± 0.12
PEG-Scl2-2	0.76 ± 0.01	0.78± 0.01	23.20 ± 0.07	23.00± 0.12	1.33± 0.05	1.45± 0.08
PEG-Scl2-3	0.76 ± 0.01	0.77± 0.01	23.70 ± 0.14	22.40± 0.55	1.34± 0.07	1.33± 0.16

[a] Results represent an average of n = 4 samples for each PEG–Scl2 formulation.

4.4.2. Cell differentiation

The effect of collagen-mimetic proteins on the osteogenic differentiation of hMSCs was evaluated. Human MSCs in PEG-Scl2 hydrogels were cultured in osteogenic medium containing dexamethasone, ascorbic acid and β-glycerophosphate for 2 weeks. The extent of calcium deposition on the different hydrogel scaffolds was examined via Calcium CPC liquid color kit after this period of time. As shown in Figure 17, quantitative CPC assays revealed a significantly increase in calcium deposits in the PEG-Scl2-2 gels relative to the PEG-Scl2-3 gels ($p < 0.021$).

In addition to calcium deposition analyses, following 14 days of culture, osteogenic differentiation markers were examined by western blot assays (Table 9). As shown in Figure 18, day 14 levels of various osteogenic markers indicated significant differences among hydrogel formulations. Specifically, although Runx2 levels did not vary between the different hydrogel formulations, cells in PEG-Scl2-3 gels expressed significantly higher levels of osterix than in PEG-Scl2-1 and PEG-Scl2-2 formulations

($p < 0.001$ and $p = 0.027$, respectively). Also, osterix expression in PEG-Scl2-2 gels was significantly higher relative to PEG-Scl2-1 gels ($p = 0.002$). Regarding osteopontin expression, both PEG-Scl2-2 and PEG-Scl2-3 gels showed apparent higher levels than Scl2-1 gels; however, statistically differences were only found between PEG-Scl2-1 and PEG-Scl2-3 gels ($p = 0.027$).

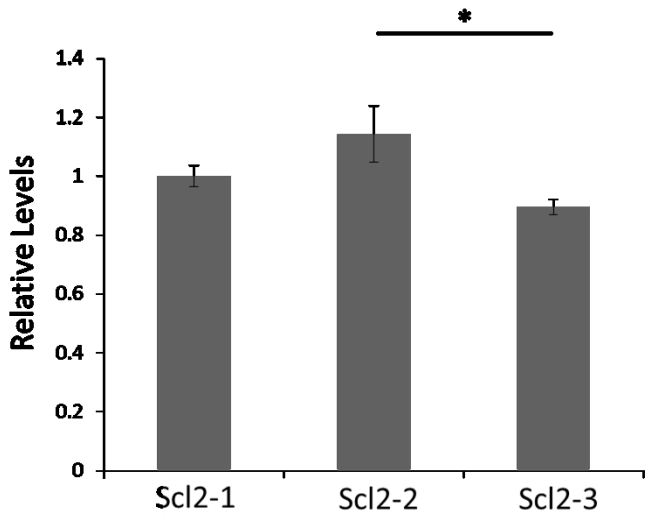

Figure 17. Calcium measures per hydrogel formulation (n = 6 per formulation). Hydrogel discs were homogenized and total calcium was quantified using 10 µl aliquots of each sample homogenate via the CPC liquid color kit.
*indicates a significant difference, $p < 0.05$.

Table 9. Osteogenic markers that were investigated in the present work.

Marker	Description
Runx2	Early osteogenic transcription factor
Osterix	Mid-term osteogenic transcription factor
Osteopontin	Bone ECM protein
Calcium deposition	Late-term bone marker

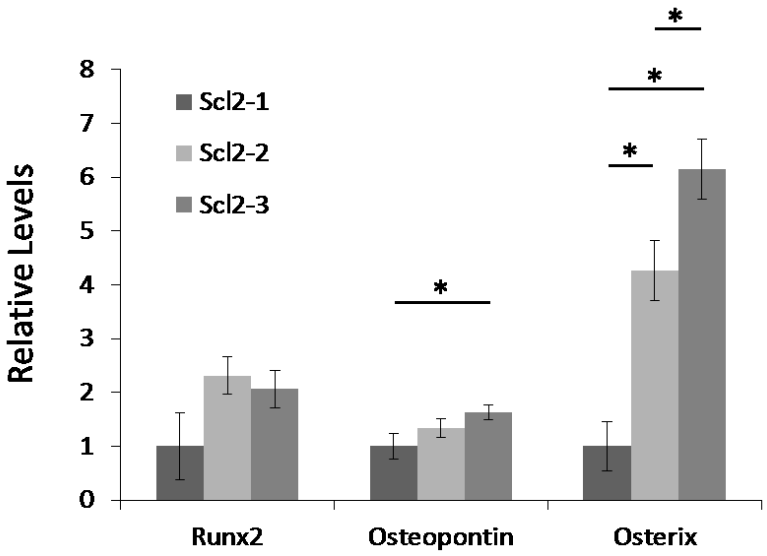

Figure 18. Expression of osteogenic markers osterix, osteopontin and Runx2 by western blot. For western blot assays, six samples per formulation (day 14) were analyzed. For the purpose of comparison, western blot measures for each protein have been normalized to the corresponding measure for PEG-Scl2-1 gels.
*indicates a significant difference, $p < 0.05$.

Data obtained for osterix and osteopontin expression indicated that PEG-Scl2-3 gels enhanced the osteogenic response of encapsulated hMSCs. Specifically, osterix and osteopontin levels in day 14 PEG-Scl2-3 gels were ~ 1.4- and 1.2-fold greater, respectively, than PEG-Scl2-2 gels. However, data collected for calcium deposition suggested that PEG-Scl2-2 gels enhanced osteogenic response of hMSCs since there was an increase in mineralization in PEG-Scl2-2 gels relative to PEG-Scl2-3 gels (~ 1.3- fold greater). The present results are consistent with previous studies in such as literature also presents conflicting reports regarding the osteoinductivity of integrin α_1 and α_2 units. Specifically, while several studies have suggested that both integrin α_1 and α_2 are involved in osteogenesis [136, 137], other studies have reported no involvement of

integrin α_1 [138, 139]. Clover et al. indicated that human bone cells primarily express integrin α_1 (osteoblasts) and integrin α_2 (osteoclasts) motifs. However, they found that expression of α_2 was independent on cell density, while expression α_1 was much greater in confluent cultures [136]. Similarly, Jikko et al. found that by function-perturbing α_1 and/or α_2 integrin subunits in murine 2T3 osteoblastic cells, not only the expression of early osteoblast markers was decreased more than 90% but also mineralization of these cells was blocked. In addition, they found that blocking by separate α_1 or α_2 integrin subunits produced partial effects by comparing the results when both subunits were perturbed combined [137]. In contrary to these studies, Foster et al. revealed that integrin α_2 plays a role in increased intracellular calcium upon cell adhesion to extracellular matrix in hMSCs differentiation toward osteoblasts [139]. Likewise, Popov et al. showed that integrin α_2 but not α_1 was significantly upregulated on osteogenic stimulation of human MSCs [138].

Several reports have also studied the independent osteoinductive role of either integrin α_1 or integrin α_2. In particular, Gronthos et al. found that incubating preosteoblasts with a function blocking antibody against integrin α_1 inhibited matrix mineralization [140]. In addition, Salaszynk et al. found that collagen I-coated surfaces stimulated human MSC matrix mineralization, and that cell interactions with these surfaces were initially mediated primarily by α_1 subunits (>90% of adhesive interactions) [26]. As with integrin α_1, integrin α_2 has also been associated with osteogenesis. Specifically, Mizuno et al. indicated that expression of osteoblastic phenotypes was suppressed by blocking the binding of integrin α_2 to collagen. Indeed,

they found a decrease of ~35% and ~50% in alkaline phosphatase and osteocalcin expression, respectively. Similarly, Reyes et al. demonstrated that α_2 integrin triggers the activation of multiple osteoblast-specific genes such as alkaline phosphatase, osteocalcin and bone sialoprotein as well as the induction of matrix mineralization in MC3T3-E1 murine immature osteoblast-like cells [141].

Although these results appear to be contradictory, they may also reflect distinct transitional phenotypes en route to hMSCs becoming osteoblasts [142]. Further work studying the influence of the initial cell signaling in osteogenesis will be conducted in order to try to better understand the influence of integrin α_1 and α_2 binding motifs in osteogenesis of hMSCs.

4.5. CONCLUSION

In the current study, toward the goal of deconvoluting the impact of integrin-based interactions on associated cell behavior, the influence of select integrin binding sequences on hMSC osteogenesis was investigated. Scl2-1, Scl2-2 and Scl2-3 proteins were conjugated into poly(ethylene glycol) diacrylate (PEGDA) hydrogels and their effects on encapsulated human MSCs were evaluated. Contradictory results were found in such as both PEG-Scl2-2 and PEG-Scl2-3 were osteoinductive. Nevertheless, this may reflect that by transmitting signals from the environment to the interior of the cell, the type of integrin expressed can influence osteogenic phenotypic behavior of hMSC. Finally, to gain insight into the origins of the found osteogenic responses, future work

that involves the study of p38 and FAK pathways in osteogenesis of hMSC will be necessary in order to establish its potential causative relationship with Scl2 proteins.

CHAPTER V

PRELIMINARY STUDY OF THE INFLUENCE OF THE P38 MAP KINASE SIGNALING IN HUMAN MESENCHYMAL STEM CELL OSTEOGENESIS USING A COLLAGEN-MIMETIC PROTEIN IN THREE DIMENSIONAL (3D) CONTEXTS

5.1. OVERVIEW

The results from the study of the effect of collagen-mimetic proteins in human mesenchymal stem cell osteogenesis were conflicting since both Scl2-2 and Scl2-3 were osteoinductive, but in different ways. To better understand the influence of the initial activation of cell signaling underlying these results, a series of experiments was conducted in which activation of p38 was inhibited. The p38 MAP kinase was selected for inhibition due to results from the study of the novel collagen-mimetic proteins that revealed that FAK and p38α MAP kinases were more activated when hMSCs were exposed to Scl2-2 protein relative to Scl2-3.

The presence of multiple MAP kinase signal transduction pathways and the extent to which each is activated during differentiation may reflect the integration of multiple signals and the balance among ERK, p38, and JNK MAP kinases. The current work examines the influence of p38α MAP kinase on osteogenic differentiation of hMSCs. However, chemical inhibitors could possibly affect more than one signaling pathway because of their reciprocal influence on cellular targets; therefore, different pathways will be analyzed as well as the osteogenic response of the cells.

Scl2-2 protein was conjugated into poly(ethylene glycol) diacrylate (PEGDA) hydrogels and p38 pathway was inhibited in order to evaluate its effect on encapsulated human MSC behavior. Specifically, MAP kinase shunts were examined at day 0 of the encapsulation in order to confirm p38 inhibition in response to the p38 inhibitor and to assess influence on the other MAP kinase pathways. In addition, following 2 weeks of culture, various osteogenic markers were examined in order to assess the impact of the p38 MAP kinase inhibition on the observed responses. The inhibition of the p38 pathway reduced the expression of osteogenic markers (Runx2, OPN and osterix), which suggest that this MAP kinase protein may regulate osteogenesis in hMSCs. Nevertheless, FAK activation was also reduced by inhibiting the p38 pathway. These results confirm that MAP kinase pathways play an important role in osteogenesis and that the extent to which each is activated during differentiation may reflect the integration of multiple signals.

5.2. INTRODUCTION

Several reports have shown opposing roles of the MAP kinase signaling pathways in osteogenic differentiation, which indicates that the role of the MAP kinase signaling pathway in osteoblastic differentiation is currently unclear. In fact, our results suggest that p38 and/or FAK pathways might be involved in osteogenesis of hMSCs. Also, several studies have shown that both FAK and p38 influence osteogenesis [18, 25, 31, 143-148]. Particularly, Salasznyka et al. indicated that by inhibiting FAK activation

by ~40%, osterix and osteogenic genes associated with osteogenic differentiation were reduced, results that suggest that FAK signaling plays an important role in regulating osteogenesis of hMSC [25]. In addition, Jaiswal et al. showed that p38 influences osteogenesis in the late stage by increasing alkaline phosphatase activity, and initiation of mineral deposition [145]. In the same way, Ortuno et al. revealed that BMP-2-activated p38 which enhances the transcriptional activity of osterix [146].

To establish the primary causative signaling mechanisms regulating osteogenic MSC differentiation in response to α_1 and α_2 integrin-mediated stimuli, human MSCs were encapsulated within PEGDA hydrogels containing defined amount of Scl2-2 protein and the p38 pathway was inhibited. Following encapsulation, MAP kinase shunts were examined in order to confirm p38 inhibition and to assess its influence in the other MAP kinases. Also, after 14 days of culture, the levels of various osteogenic markers (Runx2, osteopontin and osterix) were monitored in order to assess the impact of the p38 MAP kinase on the observed responses. Understanding the dominant signaling underlying particular cell behavior will allow biomaterials to be specifically designed to modulate these signaling cascades.

5.3. MATERIAL AND METHODS

5.3.1. Polymer and protein synthesis and characterization

5.3.1.1. PEG-diacrylate synthesis

PEGDA was prepared as previously described [50] by combining 0.1 mmol ml^{-1} dry PEG (3.4 kDa, Fluka), 0.4 mmol ml^{-1} acryloyl chloride and 0.2 mmol ml^{-1} triethylamine in anhydrous dichloromethane and stirring under argon overnight. The resulting solution was washed with 2 M K_2CO_3 and separated into aqueous and dichloromethane phases to remove HCl. The organic phase was subsequently dried with anhydrous $MgSO_4$, and PEGDA was precipitated in diethyl ether, filtered and dried under vacuum. Acrylation of the PEG end hydroxyl groups was characterized by proton nuclear magnetic resonance (^{1}H-NMR) to be ~96%.

5.3.1.2. Purification, expression and mutagenesis of Scl2 proteins

Desired bioactivity can be programmed into specific regions of the triple helix via site-directed mutagenesis of the gene encoding for Scl2. In conjunction with Dr. Russell of the Höök lab (Institute of Biosciences and Technology, Texas A&M University, System Health Science Center), two "daughter" Scl2s, Scl2-2 and Scl2-3, were engineered, which incorporate $\alpha_1\beta_1$ and/or $\alpha_2\beta_1$ integrin-binding motifs based on the collagen sequences GF/LOGER [20, 107](O; hydroxyproline). Specifically, Scl2-2 was generated by encoding for sequences GFPGER using site-directed mutagenesis of

the plasmid encoding for Scl2-1. Recombinant protein Scl2-2 was expressed using standard recombinant protein procedures in E. coli BL21 (Novagen) and purified by affinity chromatography on a StrepTrap HP column (GE Healthcare). Protein purity was determined by sodium dodecyl sulfate–polyacrylamide gel electrophoresis (SDS–PAGE) followed by Coomassie blue staining. Furthermore, Scl2 protein was dialyzed against water and stored at -20°C followed by lyophilization.

5.3.1.3. Synthesis of acrylate-derivatized Scl2 protein

In order to conjugate the different Scl2 proteins within the PEGDA-based hydrogel networks, Scl2-2 was reacted with acryloyl-PEG-N-hydroxysuccinimide (ACRL-PEG-NHS, 3.4 kDa, Nektar, San Carlos, CA) at a 1:2 molar ratio for 2 h in 50mM sodium bicarbonate buffer, pH 8.5 [50]. The resulting acrylate-derivatized products were purified by dialysis against double deionized water using a 10 kDa membrane, lyophilized and stored at -20 °C until use.

5.3.2. Cell culture and encapsulation

5.3.2.1. Cell culture

Cryopreserved hMSCs (Lonza) at passage 3 were thawed and expanded in monolayer culture per Lonza protocols. Prior to encapsulation, cells were maintained at 37 ºC and 5% CO2 in MesenPRO RSTM Media (Gibco) supplemented with 2%

MesenPRO RSTM growth supplement (Gibco). Cells at passage 5–6 were harvested and allocated for hydrogel encapsulation.

5.3.2.2. Hydrogel encapsulation

Hydrogels were fabricated by preparing: 1.) a 20 wt% 3.4kDa PEGDA solution in HEPES-buffered saline (HBS) and 2.) separate solutions of 10 mg mL^{-1} acrylate-derivatized Scl2-2 in double deionized water. A 300 mg ml^{-1} solution of UV photoinitiator 2,2-dimethoxy-2-phenyl-acetophenone in N-vinylpyrrolidone was added at 2 (v/v)% to the PEGDA mixture. The PEGDA and protein solutions were then separately sterilized by filtration, after which each protein solution was mixed with an equal volume of the 20 wt% PEGDA solution. Harvested hMSCs were resuspended in the resulting precursor solutions at $1.5x10^6$ cells ml^{-1}. The cell suspensions were then pipetted into molds composed of two glass plates separated by 0.75 mm polycarbonate spacers and polymerized by 2 min exposure to longwave UV light (Spectroline, ~6 mW cm^{-2}, 365 nm). The resulting hydrogel was removed from each mold, rinsed with phosphate buffered saline (PBS, pH 7.4; Sigma) and immersed in DMEM supplemented with 10% MSC-qualified FBS and 1% PSA (PSA. 10,000 U mL^{-1} penicillin, 10,000 mg L^{-1} streptomycin, and 25 mg L^{-1} amphotericin; Gibco) at 37 ºC and 5% CO_2. After 1 h to allow for equilibrium swelling, cells were exposed to p38 inhibitor (SB203580,Cell signaling) at 10 μM. Inhibitor was dissolved in DMSO, and therefore the control gel received equivalent volumes of vehicle (DMSO). The DMSO concentration did not exceed 0.1% of the medium volume. After 6 h of culture at 37 ºC and 5% CO_2, the

hydrogel slabs were separated into uniform gels discs using an 8 mm biopsy punch (Miltex). Each disc was transferred to a distinct 12-well culture insert fitted with porous membrane (BD Biosciences). Following transfer of the gel discs, 1.5 mL of DMEM supplemented with 10% MSC-qualified FBS and 1% PSA and osteogenic supplements (0.1 μM dexamethasone, 50 μM ascorbate-2-phosphate and 10 mM β-glycerophosphate [132]) with inhibitor supplementation was added to each well. After 24 h of culture at 37 ºC and 5% CO2, the media surrounding each sample was fully exchanged, after which full media changes were performed every two days during two weeks.

5.3.3. Day 0 hydrogel characterization

5.3.3.1. Average mesh size

PEGDA hydrogel mesh structure cannot be visualized using standard techniques such as scanning electron microscopy. In the present study, average hydrogel mesh size was therefore characterized via a series of dextran diffusion experiments based on an adaptation of the methodology of Watkins and Anseth [52]. In brief, samples were collected from the freshly prepared PEG-Scl2 hydrogels and allowed to swell overnight at 37 °C in PBS containing 0.05% azide (PBS-azide). Eight-millimeter-diameter discs were then harvested from each gel formulation, and solutions containing 0.05 mg ml^{-1} fluorescently labeled dextran (10 kDa, Invitrogen) in PBS-azide were added at 1 ml per hydrogel disc. Dextran solutions were allowed to diffuse into the hydrogels for 24 h at 37 °C. Each gel disc was then gently blotted and transferred to 1 ml fresh PBS-azide.

Dextran that had penetrated into the hydrogels was then permitted to diffuse out into the surrounding solution at 37 °C. After 24 h, the fluorescence of the PBS-azide solution surrounding each disc was measured at ex/em 488/532. Dextran standard curves were used to convert each fluorescence signal to a concentration. For each hydrogel, the measured dextran concentration was divided by gel weight [53]. The resulting value served as a quantitative indicator of hydrogel permissivity.

5.3.3.2. Hydrogel mechanical assessment

Mechanical analyses were conducted using a modification of the circumferential property testing technique validated in Johnson et al. [133] and Hiles et al. [134]. In brief, the dimensions of ring segments 2–4 cm in width were measured using digital calipers. These measures served as dimension inputs for subsequent stress and strain calculations and as swelling indicators. Each ring was mounted onto an Instron 3342 by threading opposing stainless steel hooks through the segment lumen. The hooks were then uniaxially separated at a rate of 6 mm min^{-1} until construct failure. As hook separation increased, the mounted ring was drawn into an increasingly oblong oval conformation. Johnson et al. confirmed that the force applied by the hooks to this oblong oval could be approximated as being equally distributed between two parallel rectangles, each with sides equal to the width and wall thickness, h_v, of the ring. The gauge length, l_g, was taken to be the inner diameter, D_v, of the unstretched ring plus h_v, and the elastic modulus, E, of each sample was defined as the slope of the resulting stress–strain curve at a reference stress of 20 kPa [135]. Samples remained immersed in PBS until

immediately prior to mechanical analyses, and testing was completed rapidly to avoid sample dehydration.

5.3.4. Initial and final analyses

5.3.4.1. Protein extraction

After 6 h of culture, samples were harvested from each hydrogel formulation in order to confirm p38 pathway inhibition by western blots. Samples were collected (n = 6 per formulation) and homogenized in cell extraction buffer supplemented with protease and phosphate inhibitors (1% Triton, 0.1% SDS, 10 mM sodium fluoride, 1 mM sodium pyrophosphate, 2 mM sodium orthovanadate, 1x protease cocktail (Thermo Scientific) in PBS). Supernatant was isolated by centrifugation, and a second extraction from the pellet was performed by freezing and thawing it three times. The final solution was centrifuged one more time to isolate the supernatant, which was combined with the supernatant obtained from the homogenization. Protein levels of the resulting lysates were measured by the Bio-Rad DC protein assay. The activation of FAK, ERK1/2 and p38 MAP kinases was evaluated using western blot assay.

Similarly, at day 14 of culture, samples were harvested from each hydrogel formulation for protein analyses (western blots). Samples collected for protein analyses (n = 6 per formulation) were homogenized in lysis buffer (100 mM Tris-HCl, pH 7.5, 500 mM LiCl, 10 mM EDTA pH 8.0, 1% LiDS, 5 mM dithiothreitol (DTT)). Proteins were extracted according to the same protocol followed for the after 6 h specimens.

Protein levels were assessed via CBQCA protein quantitation kit (Molecular Probes). Isolated protein solutions were used for western blot analyses.

5.3.4.2. Western blot analyses

Equal amount of protein (10 or 20 μg per lane) were loaded into different wells of a 10% polyacrylamide gel and proteins were separated by electrophoresis. Before loading the samples onto the gel, protein solutions were concentrated using 3,000 MWCO Amicon filter units (Millipore), and proteins were denatured by addition of β-mercaptoethanol solution and heating at 100 °C for 10 minutes. After electrophoresis, proteins were transferred to a nitrocellulose membrane (Thermo Scientific). The blot was cut into two parts, and wash twice with double distilled water for 5 minutes each time at room temperature. Blots were then blocked with a 5% BSA solution (Fraction V, Fisher Scientific) in Tris-buffered saline containing 0.1% Tween-20 (TBST; 25 mM Tris-HCl, pH. 7.5, 137 mM NaCl, 0.1% Tween 20) for 1 hour at room temperature. After blocking incubation, blots were briefly rinsed once with TBST. Each blot was incubated with the appropriate primary antibody diluted in TBST solution containing 5% BSA overnight at 4 °C. Further details of antibodies can be found in Table 10. After washing three times with TBST solution, 5 minutes each time at room temperature, primary antibody bound to each blot was detected using an appropriated HRP or AP conjugated secondary antibody (Jackson Immunoresearch) diluted in TBST solution containing 5% BSA for 1 hour at room temperature. Blots were again washed three times with TBST solution, 5 minutes each time at room temperature, and signal was

detected using a luminol reagent (SCBT) or an AP chemiluminescent solution (Novex). Imaging was performed using the molecular imager chemidoc XRS system (Biorad) and band intensity was quantified using Adobe Phothoshop.

5.3.5. Statistical analyses

Data are reported as mean ± standard deviation. Comparison of sample means was performed by ANOVA followed by Tukey's post hoc test (SPSS software), $p < 0.05$.

Table 10. Antibodies employed in western blot assays

Antibody	Clone	Supplier	*Western blot*
FAK	C-20	SCBT	√
p-FAK	Tyr 397	MP	√
ERK1	K-23	SCBT	√
p-ERK1/2	12E4	SCBT	√
p38α	F-9	SCBT	√
p-p38	Thr 180/ Tyr 182	SCBT	√
Runx2	M-70	SCBT	√
Osteopontin	AKm2A1	SCBT	√
Osterix	M-15-R	SCBT	√
Beta actin	mAbcam 8226	Abcam	√

[†]Abbreviations: MP – Millipore; SCBT – Santa Cruz Biotechnology

5.4. RESULTS AND DISCUSSION

The present study was designed to try to better understand the influence of p38 MAP pathway in osteogenesis of hMSC in order to establish its potential causative relationship with Scl2 proteins. Toward this goal, hMSCs were encapsulated in PEG-Scl2-2 hydrogel networks and p38 pathway was inhibited during 2 weeks of culture. After this time, osteogenic markers were evaluated using western blot assays.

5.4.1. Hydrogel material properties

A range of scaffold properties, including modulus, permeability and degradation rate, have been found to impact MSC lineage progression. Therefore, in order to attribute differences in hMSC behavior across hydrogel formulations, specifically to p38 inhibition, it was important that the remaining hydrogel material properties could be considered consistent across formulations. Hydrogels formed from pure PEGDA degrade slowly (over a period of 1–2 years) and resist cell-mediated gel contraction, ensuring consistent bulk gel properties over a broad time range [55, 56, 61-63]. In the present study, a 20:1 weight ratio of PEGDA to protein was therefore selected to ensure that the network properties of the resulting gels would be dominated by PEGDA. To confirm this, the modulus, mesh size, thickness and mass of the PEG–ECM hydrogels were characterized after encapsulation.

As shown in Table 11, the initial elastic moduli of the PEG–Scl2-2 p38 (gel that was cultured with media supplemented with p38 inhibitor) and PEG–Scl2-2 DMSO (control gel) hydrogels were similar at ~158 kPa. Similarly, average mesh size was not significantly different across hydrogels (Table 11). In addition, the initial thickness data for 8 mm gel discs was also consistent among formulations. Combined, the above data indicate that: (1) each hydrogel formulation has similar mechanical properties and (2) differences in cell responses among formulations can be attributed to differences in cell culture conditions that were used for the hydrogels, their interactions with other molecules and subsequent neo-matrix deposition.

Table 11. Comparison of the average modulus and mesh size of 8 mm discs of each PEG–Scl2 hydrogel formulation with time in culture.[a]

Gel type	Modulus (kPa)	Mesh size (μg dextran/g-gel)	Thickness (mm)	Mass of 8mm discs (mg)
PEG-Scl2-2 p38	158.30± 4.04	0.021± 0.001	0.760 ± 0.002	22.20 ± 0.12
PEG-Scl2-2 DMSO	158.00± 2.83	0.020± 0.001	0.770 ± 0.006	23.60 ± 0.28

[a] Property results represent an average of n = 4 samples for each PEG-Scl2 formulation

5.4.2. Inhibition studies

To study the influence of the p38 MAP kinase pathway in osteogenesis of hMSCs, a specific p38 inhibitor was used (SB203580). Human MSCs were encapsulated in PEG-Scl2-2 hydrogels, and cells were exposed to p38 inhibitor at 10 μM. Inhibitor was dissolved in DMSO, and therefore the control gel received equivalent volumes of

vehicle (DMSO). After 6 hours of cells being exposed to the inhibitor, samples were collected and protein was extracted in order to confirm the appropriate inhibition of p38 MAP kinase pathway. Immunoblotting was employed to examine the inhibition; for this purpose, a phosphorylated site-specific primary antibody directed against T180/Y182 p38 was used. The respective total protein (p38) was also analyzed using immunoblots. Band intensities were computed, and the activated fraction of MAP kinase protein under study was calculated by dividing the band intensity of the phosphorylated protein by the respective band intensity of the total protein. As illustrated in Figure 19, a significant decrease was observed in the activated fraction of p38 for PEG-Scl2-2 p38 gel compared to PEG-Scl2-2 DMSO gel, which suggests that p38 pathway was inhibited.

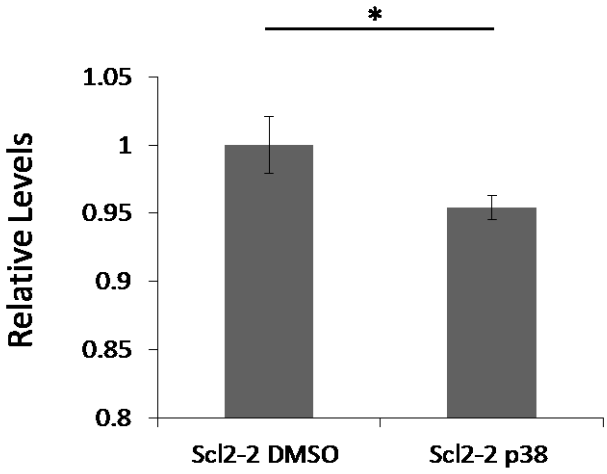

Figure 19. Relative levels of activated p38 (pp38/p38) for the different hydrogel formulations. Data of Scl2-2 DMSO was used for normalization.
*indicates a significant difference, $p < 0.05$.

Although the reagent used for inhibiting the activation of p38 MAP kinase is considered to be selective, the activation of FAK and ERK1/2 pathways was also

examined at day 0 (after 6 hours) of encapsulation to assess potential secondary effects of p38 inhibition on other MAP kinases (Figure 20). Phosphorylated site-specific primary antibodies directed against TYR 397 FAK and T202/Y204 ERK were used, and the respective total proteins (FAK and ERK) were also analyzed. Comparing the levels of activation of FAK protein between PEG-Scl2-2 p38 and PEG-Scl2-2 DMSO hydrogels, phosphorylation of FAK was significantly lower in PEG-Scl2-2 p38 relative to PEG-Scl2-2 DMSO. On the contrary, the active fraction for ERK1/2 was similar in both hydrogels (i.e. a significant difference was not observed). Cumulatively, the present data associated with initial activation of MAP kinase signaling suggested that 1) appropriate inhibition of p38 MAP kinase was observed after 6 hours of encapsulation, 2) FAK and p38 pathways may have a crosstalk relationship since FAK activation was also reduced in the hydrogel that was exposed to the p38 inhibitor and 3) cell responses may be associated with inhibition of p38α and FAK MAP kinases.

5.4.3. Cell differentiation

The effect of p38α pathway on the osteogenic differentiation of hMSCs was evaluated. Human MSCs in PEG-Scl2-2 hydrogels were cultured in osteogenic medium containing dexamethasone, ascorbic acid and β-glycerophosphate and p38 inhibitor for 2 weeks. Following this time, osteogenic differentiation markers were examined by western blot assays. As shown in Figure 21, day 14 levels of various osteogenic markers indicated significant differences among hydrogel formulations. Specifically, cells in

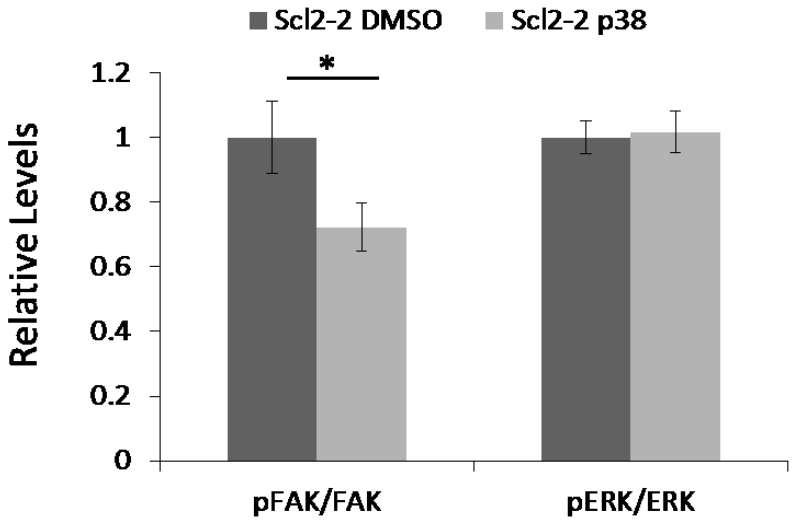

Figure 20. Activated fraction of FAK and ERK1/2 MAP kinase proteins that was investigated. Data of Scl2-2 DMSO was used for normalization.
*indicates a significant difference, $p < 0.05$.

PEG-Scl2-2 DMSO gels expressed significantly higher levels of osteopontin than PEG-Scl2-2 p38 hydrogels ($p = 0.04$). Also, Runx2 and osterix expression had an apparent, although not statistically significant, decrease in PEG-Scl2-2 p38 gels compared to PEG-Scl2-2 DMSO gels. These data suggests that the p38 pathway may be involved in osteogenesis of hMSCs. However, its influence was not completely isolated since FAK activation was also affected with the inhibition of p38 MAP kinase.

That said, the current results suggest that p38 inhibition decreases osteopontin levels, in contrast to initial results which indicated initial p38 activation decreases osteopontin levels. This may be due to complex temporal integration of signals over 14 days of culture. However, it may also be due to the fact that inhibition of one of the MAP kinase proteins does not imply that the remaining proteins involved in MAP kinase pathways will not be enhanced or inhibited, as well. As noted above, FAK activation

decreased by the inhibition of p38 pathway but ERK activation was not affected. JNK MAP kinase is another critical shunt in the MAP kinase pathway that may potentially be affected by p38 inhibition. There are several reports that have shown that JNK MAP kinase plays an important role in osteogenesis [145, 149, 150]. In particular, Guicheux et al. reported that both p38 and JNK pathways are involved in osteogenesis. Indeed, they showed that inhibition of p38 was associated with decreased alkaline phosphatase (ALP) activity, and that inhibition of JNK was associated with a reduction in osteocalcin (OC) production [149]. In addition, Jaiswal et al. showed that JNK activation plays a role in the late stage of osteogenic differentiation since its activation was related with extracellular matrix synthesis and increased calcium deposition, the two hallmarks of bone formation [145]. As a result, future work will require to include investigation of the JNK pathway in hMSC osteogenesis in order to better understand the potential causative relationship with Scl2 proteins, specifically, and the signaling induced by their integrin α_1 and α_2 binding sequences.

The present results and the data obtained in the study of the effect of collagen-mimetic proteins in human mesenchymal stem cell osteogenesis could explain the temporal relationships of kinase activation. The cumulative data suggests that FAK and p38 MAP kinases could be activated at different times, and likely regulate distinct biological functions in osteogenesis, such as commitment, differentiation and maturation. In order to gain a more detailed understanding of the reciprocal influence of MAP kinase proteins in osteogenesis, study of their activation thorough time is necessary as well as how the different osteogenic markers that were investigated vary

with time. Consequently, future studies that involve the analysis of MAP kinase activation and osteogenic marker progression at an increased number of time points will be necessary in order to help to better understand the crosstalk that may exist between the different MAP kinase pathways in osteogenesis. This will help to gain insight in the influence of the initial activation that is mediated by integrin α_1 and α_2 binding sequences.

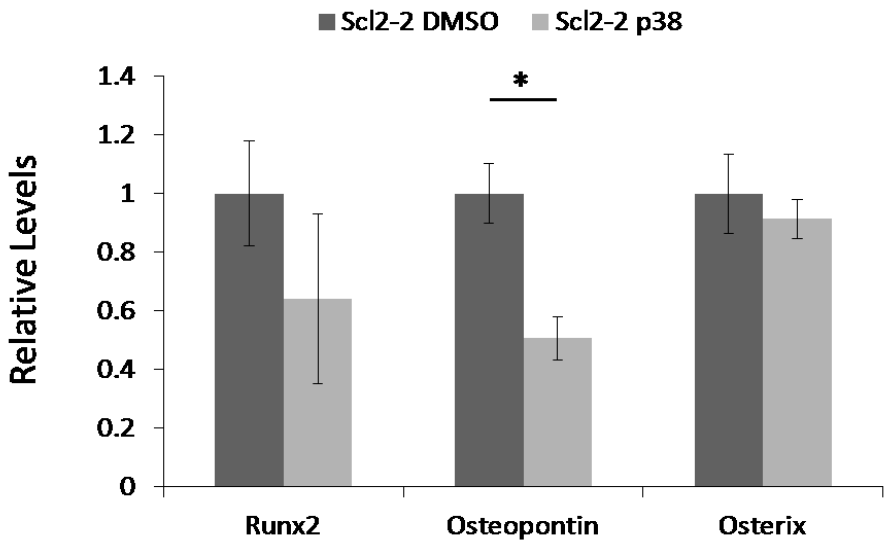

Figure 21. Expression of osteogenic markers osterix, osteopontin and Runx2 by western blot. For western blot assays, six samples per formulation (day 14) were analyzed. For the purpose of comparison, western blot measures for each protein have been normalized to the corresponding measure for Scl2-2 DMSO gel.
*indicates a significant difference, $p < 0.05$.

5.5. CONCLUSION

In the current study, the influence of p38 MAP kinase was investigated toward the goal of deconvoluting the impact of integrin α_1 and α_2 in hMSC osteogenesis. Scl2-2

protein was conjugated into PEGDA hydrogels and p38 pathway was inhibited to evaluate its effect on osteogenic differentiation of encapsulated human MSCs. The inhibition of p38 pathway reduced the expression of osteogenic markers (Runx2, OPN and osterix), which suggest that this MAP kinase protein may regulate osteogenesis in hMSCs. Nevertheless, FAK activation was also reduced by inhibiting p38 pathway. These results confirm that MAP kinase pathways play an important role in osteogenesis and that the extent to which each is activated during differentiation may reflect the integration of multiple signals and the balance among FAK, ERK1/2 and p38 MAP kinases; as a result, further research is needed for investigation of detailed mechanism of osteogenesis regulation. Finally, to gain insight into the origins of the found conflicting osteogenic responses, future studies that involve the analysis of MAP kinase activation and osteogenic marker progression at an increased number of time points will be necessary in order to help to better understand the crosstalk that may exist between the different MAP kinase pathways in osteogenesis.

CHAPTER VI

CONCLUSIONS

In this work, the first aim was to compare the osteoinductivity of select ECM components in defined 3-D environments toward the improved design of osteogenic scaffolds. The ECM components were examined within the context of scaffolds with osteogenic moduli. The associated temporal evolution in MSC lineage progression and integrin profiles were then characterized, and results indicated that both FG and LN enhanced the osteogenic response of encapsulated 10T½ cells. To gain insight into the origins of the osteogenic response associated with FG and LN, the integrin-based interactions supported by these ECM components were investigated. The results indicated that integrin α_2 and α_6 appeared to play an important role in MSC osteogenic differentiation.

Nonetheless, although results revealed that FG and LN supported osteogenesis and that integrin α_2 and α_6 play a role, native biomolecules such as FG and LN also support an array of additional signals which guide cell behavior. Consequently, the results cannot be definitively linked to integrin α_2 and α_6 signaling. In order to address this limitation, we proposed to probe MSC osteogenic response to collagen-based biochemical motifs using novel hybrid hydrogels. Collagen-mimetic protein, termed Scl2-1, provided a "blank-slate" into which desired collagen adhesion sequences were programmed by site-directed mutagenesis to include receptor binding motifs that interact with α_1 and/or α_2 integrin subunits (Scl2-2 and Scl2-3). In this way, the collagen-

mimetic proteins Scl2-1, Scl2-2, and Scl2-3 were functionalized with photocrosslinking sites to enable incorporation into a three dimensional hydrogel matrix. Bioactive hydrogels were then fabricated by combining the functionalized Scl2s with PEGDA and photocrosslinking via exposure to UV light. Characterization studies confirmed that the functionalization of the Scl2 proteins did not disrupt triple helix conformation, integrin binding, or cell adhesion. Also, initial cell studies confirmed specific hMSC adhesion to Scl2-2 and Scl2-3 proteins and appropriate activation of different MAP kinase pathways (FAK, p38α and ERK1/2) due to selective integrin binding.

Furthermore, the current work also examined the influence of integrin α_1 and α_2 binding on hMSC osteogenesis toward the goal of deconvoluting the impact of integrin-based interactions on associated cell behavior. Scl2-1, Scl2-2 and Scl2-3 proteins were conjugated into PEGDA hydrogels and their effects on encapsulated human MSCs were evaluated. Following 2 weeks of culture, various osteogenic markers were examined in order to assess the impact of integrin α_1 and α_2 on the observed responses. Contradictory results were found in that both PEG-Scl2-2 and PEG-Scl2-3 were osteoinductive, but in different ways. Finally, to gain insight into the origins of the observed osteogenic responses, the influence of the p38α pathway in hMSC osteogenesis was investigated in order to establish its potential causative relationship with Scl2 proteins. The results of the p38 inhibition studies showed that the inhibition of the p38 pathway reduced the expression of osteogenic markers (Runx2, OPN and osterix), which suggest that this MAP kinase protein may regulate osteogenesis in hMSCs. Nevertheless, FAK activation was also reduced by inhibiting the p38 pathway. These results confirm that MAP kinase

pathways play an important role in osteogenesis and that the extent to which each is activated during differentiation may reflect the integration of multiple signals and the balance among FAK, ERK1/2 and p38 MAP kinases.

Further research is needed for investigation of detailed mechanism of osteogenesis regulation. Specifically, to gain insight into the origins of the observed conflicting osteogenic responses, future studies that involve the analysis of MAP kinase activation and osteogenic marker progression at an increased number of time points will be necessary in order to help to better understand the crosstalk that may exist between the different MAP kinase pathways in osteogenesis. This should significantly advance our understanding of the processes associated with MSC osteogenic progression and ultimately allow the design of improved osteogenic scaffolds.

REFERENCES

1. Langer, R. and Vacanti, J.P., *Tissue engineering.* Science., 1993. **260**(5110): p. 920-926.

2. Lavik, E. and Langer, R., *Tissue engineering: current state and perspectives.* Appl Microbiol Biotechnol., 2004. **65**(1): p. 1-8.

3. Tuan, R.S., Boland, G. and Tuli, R., *Adult mesenchymal stem cells and cell-based tissue engineering.* Arthritis Res Ther., 2003. **5**(1): p. 32-45.

4. Shanti, R.M., et al., *Adult mesenchymal stem cells: biological properties, characteristics, and applications in maxillofacial surgery.* J Oral Maxillofac Surg., 2007. **65**(8): p. 1640-1647.

5. Pittenger, M.F., et al., *Multilineage potential of adult human mesenchymal stem cells.* Science., 1999. **284**(5411): p. 143-147.

6. Dawson, E., et al., *Biomaterials for stem cell differentiation.* Adv Drug Deliv Rev., 2008. **60**(2): p. 215-228.

7. Guilak, F., et al., *Control of stem cell fate by physical interactions with the extracellular matrix.* Cell Stem Cell., 2009. **5**(1): p. 17-26.

8. Kolf, C.M., Cho, E. and Tuan, R.S., *Mesenchymal stromal cells. Biology of adult mesenchymal stem cells: regulation of niche, self-renewal and differentiation.* Arthritis Res Ther., 2007. **9**(1): p. 204-210.

9. McBeath, R., et al., *Cell shape, cytoskeletal tension, and RhoA regulate stem cell lineage commitment.* Dev Cell., 2004. **6**: p. 483-495.

10. Sordella, R., et al., *Modulation of Rho GTPase signaling regulates a switch between adipogenesis and myogenesis*. Cell., 2003. **113**(2): p. 147-158.

11. Salinas, C.N., et al., *Chondrogenic differentiation potential of human mesenchymal stem cells photoencapsulated within poly(ethylene glycol)-arginine-glycine-aspartic acid-serine thiol-methacrylate mixed-mode networks.* Tissue Eng., 2007. **13**(5): p. 1025-1034.

12. Connelly, J.T., Garcia, A.J. and Levenston, M.E., *Inhibition of in vitro chondrogenesis in RGD-modified three-dimensional alginate gels.* Biomaterials., 2007. **28**(6): p. 1071-1083.

13. Gombotz, W.R., et al., *Protein adsorption to poly(ethylene oxide) surfaces.* J Biomed Mater Res., 1991. **25**(12): p. 1547-1562.

14. Rowley, J.A., Madlambayan, G. and Mooney, D.J., *Alginate hydrogels as synthetic extracellular matrix materials.* Biomaterials., 1999. **20**(1): p. 45-53.

15. Simmons, C.A., et al., *Cyclic strain enhances matrix mineralization by adult human mesenchymal stem cells via the extracellular signal-regulated kinase (ERK1/2) signaling pathway.* J Biomech., 2003. **36**(8): p. 1087-1096.

16. Klees, R.F., et al., *Laminin-5 activates extracellular matrix production and osteogenic gene focusing in human mesenchymal stem cells.* Matrix Biol., 2007. **26**(2): p. 106-114.

17. Lund, A.W., Stegemann, J.P. and Plopper, G.E., *Inhibition of ERK promotes collagen gel compaction and fibrillogenesis to amplify the osteogenesis of human mesenchymal stem cells in three-dimensional collagen I culture.* Stem Cells Dev., 2009. **18**(2): p. 331-341.

18. Kundu, A.K. and Putnam, A.J., *Vitronectin and collagen I differentially regulate osteogenesis in mesenchymal stem cells.* Biochem Biophys Res Commun., 2006. **347**(1): p. 347-357.

19. Heino, J., *The collagen receptor integrins have distinct ligand recognition and signaling functions.* Matrix Biol., 2000. **19**(4): p. 319-323.

20. Xu, Y., et al., *Multiple binding sites in collagen type I for the integrins alpha1beta1 and alpha2beta1.* J Biol Chem., 2000. **275**(50): p. 38981-38989.

21. Hallmann, R., et al., *Expression and function of laminins in the embryonic and mature vasculature.* Physiol Rev., 2005. **85**(3): p. 979-1000.

22. Mann, B.K., et al., *Modification of surfaces with cell adhesion peptides alters extracellular matrix deposition.* Biomaterials., 1999. **20**(23-24): p. 2281-2286.

23. Gobin, A.S. and West, J.L., *Val-ala-pro-gly, an elastin-derived non-integrin ligand: smooth muscle cell adhesion and specificity.* J Biomed Mater Res A., 2003. **67**(1): p. 255-259.

24. Klees, R.F., et al., *Dissection of the osteogenic effects of laminin-332 utilizing specific LG domains: LG3 induces osteogenic differentiation, but not mineralization.* Exp Cell Res., 2008. **314**(4): p. 763-73.

25. Salasznyk, R.M., et al., *Focal adhesion kinase signaling pathways regulate the osteogenic differentiation of human mesenchymal stem cells.* Exp Cell Res., 2007. **313**(1): p. 22-37.

26. Salasznyk, R.M., et al., *Adhesion to vitronectin and collagen I promotes osteogenic differentiation of human mesenchymal stem cells.* J Biomed Biotechnol., 2004. **2004**(1): p. 24-34.

27. Klees, R.F., et al., *Laminin-5 induces osteogenic gene expression in human mesenchymal stem cells through an ERK-dependent pathway.* Mol Biol Cell., 2005. **16**(2): p. 881-890.

28. Salasznyk, R.M., et al., *ERK signaling pathways regulate the osteogenic differentiation of human mesenchymal stem cells on collagen I and vitronectin.* Cell Commun Adhes., 2004. **11**(5-6): p. 137-153.

29. Xiao, G., et al., *Bone morphogenetic proteins, extracellular matrix, and mitogen-activated protein kinase signaling pathways are required for osteoblast-specific gene expression and differentiation in MC3T3-E1 cells.* J Bone Miner Res., 2002. **17**(1): p. 101-110.

30. Xiao, G., et al., *Role of the alpha2-integrin in osteoblast-specific gene expression and activation of the Osf2 transcription factor.* J Biol Chem., 1998. **273**(49): p. 32988-32994.

31. Salasznyk, R.M., et al., *Activation of FAK is necessary for the osteogenic differentiation of human mesenchymal stem cells on laminin-5.* J Cell Biochem., 2007. **100**(2): p. 499-514.

32. Huang, C.H., et al., *Interactive effects of mechanical stretching and extracellular matrix proteins on initiating osteogenic differentiation of human mesenchymal stem cells.* J Cell Biochem., 2009. **108**(6): p. 1263-1273.

33. Kundu, A.K., Khatiwala, C.B. and Putnam, A.J., *Extracellular matrix remodeling, integrin expression, and downstream signaling pathways influence the osteogenic differentiation of mesenchymal stem cells on poly(lactide-co-glycolide) substrates.* Tissue Eng Part A., 2009. **15**(2): p. 273-283.

34. Takeuchi, Y., Nakayama, K. and Matsumoto, T., *Differentiation and cell surface expression of transforming growth factor-beta receptors are regulated by interaction with matrix collagen in murine osteoblastic cells.* J Biol Chem., 1996. **271**(7): p. 3938-3944.

35. Benoit, D.S., Durney, A.R. and Anseth, K.S., *The effect of heparin-functionalized PEG hydrogels on three-dimensional human mesenchymal stem cell osteogenic differentiation.* Biomaterials., 2007. **28**(1): p. 66-77.

36. Hwang, N.S., et al., *Regulation of osteogenic and chondrogenic differentiation of mesenchymal stem cells in PEG-ECM hydrogels.* Cell Tissue Res., 2011. **344**(3): p. 499-509.

37. Parekh, S.H., et al., *Modulus-driven differentiation of marrow stromal cells in 3D scaffolds that is independent of myosin-based cytoskeletal tension.* Biomaterials., 2011. **32**(9): p. 2256-2264.

38. Cukierman, E., et al., *Taking cell-matrix adhesions to the third dimension.* Science., 2001. **294**(5547): p. 1708-1712.

39. Bissell, M.J., Rizki, A. and Mian, I.S., *Tissue architecture: the ultimate regulator of breast epithelial function.* Curr Opin Cell Biol., 2003. **15**(6): p. 753-762.

40. Huebsch, N., et al., *Harnessing traction-mediated manipulation of the cell/matrix interface to control stem-cell fate.* Nat Mater., 2010. **9**(6): p. 518-526.

41. Weiss, R.E. and Reddi, A.H., *Appearance of fibronectin during the differentiation of cartilage, bone, and bone marrow.* J Cell Biol., 1981. **88**(3): p. 630-636.

42. Foidart, J.M. and Reddi, A.H., *Immunofluorescent localization of type IV collagen and laminin during endochondral bone differentiation and regulation by pituitary growth hormone.* Dev Biol., 1980. **75**(1): p. 130-136.

43. Klotch, D.W., et al., *Assessment of bone formation during osteoneogenesis: a canine model.* Otolaryngol Head Neck Surg., 1995. **112**(2): p. 291-302.

44. Bueno, E. and Glowacki, J., *Biologic foundations for skeletal tissue engineering.* Morgan and Claypool Publishers., 2011.

45. Benoit, D.S., et al., *Small functional groups for controlled differentiation of hydrogel-encapsulated human mesenchymal stem cells.* Nat Mater., 2008. **7**(10): p. 816-823.

46. Ayala, R., et al., *Engineering the cell-material interface for controlling stem cell adhesion, migration, and differentiation.* Biomaterials., 2011. **32**(15): p. 3700-3711.

47. Burdick, J.A. and Anseth, K.S., *Photoencapsulation of osteoblasts in injectable RGD-modified PEG hydrogels for bone tissue engineering.* Biomaterials., 2002. **23**(22): p. 4315-4323.

48. Yang, F., et al., *The effect of incorporating RGD adhesive peptide in polyethylene glycol diacrylate hydrogel on osteogenesis of bone marrow stromal cells.* Biomaterials., 2005. **26**(30): p. 5991-5998.

49. Humphries, J.D., Byron, A. and Humphries, M.J., *Integrin ligands at a glance.* J Cell Sci., 2006. **119**(Pt 19): p. 3901-3903.

50. Bulick, A.S., et al., *Impact of endothelial cells and mechanical conditioning on smooth muscle cell extracellular matrix production and differentiation.* Tissue Eng Part A., 2009. **15**(4): p. 815-825.

51. Hummon, A.B., et al., *Isolation and solubilization of proteins after TRIzol extraction of RNA and DNA from patient material following prolonged storage.* Biotechniques., 2007. **42**(4): p. 467-470, 472.

52. Watkins, A.W. and Anseth, K.S., *Investigation of molecular transport and distributions in poly(ethylene glycol) hydrogels with confocal laser scanning microscopy.* Macromolecules., 2005. **38**(4): p. 1326-1334.

53. Armstrong, J.K., et al., *The hydrodynamic radii of macromolecules and their effect on red blood cell aggregation.* Biophys J., 2004. **87**(6): p. 4259-4270.

54. Buxton, A.N., et al., *Design and characterization of poly(ethylene glycol) photopolymerizable semi-interpenetrating networks for chondrogenesis of human mesenchymal stem cells.* Tissue Eng., 2007. **13**(10): p. 2549-2560.

55. Munoz-Pinto, D.J., et al., *Probing vocal fold fibroblast response to hyaluronan in 3D contexts.* Biotechnol Bioeng., 2009. **104**(4): p. 821-831.

56. Munoz-Pinto, D.J., Bulick, A.S. and Hahn, M.S., *Uncoupled investigation of scaffold modulus and mesh size on smooth muscle cell behavior.* J Biomed Mater Res A., 2009. **90**(1): p. 303-316.

57. Gregory, T.R., *Nucleotypic effects without nuclei: genome size and erythrocyte size in mammals.* Genome., 2000. **43**(5): p. 895-901.

58. Salinas, C.N. and Anseth, K.S., *The influence of the RGD peptide motif and its contextual presentation in PEG gels on human mesenchymal stem cell viability.* J Tissue Eng Regen Med., 2008. **2**(5): p. 296-304.

59. Salinas, C.N. and Anseth, K.S., *The enhancement of chondrogenic differentiation of human mesenchymal stem cells by enzymatically regulated RGD functionalities.* Biomaterials., 2008. **29**(15): p. 2370-2377.

60. Liao, H., et al., *Influence of hydrogel mechanical properties and mesh size on vocal fold fibroblast extracellular matrix production and phenotype.* Acta Biomater., 2008. **4**(5): p. 1161-1171.

61. Bryant, S.J. and Anseth, K.S., *Controlling the spatial distribution of ECM components in degradable PEG hydrogels for tissue engineering cartilage.* J Biomed Mater Res A., 2003. **64**(1): p. 70-79.

62. Bryant, S.J., Durand, K.L. and Anseth, K.S., *Manipulations in hydrogel chemistry control photoencapsulated chondrocyte behavior and their extracellular matrix production.* J Biomed Mater Res A., 2003. **67**(4): p. 1430-1436.

63. Peyton, S.R., et al., *The use of poly(ethylene glycol) hydrogels to investigate the impact of ECM chemistry and mechanics on smooth muscle cells.* Biomaterials., 2006. **27**(28): p. 4881-4893.

64. Jimenez-Vergara, A.C., et al., *Influence of glycosaminoglycan identity on vocal fold fibroblast behavior.* Acta Biomater., 2011. **7**(11): p. 3964-3972.

65. Steinmetz, N.J. and Bryant, S.J., *The effects of intermittent dynamic loading on chondrogenic and osteogenic differentiation of human marrow stromal cells encapsulated in RGD-modified poly(ethylene glycol) hydrogels.* Acta Biomater., 2011. **7**(11): p. 3829-3840.

66. Nuttelman, C.R., Tripodi, M.C. and Anseth, K.S., *Synthetic hydrogel niches that promote hMSC viability.* Matrix Biol., 2005. **24**(3): p. 208-218.

67. Karp, J.M., et al., *Fibrin-filled scaffolds for bone-tissue engineering: an in vivo study.* J Biomed Mater Res A., 2004. **71**(1): p. 162-171.

68. Le Nihouannen, D., et al., *Micro-architecture of calcium phosphate granules and fibrin glue composites for bone tissue engineering.* Biomaterials., 2006. **27**(13): p. 2716-2722.

69. Peled, E., et al., *A novel poly(ethylene glycol)-fibrinogen hydrogel for tibial segmental defect repair in a rat model.* J Biomed Mater Res A., 2007. **80**(4): p. 874-884.

70. Mulliken, J.B., Kaban, L.B. and Glowacki, J., *Induced osteogenesis--the biological principle and clinical applications.* J Surg Res., 1984. **37**(6): p. 487-496.

71. Schlag, G. and Redl, H., *Fibrin sealant in orthopedic surgery.* Clin Orthop Relat Res., 1988. **227**: p. 269-285.

72. Le Guehennec, L., Layrolle, P. and Daculsi, G., *A review of bioceramics and fibrin sealant.* Eur Cell Mater., 2004. **8**: p. 1-10.

73. Abiraman, S., et al., *Fibrin glue as an osteoinductive protein in a mouse model.* Biomaterials., 2002. **23**(14): p. 3023-3031.

74. Kania, R.E., et al., *Addition of fibrin sealant to ceramic promotes bone repair: long-term study in rabbit femoral defect model.* J Biomed Mater Res., 1998. **43**(1): p. 38-45.

75. Bensaid, W., et al., *A biodegradable fibrin scaffold for mesenchymal stem cell transplantation.* Biomaterials., 2003. **24**(14): p. 2497-2502.

76. Cunin, G., et al., *Experimental vertebroplasty using osteoconductive granular material.* Spine (Phila Pa)., 1976. **25**(9): p. 1070-1076.

77. Shih, Y.R., et al., *Matrix stiffness regulation of integrin-mediated mechanotransduction during osteogenic differentiation of human mesenchymal stem cells.* J Bone Miner Res., 2011. **26**(4): p. 730-738.

78. Lossdorfer, S., et al., *Microrough implant surface topographies increase osteogenesis by reducing osteoclast formation and activity.* J Biomed Mater Res A., 2004. **70**(3): p. 361-369.

79. Balloni, S., et al., *Effects of titanium surface roughness on mesenchymal stem cell commitment and differentiation signaling.* Int J Oral Maxillofac Implants., 2009. **24**(4): p. 627-635.

80. Chastain, S.R., et al., *Adhesion of mesenchymal stem cells to polymer scaffolds occurs via distinct ECM ligands and controls their osteogenic differentiation.* J Biomed Mater Res A., 2006. **78**(1): p. 73-85.

81. Tiger, C.F., et al., A*lpha11beta1 integrin is a receptor for interstitial collagens involved in cell migration and collagen reorganization on mesenchymal nonmuscle cells.* Dev Biol., 2001. **237**(1): p. 116-129.

82. Hodivala-Dilke, K.M., et al., *Novel roles for alpha3beta1 integrin as a regulator of cytoskeletal assembly and as a trans-dominant inhibitor of integrin receptor function in mouse keratinocytes.* J Cell Biol., 1998. **142**(5): p. 1357-1369.

83. Brakebusch, C., et al., *Genetic analysis of beta1 integrin function: confirmed, new and revised roles for a crucial family of cell adhesion molecules.* J Cell Sci., 1997. **110**(Pt 23): p. 2895-2904.

84. Prockop, D.J., *What holds us together? Why do some of us fall apart? What can we do about it?* Matrix Biol., 1998. **16**(9): p. 519-528.

85. Humtsoe, J.O., et al., *A streptococcal collagen-like protein interacts with the alpha2beta1 integrin and induces intracellular signaling.* J Biol Chem., 2005. **280**(14): p. 13848-13857.

86. Ruoslahti, E., *Integrins.* J Clin Invest., 1991. **87**(1): p. 1-5.

87. Xu, Y., et al., *Streptococcal Scl1 and Scl2 proteins form collagen-like triple helices.* J Biol Chem., 2002. **277**(30): p. 27312-27318.

88. Cheresh, D.A., *Structural and biologic properties of integrin-mediated cell adhesion.* Clin Lab Med., 1992. **12**(2): p. 217-236.

89. Xiong, J.P., et al., *Integrins, cations and ligands: making the connection.* J Thromb Haemost., 2003. **1**(7): p. 1642-1654.

90. Hynes, R.O., *Integrins: versatility, modulation, and signaling in cell adhesion.* Cell., 1992. **69**(1): p. 11-25.

91. Velling, T., et al., *cDNA cloning and chromosomal localization of human alpha(11) integrin. A collagen-binding, I domain-containing, beta(1)-associated integrin alpha-chain present in muscle tissues.* J Biol Chem., 1999. **274**(36): p. 25735-25742.

92. Pozzi, A., et al., *Integrin alpha1beta1 mediates a unique collagen-dependent proliferation pathway in vivo.* J Cell Biol., 1998. **142**(2): p. 587-594.

93. Camper, L., Hellman, U. and Lundgren-Akerlund, E., *Isolation, cloning, and sequence analysis of the integrin subunit alpha10, a beta1-associated collagen binding integrin expressed on chondrocytes.* J Biol Chem., 1998. **273**(32): p. 20383-20389.

94. Ivaska, J., et al., *Integrin alpha2beta1 mediates isoform-specific activation of p38 and upregulation of collagen gene transcription by a mechanism involving the alpha2 cytoplasmic tail.* J Cell Biol., 1999. **147**(2): p. 401-416.

95. Burridge, K., et al., *Focal adhesions: transmembrane junctions between the extracellular matrix and the cytoskeleton.* Annu Rev Cell Biol., 1988. **4**: p. 487-525.

96. Roux, P.P. and Blenis, J., *ERK and p38 MAPK-activated protein kinases: a family of protein kinases with diverse biological functions.* Microbiol Mol Biol Rev., 2004. **68**(2): p. 320-344.

97. Tarcic, G. and Yarden, Y., *MAP Kinase activation by receptor tyrosine kinases: in control of cell migration.* Methods Mol Biol., 2010. **661**: p. 125-135.

98. Rubin, J., Rubin, C. and Jacobs, C.R., *Molecular pathways mediating mechanical signaling in bone.* Gene., 2006. **367**: p. 1-16.

99. Ahluwalia, M.S., et al., *Targeting SRC in glioblastoma tumors and brain metastases: rationale and preclinical studies.* Cancer Lett., 2010. **298**(2): p. 139-149.

100. Han, R., et al., *Assessment of prokaryotic collagen-like sequences derived from streptococcal Scl1 and Scl2 proteins as a source of recombinant GXY polymers.* Appl Microbiol Biotechnol., 2006. **72**(1): p. 109-115.

101. Mohs, A., et al., *Mechanism of stabilization of a bacterial collagen triple helix in the absence of hydroxyproline.* J Biol Chem., 2007. **282**(41): p. 29757-29765.

102. Caswell, C.C., et al., *The Scl1 protein of M6-type group A Streptococcus binds the human complement regulatory protein, factor H, and inhibits the alternative pathway of complement.* Mol Microbiol., 2008. **67**(3): p. 584-596..

103. Caswell, C.C., et al., *Scl1-dependent internalization of group A Streptococcus via direct interactions with the alpha2beta(1) integrin enhances pathogen survival and re-emergence.* Mol Microbiol., 2007. **64**(5): p. 1319-1331.

104. Han, R., et al., *Binding of the low-density lipoprotein by streptococcal collagen-like protein Scl1 of Streptococcus pyogenes.* Mol Microbiol., 2006. **61**(2): p. 351-367.

105. Caswell, C.C., et al., *Identification of the first prokaryotic collagen sequence motif that mediates binding to human collagen receptors, integrins alpha2beta1 and alpha11beta1.* J Biol Chem., 2008. **283**(52): p. 36168-36175.

106. Seo, N., et al., *An engineered alpha1 integrin-binding collagenous sequence.* J Biol Chem., 2010. **285**(40): p. 31046-31054.

107. Kim, J.K., et al., *A novel binding site in collagen type III for integrins alpha1beta1 and alpha2beta1.* J Biol Chem., 2005. **280**(37): p. 32512-32520.

108. Knight, C.G., et al., *Identification in collagen type I of an integrin alpha2 beta1-binding site containing an essential GER sequence.* J Biol Chem., 1998. **273**(50): p. 33287-33294.

109. Knight, C.G., et al., *The collagen-binding A-domains of integrins alpha(1)beta(1) and alpha(2)beta(1) recognize the same specific amino acid sequence, GFOGER, in native (triple-helical) collagens.* J Biol Chem., 2000. **275**(1): p. 35-40.

110. Sebra, R.P., et al., *Surface grafted antibodies: controlled architecture permits enhanced antigen detection.* Langmuir., 2005. **21**(24): p. 10907-10911.

111. DeLong, S.A., Moon, J.J. and West, J.L., *Covalently immobilized gradients of bFGF on hydrogel scaffolds for directed cell migration.* Biomaterials., 2005. **26**(16): p. 3227-3234.

112. Almany, L. and Seliktar, D., *Biosynthetic hydrogel scaffolds made from fibrinogen and polyethylene glycol for 3D cell cultures.* Biomaterials., 2005. **26**(15): p. 2467-2477.

113. Zhang, G., et al., *A PEGylated fibrin patch for mesenchymal stem cell delivery.* Tissue Eng., 2006. **12**(1): p. 9-19.

114. Grace, M.J., et al., *Site of pegylation and polyethylene glycol molecule size attenuate interferon-alpha antiviral and antiproliferative activities through the JAK/STAT signaling pathway.* J Biol Chem., 2005. **280**(8): p. 6327-6336.

115. Chien, C.M., et al., *Cell phenotype analysis using a cell fluid-based microchip with high sensitivity and accurate quantitation.* J Chromatogr B Analyt Technol Biomed Life Sci., 2003. **795**(1): p. 1-8.

116. Hsu, H.J., et al., *Stretch-induced stress fiber remodeling and the activations of JNK and ERK depend on mechanical strain rate, but not FAK.* PLoS One., 2010. **5**(8): p. e12470.

117. Yamada, K.M., *Integrin signaling.* Matrix Biol., 1997. **16**(4): p. 137-141.

118. Assoian, R.K. and Schwartz, M.A., *Coordinate signaling by integrins and receptor tyrosine kinases in the regulation of G1 phase cell-cycle progression.* Curr Opin Genet Dev., 2001. **11**(1): p. 48-53.

119. Schwartz, M.A. and Ginsberg, M.H., *Networks and crosstalk: integrin signalling spreads.* Nat Cell Biol., 2002. **4**(4): p. E65-68.

120. Sawai, H., et al., *Activation of focal adhesion kinase enhances the adhesion and invasion of pancreatic cancer cells via extracellular signal-regulated kinase-1/2 signaling pathway activation.* Mol Cancer., 2005. **4**: p. 37-49.

121. Van Slambrouck, S., et al., *Activation of the FAK-src molecular scaffolds and p130Cas-JNK signaling cascades by alpha1-integrins during colon cancer cell invasion.* Int J Oncol., 2007. **31**(6): p. 1501-1508.

122. Sanders, M.A. and Basson, M.D., *Collagen IV-dependent ERK activation in human Caco-2 intestinal epithelial cells requires focal adhesion kinase.* J Biol Chem., 2000. **275**(48): p. 38040-38047.

123. Bryant, S.J. and Anseth, K.S., *Hydrogel properties influence ECM production by chondrocytes photoencapsulated in poly(ethylene glycol) hydrogels.* J Biomed Mater Res., 2002. **59**(1): p. 63-72.

124. Donald E, I., *Tensegrity-based mechanosensing from macro to micro.* Prog Biophys Mol Biol., 2008. **97**(2–3): p. 163-179.

125. Donald, I., *Integrins as mechanochemical transducers.* Curr Opin Cell Biol., 1991. **3**(5): p. 841-848.

126. Engler, A.J., et al., *Matrix elasticity directs stem cell lineage specification.* Cell., 2006. **126**(4): p. 677-689.

127. Han, R., et al., *Assessment of collagen-like sequences derived from Scl1 and Scl2 proteins as a source of recombinant GXY polymers.* Appl Microbiol Biotechnol., 2006. **72**(1): p. 109-115.

128. Hahn, M.S., Miller, J.S. and West, J.L., *Three-dimensional biochemical and biomechanical patterning of hydrogels for guiding cell behavior.* Advanced Materials., 2006. **18**(20): p. 2679-2684.

129. Mann, B.K. and West, J.L., *Cell adhesion peptides alter smooth muscle cell adhesion, proliferation, migration, and matrix protein synthesis on modified surfaces and in polymer scaffolds.* J Biomed Mater Res., 2002. **60**(1): p. 86-93.

130. Metters, A.T., Anseth, K.S. and Bowman, C.N., *A statistical kinetic model for the bulk degradation of PLA-b-PEG-b-PLA hydrogel networks: incorporating network non-idealities.* J. Phys. Chem. B., 2001. **105**(34): p. 8069-8076.

131. Anseth, K.S., et al., *In situ forming degradable networks and their application in tissue engineering and drug delivery.* J Control Release., 2002. **78**(1-3): p. 199-209.

132. Zuk, P.A., et al., *Human adipose tissue is a source of multipotent stem cells.* Mol Biol Cell., 2002. **13**(12): p. 4279-4295.

133. Johnson, C.P., et al., *A biomechanical study of the human vertebral artery with implications for fatal arterial injury.* Forensic Sci Int., 2000. **109**(3): p. 169-182.

134. Hiles, M.C., et al., *Mechanical properties of xenogeneic small-intestinal submucosa when used as an aortic graft in the dog.* J Biomed Mater Res., 1995. **29**(7): p. 883-891.

135. Hahn, M.S., et al., *Physiologic pulsatile flow bioreactor conditioning of poly(ethylene glycol)-based tissue engineered vascular grafts.* Ann Biomed Eng., 2007. **35**(2): p. 190-200.

136. Clover, J., Dodds, R.A. and Gowen, M., *Integrin subunit expression by human osteoblasts and osteoclasts in situ and in culture.* J Cell Sci., 1992. **103**(Pt 1): p. 267-271.

137. Jikko, A., et al., *Collagen integrin receptors regulate early osteoblast differentiation induced by BMP-2.* J Bone Miner Res., 1999. **14**(7): p. 1075-1083.

138. Popov, C., et al., *Integrins alpha2beta1 and alpha11beta1 regulate the survival of mesenchymal stem cells on collagen I.* Cell Death Dis., 2011. **28**(2): p. 71-84.

139. Foster, L.J., et al., *Differential expression profiling of membrane proteins by quantitative proteomics in a human mesenchymal stem cell line undergoing osteoblast differentiation.* Stem Cells., 2005. **23**(9): p. 1367-1377.

140. Gronthos, S., et al., *Integrin-mediated interactions between human bone marrow stromal precursor cells and the extracellular matrix.* Bone., 2001. **28**(2): p. 174-181.

141. Reyes, C.D. and Garcia, A.J., *Alpha2beta1 integrin-specific collagen-mimetic surfaces supporting osteoblastic differentiation.* J Biomed Mater Res A., 2004. **69**(4): p. 591-600.

142. Bennett, K.P., et al., *Proteomics reveals multiple routes to the osteogenic phenotype in mesenchymal stem cells.* BMC Genomics., 2007. **8**: p. 380-390.

143. Tamura, Y., et al., *Focal adhesion kinase activity is required for bone morphogenetic protein--Smad1 signaling and osteoblastic differentiation in murine MC3T3-E1 cells.* J Bone Miner Res., 2001. **16**(10): p. 1772-1779.

144. Lee, H.W., et al., *Berberine promotes osteoblast differentiation by Runx2 activation with p38 MAPK.* J Bone Miner Res., 2008. **23**(8): p. 1227-1237.

145. Jaiswal, R.K., et al., *Adult human mesenchymal stem cell differentiation to the osteogenic or adipogenic lineage is regulated by mitogen-activated protein kinase.* J. Biol. Chem., 2000. **275**: p. 9645-9652.

146. Ortuno, M.J., et al., *p38 regulates expression of osteoblast-specific genes by phosphorylation of osterix.* J Biol Chem., 2010. **285**(42): p. 31985-31994.

147. Ishisaki, A., et al., *Activation of p38 mitogen-activated protein kinase mediates thyroid hormone-stimulated osteocalcin synthesis in osteoblasts.* Mol Cell Endocrinol., 2004. **214**(1-2): p. 189-195.

148. Xu, D.J., et al., *Smads, p38 and ERK1/2 are involved in BMP9-induced osteogenic differentiation of C3H10T1/2 mesenchymal stem cells.* BMB Rep., 2012. **45**(4): p. 247-252.

149. Guicheux, J., et al., *Activation of p38 mitogen-activated protein kinase and c-Jun-NH2-terminal kinase by BMP-2 and their implication in the stimulation of osteoblastic cell differentiation.* J Bone Miner Res., 2003. **18**(11): p. 2060-2068.

150. Doan, T., et al., *Inhibition of JNK and ERK pathways by SP600125- and U0126-enhanced osteogenic differentiation of bone marrow stromal cells.* Tissue Eng and Reg Med., 2012. **9**(6): p. 283-294.